



METIS II

Mobile and wireless communications Enablers for the Twenty-twenty
Information Society-II

Deliverable D2.3

Performance evaluation results

Version: v1.0

2017-02-28



<http://www.5g-ppp.eu/>

Deliverable D2.3

Performance evaluation results

Grant Agreement Number:	671680
Project Name:	Mobile and wireless communications Enablers for the Twenty-twenty Information Society-II
Project Acronym:	METIS-II
Document Number:	METIS-II/D2.3
Document Title:	Performance evaluation results
Version:	v1.0
Delivery Date:	2017-02-28
Editor(s):	Michał Maternia (Nokia Bell Labs), David Martín-Sacristán (Universitat Politècnica de València)
Authors:	Jamal Bazzi (DoCoMo), Paul Arnold, Jakob Belschner, Gerd Zimmerman (Deutsche Telekom), Márten Ericson, Sachin Sharma (Ericsson), Ömer Bulakci, Emmanouil Pateromichelakis Panagiotis Spapis, Changqing Yang (Huawei), Gary Huang (ITRI), Ki Won Sung, Haris Celik (Kungliga Tekniska Högskolan), Michał Maternia, Athul Prasad, Fernando Sanchez Moya, Martti Moisio, Andreas Weber (Nokia Bell Labs), David Gutierrez Estevez, Milos Tesanovic, Yinan Qi, Mehrdad Shariat (Samsung), Giorgio Calochira, Roberto Fantini (Telecom Italia), Nandish P. Kuruvatti, Ji Lianghai (Technische Universität Kaiserslautern), David Martín-Sacristán, Jose F. Monserrat (Universitat Politècnica de València)
Keywords:	5G, performance evaluation, evaluation framework, KPIs, METIS-II, 5G PPP, 5G RAN
Status:	Final
Dissemination level:	Public

Revision History

Revision	Date	Description
1.0	2017-02-28	D2.3 v1.0 released

Acknowledgments

The editors would like to acknowledge the following people for their valuable reviews of this deliverable: Patrick Agyapong (DoCoMo), Salah Eddine El Ayoubi, Alan Stidwell (Orange), Giuseppe Piro (Politecnico di Bari) and Andreas Georgakopoulos (WINGS).



Executive summary

Key objectives of METIS-II are to develop the overall 5G radio access network (RAN) design and to provide technical enablers needed for an efficient integration and use of the various 5G technologies and components currently developed. In order to achieve these objectives, both qualitative and quantitative analysis of proposed technology components (TeCs) is needed.

This deliverable contains:

- definitions of key performance indicators (KPIs) and models constituting final METIS-II performance evaluation framework, to a large extent based on framework proposed in [MII16-D21],
- holistic assessment of hypothetical 5G system along proposed performance evaluation framework, taking into account expected advancements as well as TeCs investigated in METIS-II, and
- quantitative assessment of selected TeCs investigated for 5G RAN in METIS-II, compared against legacy solutions.

Altogether, material provided in this deliverable provides insight into the overall performance improvements that 5G can bring to the future society and on evaluation methodologies that can be used to quantify these gains.



Contents

1	Introduction	11
1.1	Objective of the document	11
1.2	Structure of the document.....	11
2	Final METIS-II 5G performance evaluation framework	12
2.1	KPIs evaluated by inspection	12
2.1.1	Bandwidth and channel bandwidth scalability	12
2.1.2	Coexistence with LTE	13
2.1.3	Deployment in IMT bands	13
2.1.4	Interworking with 3GPP legacy technologies and 802.11 Wireless Local Area Network (WLAN).....	13
2.1.5	Low cost requirements.....	13
2.1.6	Operation above 6 GHz	13
2.1.7	Spectrum flexibility	13
2.1.8	Support for wide range of services.....	13
2.2	KPIs evaluated by analysis	14
2.2.1	Control plane latency	14
2.2.2	mMTC device energy consumption improvement	14
2.2.3	Mobility interruption time	14
2.2.4	Peak data rate	14
2.2.5	User plane latency	15
2.3	KPIs evaluated by simulations	15
2.3.1	Experienced user throughput.....	15
2.3.2	Traffic volume density	16
2.3.3	E2E latency	16
2.3.4	Reliability	16
2.3.5	Availability.....	17
2.3.6	Retainability	17
2.3.7	mMTC device density	17
2.3.8	RAN energy efficiency	17
2.3.9	Supported velocity	17



2.4	Main KPIs evaluated with simulations and corresponding simulation parameters	.18
3	METIS-II 5G evaluation	21
3.1	Evaluation through inspection	21
3.1.1	Bandwidth and channel bandwidth scalability	21
3.1.2	Coexistence with LTE	21
3.1.3	Deployment in IMT bands	21
3.1.4	Interworking with 3GPP legacy technologies and 802.11 WLAN	22
3.1.5	Operations above 6 GHz	22
3.1.6	Spectrum flexibility and sharing	22
3.1.7	Support of wide range of services	22
3.1.8	Low cost requirements	22
3.2	Analytical evaluation	22
3.2.1	Control plane latency	22
3.2.2	User plane latency	25
3.2.3	mMTC device energy consumption improvement	26
3.2.4	Mobility interruption time	28
3.2.5	Peak data rate	28
3.3	Evaluation through simulation	29
3.3.1	UC1 – Dense Urban Information Society	29
3.3.2	UC2 – Virtual Reality Office	34
3.3.3	UC3 – Broadband Access Everywhere	36
3.3.4	UC4 – Massive Distribution of Sensors and Actuators	40
3.3.5	UC5 – Connected Cars	42
3.3.6	RAN energy efficiency	47
4	Performance of selected METIS-II 5G RAN components	49
4.1	xMBB	51
4.1.1	Tight integration of 5G with LTE-A	51
4.1.2	Flexible interference management for 5G AIVs	52
4.1.3	Joint transmission with dummy symbols for dynamic TDD	53
4.1.4	Diurnal mobility prediction to assist context aware RRM	54
4.1.5	5G user-centric interference management in UDNs	56



4.1.6	Dynamic cell switch off.....	57
4.1.7	Mobility management framework for D2D communication	58
4.1.8	Resource management and traffic steering in heterogeneous environments	59
4.2	mMTC.....	60
4.2.1	FQAM-FBMC design and its application to mMTC	60
4.2.2	Group based system access.....	61
4.2.3	RRC state handling improvements – Connected Inactive	62
4.2.4	Context-aware D2D communication for mMTC	63
4.3	uMTC.....	64
4.3.1	AIV harmonization for V2V communication	64
4.4	TeCs addressing mixed services	65
4.4.1	RACH multiplexing in support to diverse access requirements	65
4.4.2	Regular resource grid for new waveform.....	66
4.4.3	Flexible multi-service scheduling framework	68
4.4.4	Multi-AI traffic steering framework.....	69
4.4.5	RRM for network slicing	70
5	Conclusions	72
6	References	74
A	Annex: Final METIS-II 5G performance evaluation framework.....	80
A.1	Simulation KPIs	80
A.1.1	Detailed RAN energy efficiency evaluation procedure.....	80
A.2	Simulation parameters for deployment scenarios.....	84
A.2.1	Synthetic deployment scenarios	84
A.2.2	BS antenna pattern.....	86
A.2.3	Realistic deployment scenarios.....	87
A.3	Models for individual use cases	89
A.3.1	Dense Urban Information Society	90
A.3.2	Virtual Reality Office	91
A.3.3	Massive Distribution of Sensors and Actuators	92
A.3.4	Connected Cars.....	92
B	Annex: METIS-II 5G evaluation.....	97



B.1	Control plane latency	97
B.2	UC2	100
B.3	UC4	101
C	Annex: Performance of METIS-II key 5G RAN components.....	103
C.1	xMBB	103
C.1.1	Tight integration of 5G with LTE-A	103
C.1.2	Diurnal mobility prediction to assist context aware RRM	104
C.1.3	5G user-centric interference management in UDNs.....	104
C.1.4	Dynamic cell switch off.....	108
C.1.5	Mobility management framework for D2D communication	109
C.1.6	Resource management and traffic steering in heterogeneous environments	111
C.2	mMTC.....	112
C.2.1	FQAM-FBMC design and its application to mMTC	112
C.2.2	Group based system access.....	112
C.2.3	RRC state handling improvements – Connected Inactive	114
C.2.4	Context-aware D2D communication for mMTC	114
C.3	uMTC.....	119
C.3.1	AIV harmonization for V2V communication	119
C.4	TeCs addressing mixed services	121
C.4.1	Regular resource grid for new waveform.....	121
C.4.2	Flexible multi-service scheduling framework	121
C.4.3	Multi AI traffic steering framework	122

List of Abbreviations and Acronyms

3G	Third Generation
3GPP	Third Generation Partnership Project
4G	Fourth Generation
5G	Fifth Generation
5G PPP	5G Infrastructure Public Private Partnership
AASE	AIV-Agnostic Slice Enabler
ACK	ACKnowledgement
AI	Air Interface
AIV	Air Interface Variant
AN-I	Access Network-Inner
AN-O	Access Network-Outer
AWGN	Additive White Gaussian Noise
BER	Bit Error Rate
BLER	Block Error Rate
BS	Base Station
BW	BandWidth
C/I	Carrier-to-Interference
CBR	Constant Bit Rate
CCH	Control Channel
cmW	Centimeter Wave
CN	Core Network
CoMP	Coordinated MultiPoint
CP	Control Plane
CP-OFDM	Cyclic Prefix Orthogonal Frequency Division Multiplexing
C-RAN	Cloud Radio Access Network
D2D	Device-to-Device
DC	Dual Connectivity
DL	DownLink
DPB	Dynamic Point Blanking
DPS	Dynamic Point Selection
DRX	Discontinuous Reception
DTX	Discontinuous Transmission
E2E	End-to-End

eNB	Enhanced Node B
EVA	Extended Vehicular A
FBMC	Filter Bank MultiCarrier
FBR	Front-to-Back Ratio
F-OFDM	Filtered Orthogonal Frequency Division Multiplexing
FQAM	Frequency and Quadrature-Amplitude Modulation
FS	Fast Switch
FTP	File Transfer Protocol
GSM	Global System for Mobile communications
HARQ	Hybrid Automatic Repeat reQuest
HetNet	Heterogeneous Network
HH	Hard Handover
ICI	Inter-Cell Interference
IEEE	Institute of Electrical and Electronics Engineers
IMT-A	International Mobile Telecommunications – Advanced
IoT	Internet of Things
ISD	Inter-Site Distance
ITS	Intelligent Transportation Systems
ITU	International Telecommunication Union
JT	Joint Transmission
KPI	Key Performance Indicator
LoS	Line-of-Sight
LTE	Long Term Evolution
LTE-A	Long Term Evolution-Advanced
MAC	Medium Access Control
mMTC	Massive Machine-Type Communication
mmW	Millimeter Wave
MTC	Machine-Type Communication



NACK	Negative ACKnowledgement
NAS	Non-Access Stratum
NLoS	Non Line-of-Sight
NN	Nomadic Node
NR	New Radio
OFDM	Orthogonal Frequency Division Multiplexing
OFDMA	Orthogonal Frequency Division Multiple Access
OOB	Out-of-Band
OSC	Outdoor Small Cell
PAPR	Peak-to-Average Power Ratio
PDCP	Packet Data Convergence Protocol
PGIA	Pre-emptive Geometrical-based Interference Analysis
PRB	Physical Resource Block
PRR	Packet Reception Ratio
PSD	Power Spectral Density
QAM	Quadrature Amplitude Modulation
QoS	Quality of Service
QPSK	Quadrature Phase Shift Keying
RACH	Random Access Channel
RAN	Radio Access Network
RAT	Radio Access Technology
RB	Resource Block
RFSP	RAT/Frequency Selection Priority
RMa	Rural Macro
RNTP	Relative Narrow-band Transmit Power

RRC	Radio Resource Control
RRM	Radio Resource Management
RSC	Resource Sharing Cluster
RSRP	Reference Signal Received Power
RTT	Round Trip Time
SC	SubCarrier
SFN	Single Frequency Network
SINR	Signal-to-Interference-plus-Noise Ratio
SIR	Signal-to-Interference Ratio
SLA	Service Level Agreement
SNR	Signal-to-Noise Ratio
SON	Self-Organizing Network
SPB	Small Packet Blocks
TCP	Transmission Control Protocol
TDD	Time Division Duplexing
TeC	Technology Component
TTI	Transmission Time Interval
UC	Use Case
UDN	Ultra-Dense Network
UE	User Equipment
UL	UpLink
UMa	Urban Macro
UMi	Urban Micro
uMTC	Ultra-reliable Machine-Type Communication
UP	User Plane
V2V	Vehicle-to-Vehicle
VoIP	Voice over Internet Protocol
WLAN	Wireless Local Area Network

1 Introduction

Starting from the introduction of Global System for Mobile communication (GSM), mobile phones and associated applications have become a commodity for the people worldwide. However, modern societies not only expect faster data rates and cheaper services. Contemporary cellular users and mobile network operators shift attention also to machine type communication (MTC) expected to form so-called Internet of Things (IoT), and to ultra-reliable communication that will lift probability of service successful completion to unprecedented level and duration.

All these expectations will to be catered by fifth generation of cellular communication known as 5G. 5G will allow peak data rates up to several Gbps for extreme mobile broadband (xMBB) services, energy efficient data transmission for massive MTC (mMTC) devices deployed in enormous volumes, and finally, low latencies and service robustness using ultra-reliable MTC (uMTC).

The last mile access is often a bottleneck that limits the potential service experience in telecommunication systems, therefore an efficient radio access network (RAN) is a crucial element of every wireless technology. METIS-II project aims at tackling this challenge for 5G and investigates technical solutions (denoted further as technology components (TeCs)) that enable different features of the 5G system with the overall goal of providing high performing 5G RAN.

1.1 Objective of the document

The objective of this document is threefold. Firstly, it provides an evaluation framework that can be used for a fair assessment of key performance indicators (KPIs). This framework is expected to be similar as the one that will be issued by International Telecommunication Union (ITU) for “International Mobile Telecommunication for 2020 and beyond” (IMT-2020) (cf. [ITUR15-M2083] [ITUR17-C508]). Secondly, assessment of a hypothetical 5G RAN along proposed performance evaluation framework is done, taking into account expected advancements as well as TeCs investigated in METIS-II. Finally, a crisp overview of selected TeCs developed in METIS-II is provided, showing their potential impact on the performance of 5G end users and network, mainly through system-level simulations.

1.2 Structure of the document

Section 2 contains the final METIS-II 5G performance evaluation framework consisting of KPIs, models and evaluation scenarios. It is used for assessment of the METIS-II 5G RAN design, taking into account five generic use cases (UCs) defined for 5G in [MII16-D11]. This assessment is carried out in Section 3. Finally, a crisp overview and quantitative evaluation of selected METIS-II TeCs is given in Section 4, followed by the conclusions and recommendations in Section 5.

2 Final METIS-II 5G performance evaluation framework

To quantify gains of certain technical solutions or RAN design concepts proposed for 5G, specific metrics are needed. This section gives definitions of 5G KPIs and provides detailed guidelines and instructions on how to assess them, similarly to the coarse framework proposed in [ITUR15-M2083] that follows [ITUR08-M2134] defined for evaluation of International Mobile Telecommunications – Advanced (IMT-A)/Fourth Generation (4G). Specifically, the following assessment methods can be distinguished for proposed framework:

- In case of **inspection** methods, the evaluation is based on statements (Section 2.1).
- For **analytical** procedures, the evaluation is done through calculations based on available technical information and/or performance that is predictable and repeatable in a given scenario (Section 2.2). Analytical procedures that are formulated in steps are generic and should not favour any particular technology. Depending on a specific technical solution, only a subset of these steps may be required to be included in the evaluation.
- In case of evaluations through **simulations**, both system and link level simulation are used to derive results, which can't be precisely assessed using inspection or analytical methods (Section 2.3).

For the latter group, specific deployment scenarios, hardware configurations and models for METIS-II UCs are given in Section 2.4.

Altogether, information captured in this section constitutes the final METIS-II performance evaluation framework. It is based to a large extent on a performance evaluation framework captured in [MII16-D21]. The latter contains also state-of-the-art analysis and additional information why certain KPIs or models were dropped, added or changed comparing to the evaluation framework proposed for evaluation of IMT-A/4G [ITUR08-M2134]. Detailed information on the METIS-II UCs, KPIs and expected performance, also with respect to studies of ITU, Next Generation Mobile Networks alliance and Third Generation Partnership Project (3GPP), can be found in [MII16-D11].

Finally, 5G evaluation assessed according to METIS-II 5G performance evaluation framework presented in this section can be found in Section 3.

2.1 KPIs evaluated by inspection

2.1.1 Bandwidth and channel bandwidth scalability

Scalable bandwidth is the ability of the 5G system to operate with different bandwidth allocations. This bandwidth may be supported by single or multiple radio frequency carriers.

The 5G system shall support a scalable bandwidth of at least 1 GHz. Proponents are encouraged to consider extensions to support operation in wider bandwidths (e.g. up to 3.5 GHz) as will be detailed in Section 3.1.1.

2.1.2 Coexistence with LTE

The new 5G Air Interface¹ (AI) must be able to coexist with Long Term Evolution (LTE) from Release 8 and onward. This coexistence refers to the ability of the 5G access technology to share resources with a LTE technology operating in the same block of spectrum with possible bandwidth overlap. In this sense, the new AI must be able to support flexible allocation of resources both in frequency and in time domain.

2.1.3 Deployment in IMT bands

Deployment of the 5G system must be possible in at least one of the identified IMT bands. Proponents are encouraged to clarify the preferred bands for the proposed candidate/s.

2.1.4 Interworking with 3GPP legacy technologies and 802.11 Wireless Local Area Network (WLAN)

Interworking refers to the capability of the 5G AI terminals to switch multimode terminals to another technology depending on the coverage and achievable Quality of Service (QoS).

2.1.5 Low cost requirements

The 5G AI shall support the connection of low cost devices and low cost operations.

2.1.6 Operation above 6 GHz

The 5G AI shall be able to operate in centimetre wave (cmW) and/or millimetre wave (mmW) bands with one or several Air Interference Variants² (AIVs) especially suited to these bands.

2.1.7 Spectrum flexibility

The ability of the 5G AI with one or several AIVs to be adapted to suit different downlink (DL) / uplink (UL) traffic patterns and capacity needs for both paired and unpaired frequency bands [3GPP15-152129].

2.1.8 Support for wide range of services

The ability of the 5G AI to meet the connectivity requirements of a range of existing and future (as yet unknown) services to be operable on a single continuous block of spectrum in an efficient manner [3GPP15-152129].

¹ An AI is here defined as the RAN protocol stack and all related functionalities describing the interaction between infrastructure and device and covering all services, bands, cell types etc. that are expected to characterize the overall 5G system.

² An AIV is defined in the same way as an air interface, but covers only a subset of services, bands, cell types expected to characterize the overall system.

Note that hybrid services including xMBB, mMTC and uMTC may be supported in the same band.

2.2 KPIs evaluated by analysis

2.2.1 Control plane latency

Control Plane (CP) latency (in ms) is a transition time from an energy efficient connection mode (e.g., idle) to active mode. Total CP latency must be provided together with the latencies of all intermediate steps, if any. Note that the full set of steps represents the idle to active state transition. However, the proponent must clarify intermediate states that could be included in the AIV, like a connected-inactive state, and the latencies associated with each intermediate state.

The following steps need to be considered (not all steps are required):

- Step 0: User Equipment (UE) wakeup time
- Step 1: DL scanning and synchronization + acquisition of broadcast channel
- Step 2: Random access procedure
- Step 3: UL synchronization
- Step 4: Capability negotiation + hybrid automatic repeat request (HARQ) retransmission
- Step 5: Authorization and authentication/ key exchange + HARQ retransmission
- Step 6: Registration with the Base Station (BS) + HARQ retransmission
- Step 7: Radio Resource Control (RRC) connection establishment/ resume + HARQ retransmission

2.2.2 mMTC device energy consumption improvement

mMTC device energy consumption improvement is defined as the lifetime of a battery (in hours, days or years) for a 5G device comparing to LTE-A one, under the assumption that the device is stationary and the energy consumption is related only to operations in AI. If not mentioned explicitly, energy consumption in RRC idle state is assumed the same for LTE-A and 5G devices.

Following steps need to be considered (not all steps are required):

- Step 0: Synchronization
- Step 1: Transmit scheduling request
- Step 2: Receive grant
- Step 3: Transmit 125 B data
- Step 4: HARQ retransmission

2.2.3 Mobility interruption time

Mobility interruption time (in ms) is defined as the time span during which a UE cannot exchange User Plane (UP) packets with any BS during transitions [3GPP15-152129]. It can be regarded as intra-system handover interruption time.

2.2.4 Peak data rate

Peak data rate (in Gbps) is the highest theoretical single user data rate, i.e., assuming error-free transmission conditions, when all available radio resources for the corresponding link direction

are utilized (i.e., excluding radio resources that are used for physical layer synchronization, reference signals or pilots, guard bands and guard times). Peak data rate calculation shall include the details on the assumed Multiple-Input Multiple-Output (MIMO) configuration and bandwidth.

2.2.5 User plane latency

UP latency (in ms) is defined as the one-way transmission time of a packet between the transmitter and the availability of this packet in the receiver. The measurement reference is the Medium Access Control (MAC) layer in both transmitter and receiver side. Analysis must distinguish between UP latency in an infrastructure-based communication and in a direct Device-to-Device (D2D) communication.

Following steps need to be considered (not all steps are required):

- Step 0: Transmitter processing delay at BS (or UE in D2D communication)
- Step 1: Frame alignment
- Step 2: Synchronization
- Step 3: Number of Transmission Time Intervals (TTIs) used for data packet transmission (unloaded condition is assumed)
- Step 4: HARQ retransmission (assuming 10% error probability)
- Step 5: Receiver processing delay in UE

2.3 KPIs evaluated by simulations

2.3.1 Experienced user throughput

Experienced user throughput (in Mbps) is evaluated using deployment scenarios and models for METIS-II xMBB UCs (UC1, UC2 and UC3 [MII16-D11]). It refers to an instantaneous data rate between Layer 2 and Layer 3, calculated as:

$$U_{Tput} = \frac{S}{T},$$

where S is the transmitted packet size and T is the packet transmission duration between the time when the entire packet is correctly received at the destination and the time when packet is available for transmission. It is calculated separately for DL (transmission from source radio points to UE), UL (transmission from UE to destination radio points) and (potentially) for D2D (transmission directly between involved UEs).

Note that experienced user throughput depends on the system bandwidth, and therefore this parameter shall be clearly identified in the simulation analysis.

Experienced user throughput is linked with a certain level of availability and retainability (cf. Table 2-1).

2.3.2 Traffic volume density

Traffic volume density (in Gbps/km²) is evaluated using deployment scenarios and models for METIS-II xMBB UCs (UC1, UC2 and UC3 [MII16-D11]). It is defined as the aggregated number of correctly transferred bits (*Nbits*) received by all destination UEs from source radio points (DL traffic) or sent from all source UEs to destination radio points (UL traffic), over the active time of the network, to the area size covered by the radio points belonging to the RAN(s) where UEs can be deployed. Here active time of the network (*T_{sim}*) is the duration in which at least one session in any radio point of the RAN is activated. Traffic volume density can be calculated as

$$\text{Traffic volume density} = \frac{\sum_{n=1}^N (Nbits_{DL}^n + Nbits_{UL}^n + Nbits_{D2D}^n)}{T_{sim} \times \text{Simulation area}}$$

Where *N* is a total number of UEs in simulation and *Nbits_{DL}ⁿ*, *Nbits_{UL}ⁿ* and *Nbits_{D2D}ⁿ* is a total number of transferred bits for DL, UL and D2D traffic, respectively.

Note that D2D traffic should be evaluated independently from the cellular one. Besides, the link between source and destination may cover multiple hops especially when non-ideal backhaul is taken into consideration.

Again, system bandwidth assumption must be clearly identified.

2.3.3 E2E latency

Different types of latency are relevant for different applications. E2E latency (in ms), or one trip time (OTT) latency, refers to the time it takes from when a data packet is sent from the transmitting end to when it is received at the receiving entity, e.g., internet server or other device. Another latency measure is the round trip time (RTT) latency which refers to the time from when a data packet is sent from the transmitting end until acknowledgements are received from the receiving entity. The measurement reference in both cases is the interface between Layer 2 and 3.

2.3.4 Reliability

Reliability (in percentage) is evaluated using deployment scenarios and models for METIS-II uMTC UC5 [MII16-D11]. It refers to the continuity in the time domain of correct service and is associated with a maximum latency requirement. In effect, reliability accounts for the percentage of packets properly received within the given maximum E2E latency (OTT or RTT depending on the service).

More specifically, for vehicular-to-anything transmission, reliability is evaluated through the packet reception ratio (PRR), following the 3GPP definition [3GPP15-154981]. PRR is calculated for each transmitted packet as *X/Y*, where *Y* is the number of UEs/vehicles located in the certain range (20 m range bins are assumed) from the transmitter, and *X* is the number of UEs/vehicles with successful reception among *Y*.

Reliability of uMTC at a specific level is achieved when a given PRR (equal to the reliability) can be guaranteed at a specific distance, for the messages successfully received within a specific time interval.

In general reliability is linked with a certain level of availability and retainability (cf. Table 2-1).

2.3.5 Availability

Availability (in percentage) is defined as the number of places (related to a predefined area unit or pixel size) where the Quality of Experience (QoE) level requested by the end-user is achieved, divided by the total coverage area of a single radio cell or a multi-cell area (equal to the total number of pixels) times 100.

2.3.6 Retainability

Retainability is defined as the percentage of time where transmissions meet the target experienced user throughput or reliability.

2.3.7 mMTC device density

mMTC device density (in the number of mMTC devices per km²) is defined as the maximum supported number of mMTC devices in a given area. It is evaluated using deployment scenarios and models for METIS-II mMTC UC4 [MII16-D11] and it is achieved when a given radio network infrastructure can correctly receive a specific percentage of access attempts (equal to availability) from mMTC devices.

2.3.8 RAN energy efficiency

Energy efficient network operation is one of the key design objectives for 5G. RAN energy efficiency (in arbitrary units) is defined as the overall energy consumption of 5G access nodes in the RAN comparing to a performance of legacy access nodes. In order to prove expected energy efficiency both spatial (entire network) and temporal (24 hours) traffic variations need to be taken into account. Detailed steps for evaluation of the 5G RAN energy efficiency are given in Annex A.1.1.

2.3.9 Supported velocity

Velocity (in km/h) is supported when at a given velocity, device link data rate is equal or greater than required value and required bit error rate.

Following steps should be taken to evaluate the velocity support:

Step 1: Run system level simulations with parameters as defined for a given deployment scenario defined for a specific use case in Section 2.4 with the exception of setting the speed to a given value and using full buffer traffic model to collect the overall statistics for downlink Cumulative Distribution Function (CDF) of pilot signal power.

Step 2: Use the CDF of this received power to collect the given CDF percentile value required by desired availability (e.g., for availability of 95% a 5th percentile value should be chosen).

Step 3: Run the downlink link-level simulations for settings defined in Section 2.4 and for a given velocity for both Line-of-Sight (LoS) and non LoS (NLoS) conditions to obtain link data rate and bit error rate as a function of the pilot signal power. It is sufficient if one of the spectral efficiency values of either LoS or NLoS channel conditions fulfils the threshold.

2.4 Main KPIs evaluated with simulations and corresponding simulation parameters

METIS-II proposes 5 distinctive UCs [MII16-D11] for evaluation of different simulation KPIs introduced in Section 2.3. UC1 *Dense Urban Information Society* focuses on evaluation of heterogeneous networks (HetNet) in a dense urban environment, UC2 *Virtual Office* targets indoor deployments and UC3 *Broadband Access Everywhere* aims at assessment of 5G performance in rural and suburban areas. These three UCs address evaluation of xMBB services, while UC4 *Massive Distribution of Sensors and Actuators* and UC5 *Connected Cars* address evaluation of mMTC and uMTC services, respectively.

Main targets for simulation KPIs defined for METIS-II UCs can be found in Table 2-1 and major evaluation parameters are captured in Table 2-2. Remaining parameters and models can be found in Annex A.2 and Annex A.3.

Table 2-1. Requirements for KPIs of METIS-II UCs

UC	KPI	Requirement
UC1 Dense Urban Information Society	Experienced user throughput	300 Mbps in DL and 50 Mbps in UL at 95% availability and 95% retainability
	E2E RTT latency	Less than 5 ms (augmented reality applications)
UC2 Virtual Reality Office	Experienced user throughput	5 (1) Gbps in DL and UL at 20% (95%) availability and 99% retainability
UC3 Broadband Access Everywhere	Experienced user throughput	50 Mbps in DL and 25 Mbps in UL at 99% availability and 95% retainability
UC4 Massive Distribution of Sensors and Actuators	mMTC device density	1 000 000 devices/km ² transmitting from few bytes per day to 125 B per second with 99.9% availability
	mMTC device energy consumption improvement	10 years (assuming 5 Wh battery)

UC5 Connected Cars	E2E OTT latency	5 ms (traffic safety applications) at 99.999% reliability
	Experienced user throughput	100 Mbps in DL and 20 Mbps in UL (for non-traffic safety related services) at 99% availability and 95% retainability
	Supported velocity	Up to 250 km/h

Table 2-2. Key evaluation parameters and models.

Use case	UC1	UC2	UC3	UC4	UC5
BS deployment	HetNet	Indoor Hotspot (InH)	Rural Macro (RMa)	Urban Macro (UMa)	HetNet/RMa (urban/motorway)
Inter-site Distance (ISD)	200 m for macro and >20 m for small cells	20 m	1732 m	500 m	500 m
Carrier frequency	3.5 GHz for macro and 25 GHz for small cell	3.5 GHz and 70 GHz	800 MHz	800 MHz	5.9 GHz
UE deployment	10 UEs per macro cell and 5 UEs per small cell	10 UEs	10 UEs per cell	24000 per cell	< 1000 cars per square km (urban) < 100 cars per km (motorway)
Number of UE antenna elements (TX/RX)	16/16	16/16	8/8	2/2	2/4
Number of UE antenna ports (TX/RX)	8/8 for <6 GHz 4/4 for >6 GHz	8/8 for <6 GHz 4/4 for >6 GHz	4/4	1/1	1/2



UE speed (for fast fading calculation)	3 km/h in small cells and 30 km/h in macro	3 km/h	120 km/h	3 km/h	60 km/h for urban and 140 km/h for motorway
Indoor / Outdoor ratio	80/20	100/0	0/100	80/20	0/100
Traffic model	Full buffer and bursty	Full buffer and bursty	Full buffer and bursty	Bursty (periodic)	Bursty (periodic + event driven)

3 METIS-II 5G evaluation

This section contains qualitative and quantitative assessment of performance that can be achieved by the hypothetical 5G system taking into account solutions developed in METIS-II. This assessment is done according to METIS-II performance evaluation framework defined in Section 2.

3.1 Evaluation through inspection

3.1.1 Bandwidth and channel bandwidth scalability

METIS-II system can operate with different bandwidth allocations [MII16-D41] and in bands up to 100 GHz [MII16-D31].

Here, we provide an exemplary bandwidth evaluation based on the application-based methodology described in [ITUR15-WP5D]. This example considers the analysis of a crowded dense urban scenario, where the user or device density is assumed to be 1 per 4 m². With user activity factor of 0.8, this leads to the connection density of 200 000 devices/km², in line with UC1, i.e., dense urban information society [MII16-D11]. Multiple applications are considered with data rates ranging from 1 Gbps for super-high data rate applications (e.g. virtual reality) to 500 Mbps for the high data rate applications (e.g., 8K Ultra High Definition (UHD)) and then to 100 Mbps for the medium data rate cases (e.g., 4K UHD). We assume that the traffic activity factor for medium, high and super high data rate applications are 2%, 1% and 0.5%, respectively. Furthermore, we assume that the ISD is 200 m. The spectrum efficiency in 5G is supposed to be improved to 7.3 bps/Hz/cell [ITUR13-M2290] via advanced Physical Layer (PHY) and possibly upper layer techniques as also illustrated in [MAG-D11]. It is also proposed in 3GPP that Orthogonal Frequency Division Multiplexing (OFDM)-based waveform will be employed in New Radio (NR) Phase-I [3GPP15-150073] system design (for xMBB and uMTC applications), which requires around 10% guard band. Based on all the identified parameters, we can easily calculate that the required spectrum can be around 3.5 GHz to support a scenario as above.

3.1.2 Coexistence with LTE

The METIS-II 5G RAN is designed for coexistence with LTE (cf. e.g., Radio Resource Management (RRM) schemes or RAN moderation solutions captured in [MII16-D51], and the same spectrum bands can be used by both technologies, which could share resources depending on the specific AI needs. This flexible allocation also contemplates re-farming of spectrum for LTE to the 5G technology.

3.1.3 Deployment in IMT bands

Deployment in at least one identified IMT bands is an operational requirement for the 5G RAN captured in [3GPP16-38913]. 5G may be widely adopted in additional bands such as 3.4-3.8 GHz that may address some IMT-2020 needs and which is discussed in Europe [ECC16-PT1083]. METIS-II addresses this KPI through work in [MII16-D31].

3.1.4 Interworking with 3GPP legacy technologies and 802.11 WLAN

METIS-II 5G RAN is designed to support interworking with 3GPP legacy technologies (cf. Section 2.3.2 in [MII16-D61]) and IEEE 802.11 family of WLANs (cf. Section 6.2 in [MII16-D61]).

3.1.5 Operations above 6 GHz

Operations above 6 GHz are considered for 5G. METIS-II addresses this KPI through spectrum-related activities in [MII16-D31] (e.g. analysis of coexistence with fixed service links operating on mmW, or feasibility studies for outdoor-to-indoor deployment at higher frequencies) as well as through appropriate UP and CP design [MII16-D41] [MII16-D51] [MII16-D61].

3.1.6 Spectrum flexibility and sharing

The ability to adapt to different DL/UL traffic patterns and capacity for paired and unpaired bands is addressed by METIS-II through specific UP design concepts [MII16-D41] and system level solutions (cf. e.g., Sections 4.1.2 and 4.4.3). METIS-II investigates also mechanisms to allow sharing licensed or unlicensed spectrum with other technologies [MII16-D31].

3.1.7 Support of wide range of services

Support of a wide range of services is addressed by METIS-II through numerous technical solutions captured e.g. in Section 4.

3.1.8 Low cost requirements

METIS-II 5G RAN is designed to support low cost devices, as well as low cost operation and maintenance enabled by e.g., mMTC solutions captured in Section 4.2, lean signalling and energy efficiency [MII16-D51] [MII16-D61], spectrum sharing [MII16-D31] and self-organizing networks [MII16-D51].

3.2 Analytical evaluation

3.2.1 Control plane latency

For CP latency calculations, faster UE and BS processing delays for 5G are expected due to improvements in hardware processing delays and reduced sub-frame durations for 5G. In [3GPP16-165538] reduction of processing delay up to a factor of 4 compared to LTE-A is given and this assumption is used in calculations below. Additionally, for calculation of CP latency a 5G sub-frame of 0.25 ms is selected.

For transition between RRC Connected Inactive state to RRC Connected state (cf. Section 3.4.1 in [MII16-D61]) the CP latency calculation steps are as presented in Table 3-1.

Table 3-1. Evaluation 5G CP latency for transition from RRC Connected Inactive state to RRC Connected state.

Step	Description	Component	5G latency
0	UE wakeup time		Implementation dependent and neglected in further calculation 0 ms
1	DL scanning and synchronization + broadcast channel (BCH) acquisition		UE in RRC Connected Inactive state keeps listening to BCH so delays related to DL scanning and broadcast channel acquisition are neglected in further calculations 0 ms
2	Random access (RA) procedure	Average delay due to Random Access Channel (RACH) scheduling period	5G sub-frame of 0.25 ms results in average delay of RACH scheduling period, preamble transmission, detection and RA response equal to 0.125, 0.25 and 0.75 ms respectively. Assuming faster UE processing, delay of the last component of this step is assumed to be to 1.25 ms 2.375 ms
		RACH Preamble	
		Preamble detection and transmission of RA response	
		UE processing delay (decoding of scheduling grant, timing alignment and identifier assignment + encoding of RRC CONNECTION RESUME REQUEST)	
3	UL synchronization		After RA procedures UL synchronization is achieved 0 ms
4	Capability negotiation + HARQ retransmission probability	n.a.	Context information on UE capabilities is available at the serving BS (assuming that UE position is known to 5G RAN at the cell level, cf. Section 4.5.2 in [MII16-D61]) 0 ms

5	Authorization and authentication/ key exchange + HARQ retransmission probability	n.a.	Authorization and authentication keys are available at the serving BS (assuming that UE position is known to 5G RAN at the cell level, cf. Section 4.5.2 in [MII16-D61]) 0 ms
6	Registration with the BS + HARQ retransmission probability	n.a.	Context information on UE capabilities is available at the serving BS (assuming that UE position is known to 5G RAN at the cell level, cf. Section 4.5.2 in [MII16-D61]) 0 ms
7	RRC connection establishment/ resume + HARQ retransmission probability	Transmission of RRC CONNECTION RESUME REQUEST	Assuming 0.25 ms sub-frame for transmission of RRC CONNECTION RESUME REQUEST, RRC CONNECTION RESUME and acknowledgement, faster processing in BS and UE (1 ms and 3 ms, respectively) 4.75 ms
		Processing delay in BS (L2 and RRC)	
		Transmission of RRC CONNECTION RESUME to UE with e.g. UE ID	
		Processing delay in the UE (L2 and RRC)	
		Transmission of RRC CONNECTION RESUME acknowledgement to BS	
Total delay			7.125 ms

Based on calculations in Table 3-1 for transition from RRC Connected Inactive to RRC Connected, CP latency as short as 7.125 ms is expected for 5G. However, such performance can be only achieved when UEs are stationary or if mechanisms such as RAN Based Paging (cf. [MII16-D61]) are in place so the context information is available at the BS.

Additional considerations for CP latency calculations can be found in Annex B.1.

It should be noted that further reduction of CP latency for 5G can be obtained if e.g., sub-frame duration of 0.125 ms is used, as proposed for several physical layer numerologies in [MII16-D41]. In addition, reduction of CP delay due to improvements in UE and BS processing capabilities is

more likely for RRC Connected Inactive operation due to lightweight nature of signalling for this state.

3.2.2 User plane latency

Table 3-2 provides necessary steps for calculations of UP latency. Evaluation of Time Division Duplexing (TDD) mode is chosen as it is more challenging. 5G offers reduction of processing time by a factor of 4, as explained in Section 3.2.1. LTE-A values from 3GPP evaluation of TDD DL with optimal slot configuration (cf. UL/DL configuration #2 from [3GPP15-36912]) are used as a baseline. For 5G TDD a sub-frame duration of 0.125 ms is assumed as the shortest value for several physical layer numerologies proposed in [MII16-D41].

Table 3-2. Evaluation of 5G UP latency.

Step	Description	5G latency
0	Transmitter processing delay (BS)	4-time reduction comparing to LTE-A [3GPP15-36912] 0.25 ms
1	Frame alignment	In 5G more dynamic UL/DL configuration, compared to LTE-A will be used [MET14-D23]. If all sub-frames are configured for a given transmission direction, delay of this step is 0 ms
2	Synchronization	0 ms (in D2D communications, the user terminal may need some time for synchronization, though solutions proposed in [MII16-D41] for asynchronous transmission, reduce delay of this step for D2D transmission down to 0 as well)
3	Number of TTIs used for data packet transmission (unloaded condition is assumed)	1 TTI 0.125 ms
4	HARQ retransmission (assuming 10% HARQ probability)	$0.1 * 0.125 \text{ ms}$ 0.013 ms
5	Receiver processing delay (UE)	4-time reduction comparing to LTE-A [3GPP15-36912] 0.375 ms
	Total delay	0.763 ms

UP latency calculation presented in Table 3-2 indicates that UP latency can be reduced from 5.18 ms in LTE-A (optimal TDD slot configuration in DL [3GPP15-36912]) down to 0.763 ms for 5G. Further reduction of 5G UP latencies cannot be precluded as UE and BS processing delays for 5G could be even more evident for UP delays (for CP delay processing of signalling messages is done up to RRC level, while for UP delay it is done up to MAC level).

3.2.3 mMTC device energy consumption improvement

To compare LTE-A performance with 5G, mMTC devices are assumed to be equipped with a battery having energy capacity of 5 Wh (or 18 kWh) [MII16-D11]. It is assumed that UEs synchronize to the network before initial access. After synchronization, depending on the availability of data for transmission, mMTC devices either keep receive (RX) chains to read system information, read paging information or additionally turn on transmit (TX) chains to upload data to serving BS. Payload (125 B) is transmitted over 1 ms (in line with e.g. maximum transport block size for UL transmission for Narrow Band (NB)-IoT [3GPP16-36213]). Data upload is hindered with 10% retransmission probability.

It should be noted that some modifications to the calculation below can be caused by, e.g., semi-persistent scheduling, relaxation of synchronization requirements, binding data transmission with RACH request, etc. No tracking area updates are considered (such behaviour can be enforced by setting T3412 timer [3GPP16-24301] to 0 starting from 3GPP Rel 9), but it is assumed that device needs to change from energy efficient state to RRC Connected, before uploading the data.

Table 3-3. Duration and instantaneous power consumption levels used for calculations of mMTC device energy consumption improvements.

	Power consumption [mW]		Duration [ms]	
	LTE-A	NB-IoT, 5G	LTE-A, NB-IoT	5G
Data transmission + 10% HARQ (TX/RX on)	300	150	1.1	1.1
CP establishment (TX/RX on)	200	100	50	7.125
Synchronization (RX on)	100	50	15	7.5
Listening for sys. information and paging (RX on)	100	50	10	5

Calculations were done for sporadic (4 per day) and frequent (1 per 10.24 s) transmission periodicity. For less frequent transmission periods, discontinuous reception (DRX) cycles of 2.56 s are assumed for LTE-A, 10485.76 s (~3 hours) for NB-IoT [3GPP16-36304]. Extension of DRX cycle to 6 hours is assumed for 5G. Synchronization is performed after every DRX cycle. Energy efficient state is RRC IDLE for LTE-A and NB-IoT and RRC Connected Inactive for 5G (cf. Section 3.2.1). In addition to values captured in Table 3-3, power consumption in sleep mode and deep sleep mode is equal to 0.001 mW and 0.00002 mW, respectively [RVX+16], [R2-132394].

Power consumption for NB-IoT and 5G was halved comparing to LTE-A due to narrowband operations. Deep sleep mode is introduced only for NB-IoT and 5G. For 4G solutions duration of synchronization is based on synchronization signal periodicity (10 ms) and averaged time misalignment after DRX cycle (5 ms). The final value of 15 ms is close to empirical values reported e.g., in [LNS+14]. For 5G this value is halved to account for potential improvement in configurability and duration of synchronization signals (cf. [R1-1700294], [R1-1700329]). System information reading duration for 4G is linked with the structure of Physical Broadcast Channel. To account for lean control plane design improvement in system information readouts in 5G (cf. Section 4.2 in [MII16-D61], [R2-1700309]) corresponding duration is halved comparing to 4G.

Table 3-4. Assessment of overall power consumption of mMTC devices for frequent and sporadic data transmissions.

Daily summary	Rel 10, frequent	Rel 10, sporadic	NB-IoT, frequent	NB-IoT, sporadic	5G, frequent	5G, sporadic
# data transmission per day	8437	4	8437	4	8437	4
Time for data transmission [s]	9.28	0.004	9.28	0.004	9.28	0.004
Time for CP establishment [s]	421.85	0.2	421.85	0.2	60.11	0.028
Time for listening to system information and paging [s]	337.5	337.5	84.37	0.08	42.185	0.02
Time for synchronization [s]	506.25	506.25	126.56	0.12	63.28	0.03
Time in sleep mode [s]	85125.1	85556	0	0	0	0
Time in deep sleep [s]	n.a.	n.a.	85758	86399	86225	86399
Overall power consumption [W]	256.68	169.97	55.84	1.76	17.56	1.73

Based on calculations provided in Table 3-4 and assuming average battery energy storage of 5 Wh, MTC device would last without battery exchange between 70 and 106 days for Rel 10 LTE-A, between 322 days and 28 years for NB-IoT, and between 2.8 and 28.5 years for 5G, depending on the data transmission frequencies. This is depicted in Figure 3-1.

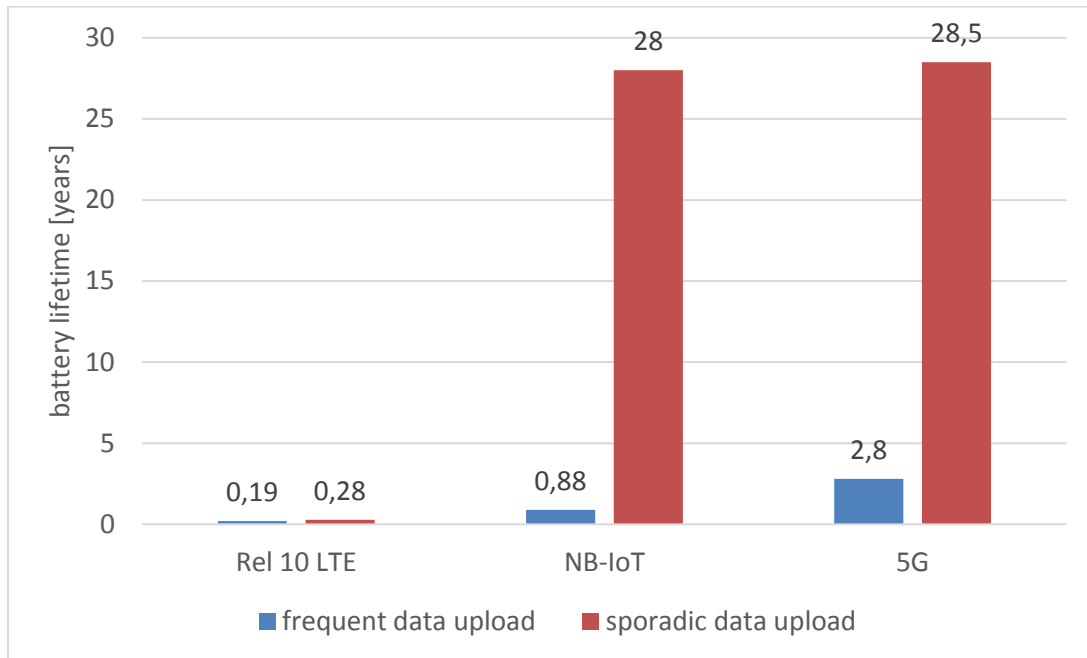


Figure 3-1. Lifetime of a 5 Wh battery of mMTC device for different data upload periodicity and for different technologies.

It should be noted that these values can be further impacted by additional power consumptions caused by e.g. wake up or down phases experienced by device exploiting DRX operations, and battery leakage. However, these aspects are heavily implementation dependent and are beyond the scope of the system level evaluation captured in this document.

3.2.4 Mobility interruption time

Mobility interruption time can be reduced to 0 through multi-connectivity concepts, giving that make-before-break approach is used (cf. [MII16-D51]). Note that in 5G system, handover between adjacent BS may no longer exist due to solutions based on multi-connectivity and CP / UP decoupling.

3.2.5 Peak data rate

The analysis assumes a 100 MHz component carrier bandwidth channel in TDD mode, but with flexible UL/DL allocation which allows a full allocation of bandwidth in the peak data rate analysis. Our exemplary 5G RAN³ assumes two simultaneously used bands, one centred in the 3.5 GHz with 100 MHz allocated per operator (one single component carrier), and another at 28 GHz with 500 MHz available for the operator (five aggregated component carriers). At 3.5 GHz 16 spatial parallel flows are transmitted, whereas at 28 GHz only 8 spatial flows are possible, with a massive

³ This computation is based on a given exemplary METIS-II system with realistic parameters, but the final settings of an AIV may deviate.



MIMO 256x256 antenna system. A maximum of 64 QAM modulation is assumed due to the huge data rate at hand. The exemplary 5G transmission has the following characteristics:

- 2048 FFT is assumed for each component carrier.
- Subcarrier spacing is set to 60 kHz.
- 100 MHz bandwidth per component carrier encompasses 1650 subcarriers and thus 110 Resource Blocks (RBs) in frequency domain, each with 15 subcarriers. In fact, these 1650 carriers cover only 99 MHz with remaining 1 MHz used as a guard band for the purpose of calculation.
- Cyclic prefix is set to 1.17 μ s, resulting in an OFDM symbol duration of 17.84 μ s.
- A total of 56064 OFDM symbols are transmitted per second, reserving 10% of symbols for signalling purposes and 20% of subcarriers for channel reference signals.
- The modulation is assumed to be 64 QAM (6 bits per symbol).
- Since error-free assumptions can be assumed, channel coding rate is equal to 1.
- 16 layers spatial multiplexing is assumed for below 6 GHz bands and 8 for above 6 GHz bands.
- Peak data rate per component carrier results in $56064 \cdot 1650 \cdot (0.7)^6 \cdot 16 = 6216376320$ bps, i.e. about 6.2 Gbps for below 6 GHz band, and in $56064 \cdot 1650 \cdot (0.7)^6 \cdot 8 = 3108188160$ bps, i.e. about 3.1 Gbps for above 6 GHz band.

In the aggregation case for the DL, 5 component carriers (500 MHz) at above 6 GHz and 1 at below 6 GHz (100 MHz) will result in a total peak data rate of 21.7 Gbps. In the UL, 2 component carriers at 28 GHz and 1 component carrier at 3.5 GHz will result in a total peak data rate of 12.4 Gbps. The ratio of 3 to 6 component carriers between UL and DL is due to the power limitations existing in handheld devices.

Finally, it is worth recalling that this peak calculation is just an example of the procedure, with an arbitrary but realistic selection of the AIV characteristics

3.3 Evaluation through simulation

This subsection covers performance evaluation via simulation of a hypothetical 5G system along the METIS-II UCs. The detailed specification of 5G is not yet known, but expected advancements are taken into account. However, this analysis doesn't focus explicitly on any TeC proposed in Section 4.

3.3.1 UC1 – Dense Urban Information Society

In UC1, a large number of resources in terms of bandwidth, sites and antennas is used to provide consistent and good user experience. On one hand, urban macro layer provides wide network coverage and cater for the edge users' experience. This is enabled using operations on lower carrier frequencies and high spectral efficiency over large bandwidth. Wide coverage of macro

BS also benefits the mobility performance for users on the move. On the other hand, small cell BSs boost available capacity over specific hotspot areas, as much wider bandwidth can be exploited at higher frequency range. Therefore, in order to evaluate the performance of UC1, site deployments, antenna configurations, channel and bandwidth extensions should be explicitly modelled. Key evaluation parameters are captured in Table 3-5.

Table 3-5. Evaluation parameters for UC1.

Deployment scenario	Urban macro layer	HetNet outdoor small cell layer
BS antenna height	25 m, above rooftop	10 m on the lamppost / below the rooftop
Number of BS antenna elements (TX/RX)	32/32	32/32
Number of BS antenna ports	8	8
BS antenna gain	8 dBi (per element)	5 dBi (per element)
Maximum BS TX power	49 dBm per band (in 20 MHz)	23 dBm per band (in 80 MHz)
Carrier centre frequency	3.5 GHz	30 GHz
Carrier bandwidth	20 MHz	80 MHz
System bandwidth	200 MHz	800 MHz
ISD	200 m	> 20 m
UE deployment	10 UEs per macro cell	5 UEs per small cell
UE height	cf. Annex A.3.2	
UE antenna pattern	2D omni-directional	
Number of UE antenna elements (TX/RX)	4/4	4/4
Number of UE antenna ports (TX/RX)	4/4	4/4
UE antenna gain	0 dBi	

UE speed for fast fading calculation	3 km/h for indoor and 30 km/h for outdoor	
Min 2D UE-BS distance	35 m	5 m
Indoor / Outdoor ratio	80/20	
Channel model	3D UMa [3GPP15-36873]	High frequency UMi [3GPP16-38900]
Traffic model	File Transfer Protocol (FTP) Model 3 [3GPP13-36872] with packet size 3.5 MB	

Figure 3-2 shows UC1 network performance against overall traffic load being a function of packet inter-arrival time for individual UEs. It is shown that as the packet arrival rate increases, the traffic volume density grows accordingly until the network is fully loaded. Based on considered evaluation assumptions, the maximal supported DL traffic volume density of UC1 is about 560 Gbps/km², which is lower than required 750 Gbps/km² assumed in [MII16-D11]. It is, however, expected that if more resources are available, e.g., site, bandwidth, antenna, power, or more advanced transmission technologies are implemented, the target traffic volume density could be achieved. To exemplify, BW comparing for dense urban deployments can be as high as 1 GHz. Considering 100 MHz used for evaluation, improvement by a factor of 10 (at least, as pooling and multiplexing gains are also expected) could be applied for achieved data rates and traffic volumes densities.

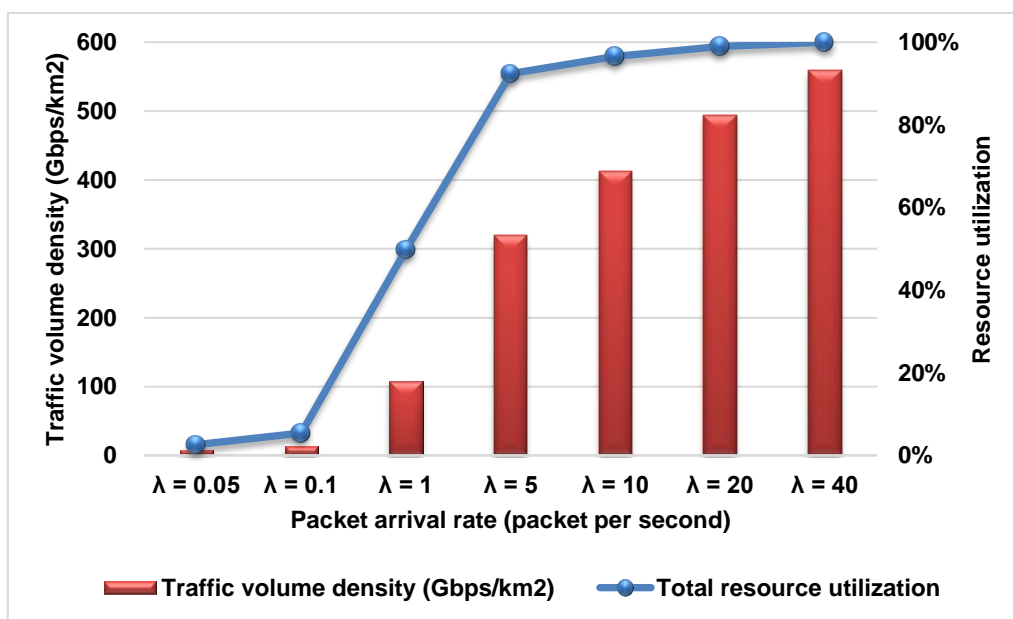


Figure 3-2. Traffic volume density and radio resource utilization vs. packet arrival rate (λ) for UC1.

From Figure 3-3 it can be observed that a high user experienced data rate is achievable in UC1 especially at low load state, in which interference level is also low. As more traffic is generated, the resource utilization becomes higher and stronger co-channel interference is expected. Note that under current assumption, the required DL user experienced data rate, e.g., 300 Mbps, could be achieved when load level is below 3%. It is expected that further enhancement of the network (e.g. more advanced antenna systems)could make the target achieved at higher load level.

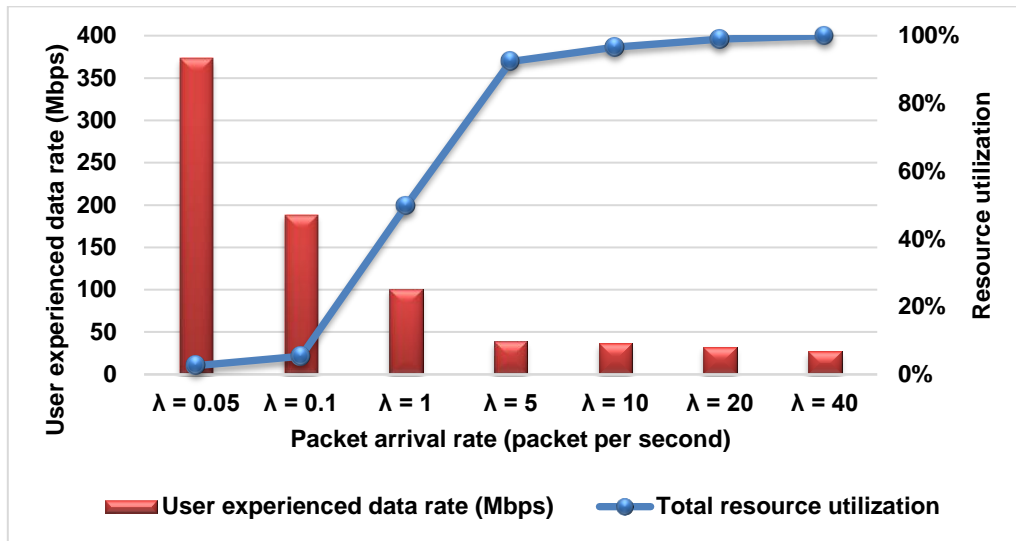


Figure 3-3. Experienced user data rate and radio resource utilization vs. packet arrival rate for UC1.

RAN energy efficiency is one of key KPIs foreseen for 5G. Therefore, as a large number of sites, bandwidth allocations and antennas are deployed to support the high-performance requirement in terms of data rates, power consumption should also be taken into account in order to achieve sustainable development in terms of cost and environmental impact. From the Figure 3-4 it can be observed that higher RAN energy efficiency performance is expected for higher traffic load levels, as more traffic can be delivered while the ratio of load-independent static power consumption could be reduced accordingly. In addition, it is also shown that advanced sleeping strategy can achieve significant performance gain especially in low load level scenarios.

In Figure 3-5, further comparison is given for the RAN energy efficiency performance with baseline, i.e., UMa scenario defined in IMT-A system. Note that most assumptions were defined in [ITUR08-M2135] for IMT-A/4G, except the traffic model parameters and user densities. In order to simplify the comparison, same user density number per macro sector in IMT-A/4G (ISD = 500 m) and 5G (ISD = 200 m) is assumed while the traffic amount per sector of IMT-A/4G is only 1/1000 of 5G in UC1 (i.e., packet size is 1/100 while packet arrival rate is 1/10 for IMT-A/4G compared with 5G). It is shown that when the load level is low, high performance gain can be achieved, and this gain increases as more advanced sleeping strategy is implemented. Even when the system load level is very high, e.g., fully loaded, the energy efficiency performance gain is noticeable, which is mainly due to the introduction of small cells and more advanced and energy efficient hardware.

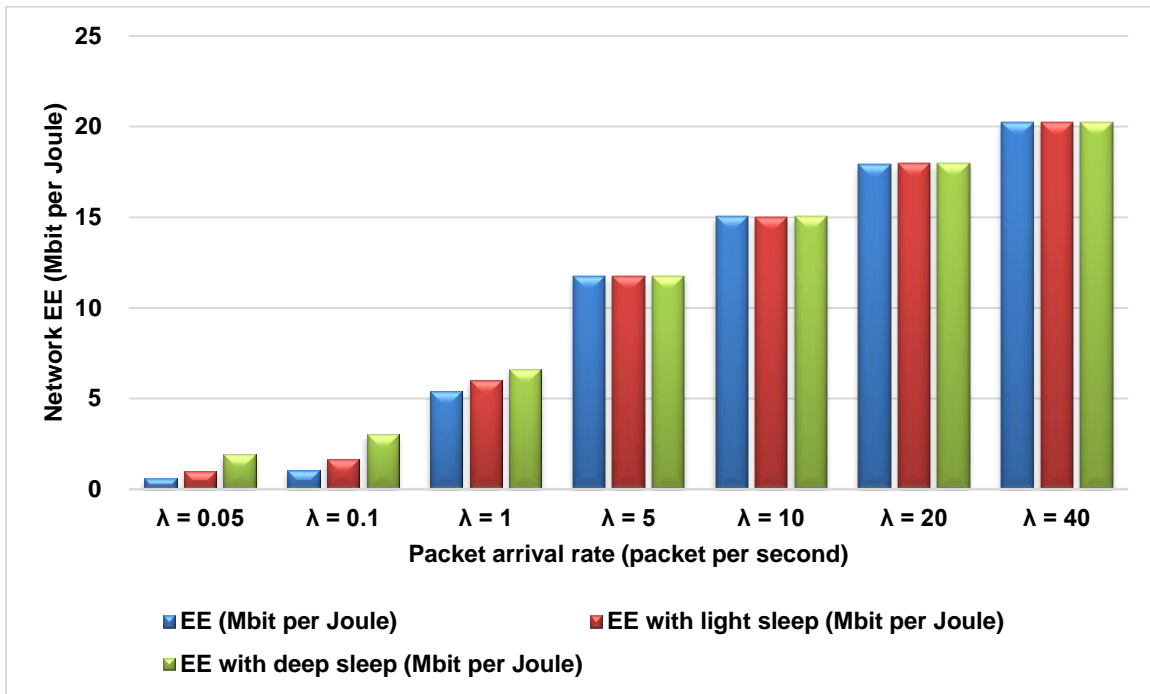


Figure 3-4. RAN energy efficiency (EE) performance of UC1.

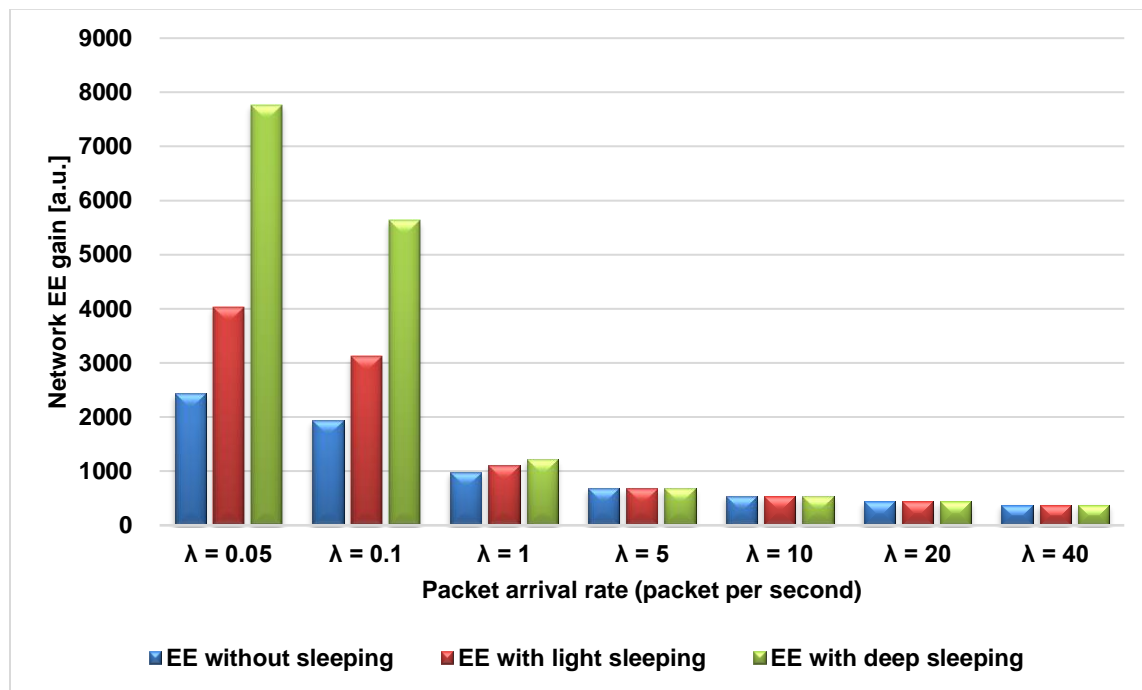


Figure 3-5. RAN energy efficiency performance gain of 5G UC1 over UMa of IMT-A/4G.

More details on RAN energy evaluation methodology can be found in Annex A.1.1.

3.3.2 UC2 – Virtual Reality Office

The main goal of UC2 is to evaluate 5G capability in providing xMBB services indoors. Edge requirements of this UC are dictated by the fact that in such scenarios end users expect experience comparable to the one achieved using wired solutions. Additionally, limited area of the indoor office pushes traffic volume density to extreme.

Comparing to LTE-A, the main technical enabler to achieve these goals is the exploitation of high frequency bands and massive antenna systems. Table 3-6 provides the main parameters for system level simulations considered for evaluation of UC2.

Table 3-6. Evaluation parameters for UC2.

Deployment scenario	Virtual reality office
BS antenna height	3 m
Number of BS antenna elements (TX/RX)	64/64
Number of BS antenna ports	2
BS antenna gain	5 dBi (per element)
BS antenna pattern	[3GPP16-165850] alternative 3
Maximum BS TX power	23 dBm per band (in 80 MHz)
Carrier centre frequency	30 and 70 GHz
Carrier bandwidth	40 MHz
ISD	20 m
UE deployment	10 UEs per cell
UE height	1 m
UE antenna pattern	3D omni-directional
Number of UE antenna elements (TX/RX)	32/32
UE antenna gain	5 dBi
UE speed for fast fading calculation	3 km/h
Minimum 2D UE-BS distance	0 m

Indoor / Outdoor UE ratio	100/0
Channel model	5G InH [3GPP16-38900]
Traffic model	FTP Model 3 [3GPP13-36872] with packet size 3.5 MB

For complexity reasons, UC2 was evaluated using 40 MHz bandwidth, but for proper assessment of UC2 KPIs we need to take into account the assumption of availability of 1 GHz bandwidth. However, considering bursty traffic, performance results should not be simply multiplied by the bandwidth ratio (1000 MHz/40 MHz = 25) as additional gains related to statistical multiplexing imply a higher impact factor. Factor of 25 is nevertheless used, but should be treated as a minimum improvement, lower than what could be achieved if entire 1 GHz band was simulated.

Based on the results captured in Figure 3-6, supported traffic volume density reaches 593 Gbps/km² equivalent to 0.59 Mbps/m² with our simulations at the level of resource consumption close to 100%. Taking into account the bandwidth scaling explained above, it can reach at least ~15 Mbps/m².

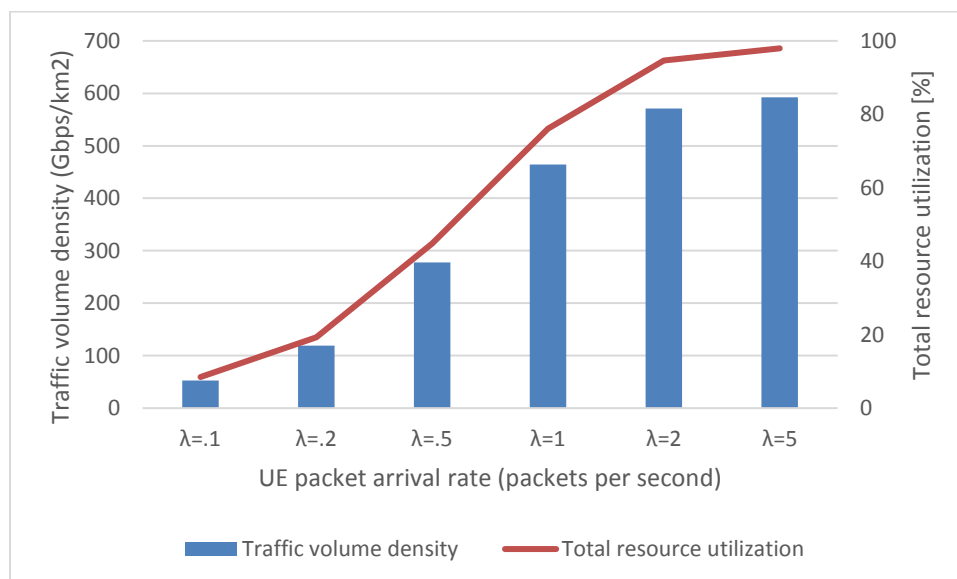


Figure 3-6. Traffic volume density and resource usage in UC2.

As depicted in Figure 3-7 experienced user data rates (5%-ile) for 50% resource consumption level (one 3.5 MB/ 14 Mbps packet generated for each user every two seconds) are as high as 48.1 Mbps (or at least 1.21 Gbps after bandwidth scaling). For 20% of the entire UE populations, transfer speed of 314 Mbps is achievable (or at least 7.85 Gbps after bandwidth scaling).

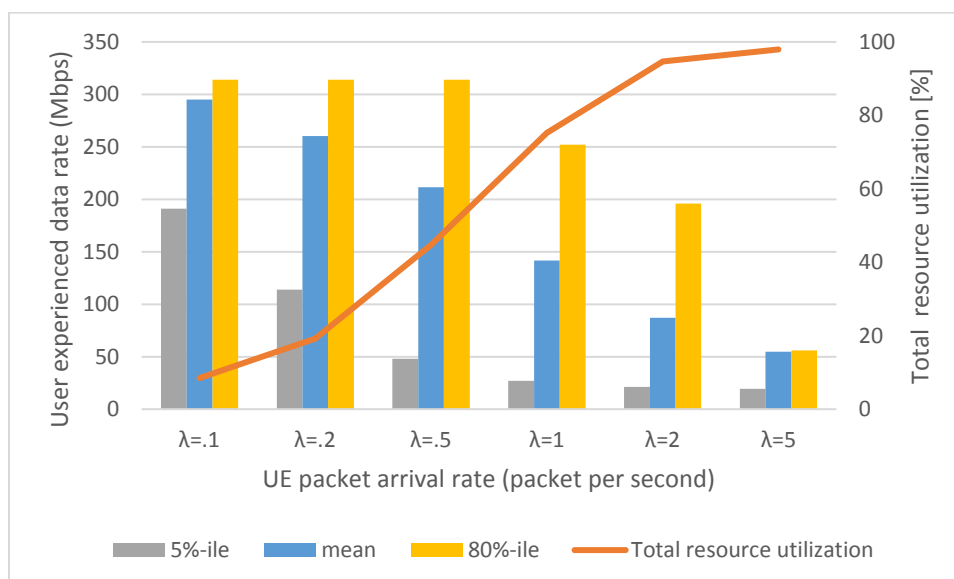


Figure 3-7. Experienced downlink user data rates in UC2.

Performance evaluation results for UC2 at carrier frequency of 30 GHz are given in Annex B.2.

3.3.3 UC3 – Broadband Access Everywhere

The focus of this section is to present the system level simulation results including the RAN energy performance for the UC3 in the rural macro deployment scenario (RMA). The simulation parameters used for evaluation are shown in Table 3-7. Three deployment options are evaluated: 800 MHz carrier frequency with and without beamforming capabilities and 3.5 GHz carrier frequency with larger antennas and beamforming capabilities to assess the performance with respect to experienced user throughput and RAN energy consumption. The case with 800 MHz without beamforming is assumed to be the baseline case for comparison.

Table 3-7. Evaluation parameters for UC3.

Deployment option	RMa without beamforming	RMa with beamforming	RMa for 3.5 GHz
BS antenna height [m]	35	35	35
BS antenna gain [dBi]	17	17	17
No. of BS antenna elements (TX/RX)	1/1	32/32	256/256
BS TX power [dBm]	49	49	49
BS noise figure [dB]	5	5	5

Carrier center frequency [MHz]	800	800	3500
Carrier bandwidth [MHz]	30	30	200
ISD [m]	1732	1732	1732
UE noise figure [dB]	9	9	9
UE antenna gain [dBi]	0	0	0
UE TX power [dBm]	24	24	23
Indoor / Outdoor UE ratio	0/100	0/100	0/100

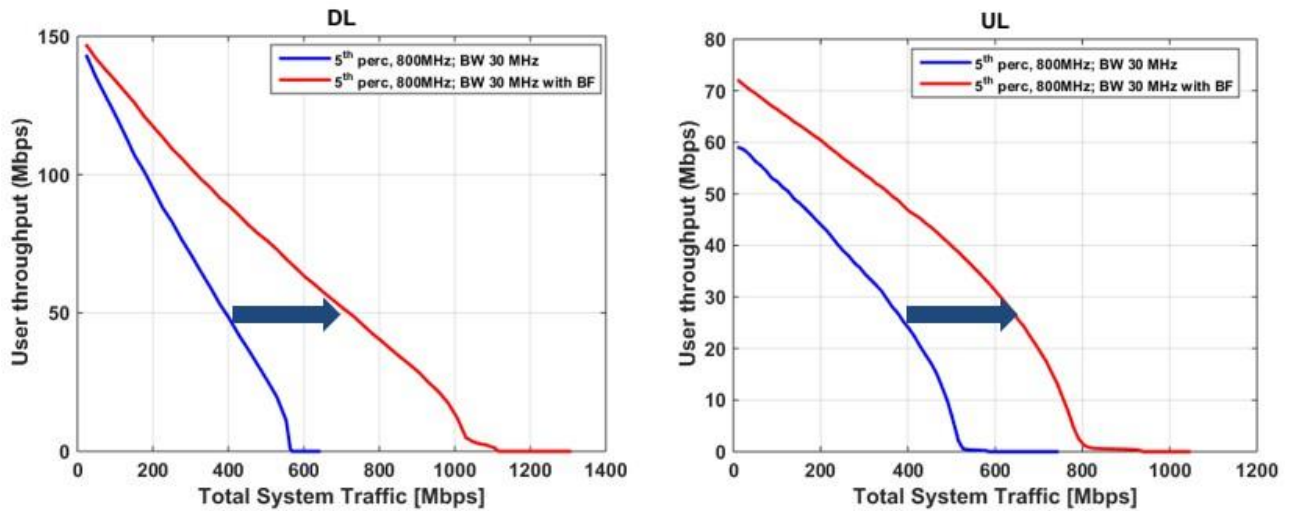


Figure 3-8. DL and UL 5%-ile user throughput vs. total system traffic.

Figure 3-8 shows the 5%-ile DL and UL user throughput for two deployments operating at 800 MHz with and without beamforming capabilities as a function of total system throughput for the DL and UL separately. A significant improvement in the 5%-ile DL and UL user throughput can be observed if more antenna elements are used at the base station side enabling beamforming capabilities. As depicted in Figure 3-8, the capacity is increased by a factor of almost 2 meaning that the network can handle two times more traffic while maintaining the minimum experienced user throughput requirement of UC3 (50 Mbps for the DL and 25 Mbps for the UL). Similarly, Figure 3-9 shows the 5%-ile DL and UL user throughput for all deployment options including 3.5 GHz, where it can be observed that the capacity is increased by almost a factor of 20 when compared to the 800 MHz case without beamforming case. Therefore, despite higher

propagation loss, 3.5 GHz can be a good candidate in rural areas to extend the cell range using the benefit of beamforming with bigger antennas and larger bandwidth.

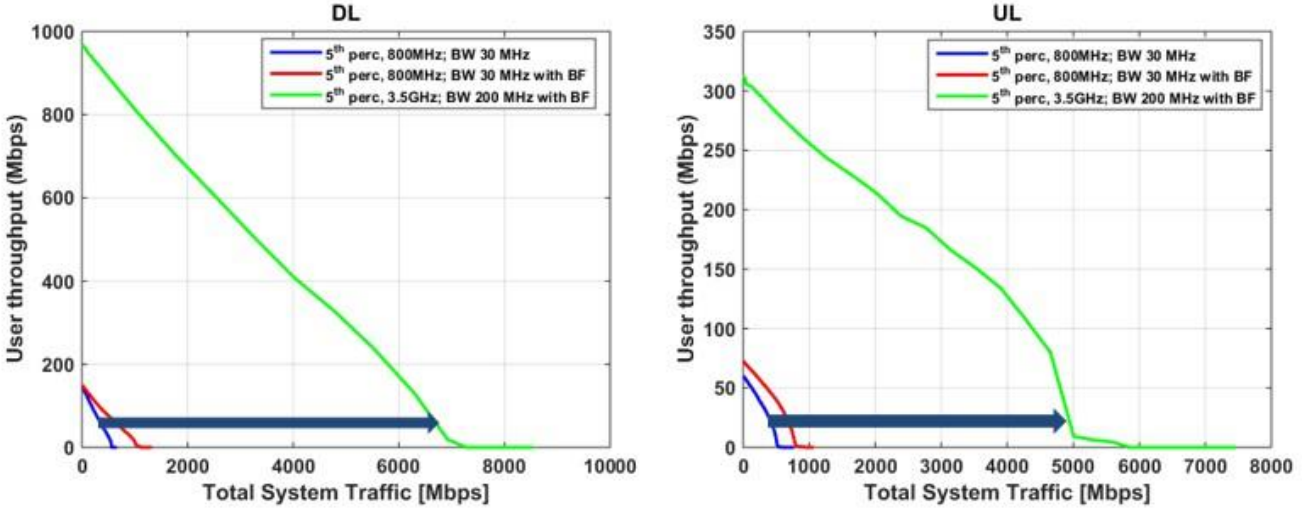


Figure 3-9. DL and UL 5%-ile user throughput vs. total system traffic.

The energy performance is defined as the daily averaged area power consumption. Therefore, for a given network with N_{BS} BSs covering A km², energy performance can be written as:

$$EP = \frac{1}{24} \sum_{t=1}^{24} \sum_{i=1}^{N_{BS}} \left[(P_{active}) \eta_i^t + P_{sleep} (1 - \eta_i^t) \right] / A$$

Here P_{active} and P_{sleep} are the power consumption of each BS when it is transmitting and when it is in sleep mode, respectively. Note that the power consumption parameter settings for the equation will be different for the case with and without beamforming capabilities. On the other hand, η_i^t represents the resource utilization of the BS i during given hour t . Here, the resource utilization is defined as the fraction of time-frequency resources that are scheduled for data transmission in a given cell in a given time frame. It also represents the probability that BS i is transmitting.

In this study, the daily average power consumption is calculated by identifying the resource utilization of each BS in the network throughout the day using the daily traffic fluctuation pattern as in Annex A.1.1 (cf. Figure A-1) and a given peak data traffic demand in the cell (Mbps/cell).

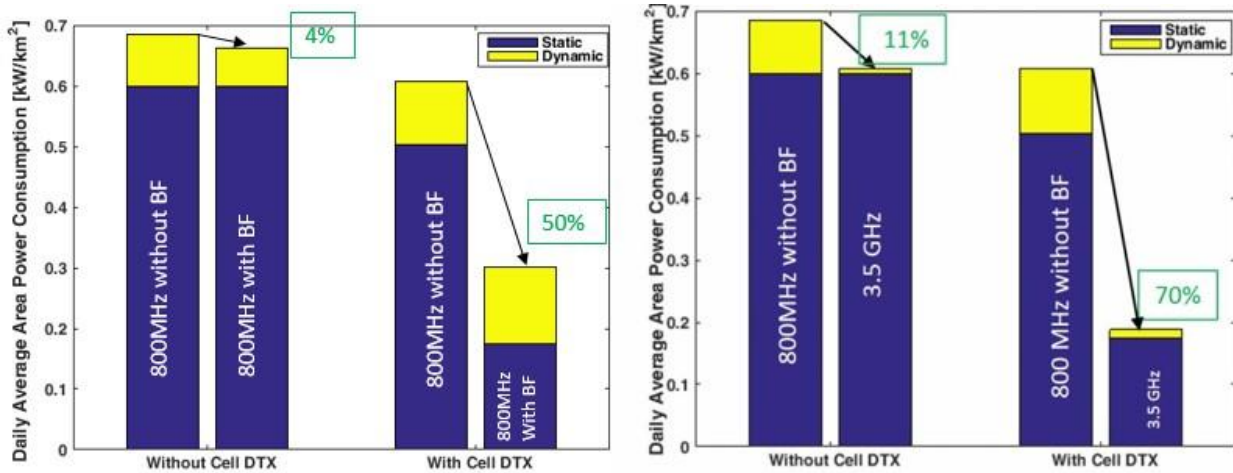


Figure 3-10. Energy performance comparison of UC3 with and without cell DTX for static and dynamic power consumption for 800 MHz with vs. without beamforming (left) and baseline scenario vs 3.5 GHz (right) (cf. [MII16-D21]).

Figure 3-10 illustrates the daily average area power consumption (in kW/km²) based on two components: i) static (power consumed even when there is no traffic), and ii) dynamic (power consumed based on the served traffic) and for two cases i) BSs don't have cell DTX capability and a BS cannot be put into sleep mode when there is no traffic; ii) BSs have cell DTX capability and power consumption of a BS will be reduced when there is no traffic in the network. In this evaluation, a rush hour (i.e., high traffic of 26 Mbps/cell) is considered when the average radio resource utilization in a cell is around 60% for the baseline case i.e. 800 MHz without beamforming. In order to make a fair comparison, the same peak traffic level is considered for evaluating the daily average area power consumption for all the deployment options considered for UC3. In considered deployments it is observed that the static power consumption strictly dominates the total power consumption. This highlights the importance of sleep mode solutions in order to reduce the energy consumption in wireless access networks.

When the BSs do not have sleep capability, the daily average power consumptions of UC3 with and without beamforming are very similar. In Figure 3-10 (left) it is observed that dynamic power consumption is slightly lower in deployments with beamforming, despite the fact that during transmission the power consumption of beamforming capable BSs is higher compared to those without this feature, due to the increased number of RF chains. The reason behind this reduction is the fact that the same traffic is served in shorter time, thanks to beamforming capabilities enabling higher data rates. This results in lower cell utilization compared to baseline scenario (i.e., utilization goes down from 60% to 20%) which enables 4% reduction in energy consumption when the BSs do not have DTX capability. On the other hand, if BSs can exploit DTX when there is no transmission, it is observed that UC3 with beamforming consume much less power as the ultra-lean design enables the beamforming capable BSs to exploit longer DTX duration and deeper sleep mode levels. In this case, there is around 50% reduction in a daily average area power consumption. In case of 3.5 GHz deployment scenario, it can be seen in Figure 3-10 (right) that beamforming capable BSs together with cell DTX enables energy saving up to the level of 70%.

The main reason behind this is the fact that in 3.5 GHz deployment scenario the bandwidth and the number of antenna elements are much higher when compared to 800 MHz deployments. The combined effect of these reduces the resource utilization even further down to 2.6% in the same traffic level (26 Mbps/cell). As a result, higher savings are observed in both dynamic and static power consumption. Therefore, it can be concluded that the 3.5 GHz band does not only prove to be a potential candidate band for providing enhanced capacities but also for enable enhanced energy performance in the rural deployment scenarios.

3.3.4 UC4 – Massive Distribution of Sensors and Actuators

Assessment of METIS-II UC4 has been performed based on [MII16-D21] assumptions complemented with settings from 3GPP’s urban coverage for massive connection defined in [3GPP16-38913]. Main evaluation assumptions are captured in Table 3-8. Further information on the evaluated concepts can be found in Annex B.3.

Table 3-8. Simulation parameters for UC4.

Deployment scenarios	Urban macro (7 sites and 3 sectors per site, wrap-around)
BS antenna height	25 m, above rooftop
BS antenna configuration	RX: 8 antenna ports: 4 columns of X-pol elements and 10 X-elements per column, horizontal spacing 10 lambda, vertical spacing 0.5 lambda
BS antenna tilt	4 deg electrical downtilt
BS antenna element gain + connector loss	8 dBi, including 3 dB cable loss
Carrier frequency centre	700 MHz
Carrier bandwidth	20 MHz
UE height	cf. Annex A.3.3
Max UE TX power	23 dBm
UE antenna gain	-4 dBi
UE speed for fast fading calculations	3 km/h



Indoor / Outdoor UE ratio	80/20
Traffic model	Non-full buffer small packet. 840 bits per Small Packet Blocks (SPB), one SPB consists of 7 Physical RBs (PRBs), QPSK modulation, the max. number of data transmission trials per data packet is 4
BS receiver	Minimum mean square error receiver with interference rejection combining. No multi-user detection. No chase combining
UL power control	Open loop power control, $P_0 = -110$ dBm, P_0 increased by +2 dB increments for each transmission retriel (max. TX power is thus -104 dBm), $\alpha = 1.0$ (full pathloss compensation)
Channel estimation	Realistic according to [3GPP14-36866]
Scheduling request	6 PRBs for scheduling request used per TTI, max number of scheduling request trials is 4 One-stage protocol: Ideal detection assumed Two-stage protocols: Explicit and realistic modelling of scheduling request transmission and detection with up to 64 preambles.

In order to measure the number of supported mMTC devices in UC4, the initial access rate, i.e. the average rate of new transmission requests, was set between 1000 requests/s/sector and 11000 requests/s/sector. A KPI of 1% maximum ratio of finally lost transmissions is selected as a cut off value for calculating initial access attempts and the number of supported mMTC devices. It is assumed that a UE can try four times to transmit its small packet. If it receives a final NACK for the last trial it will stop the transmit procedure. For 1% of final NACK rate more than 1500 initial access events/s/sector for *one-stage* access can be supported (cf. Figure 3-11). For *two-stage tagged* approach this number is increased to more than 3000 events/s/sector and for *two-stage pooled* more than 5000 events/s/sector. Considering a sector area of 0.0722 km² (corresponding to 500 m ISD) and assuming an initial request rate of 1/100 s per sensor, the supported density of mMTC devices is more than 2.1 million devices per km² for *one-stage* access. For *two-stage tagged* more than 4.2 million devices per km² can be supported. Finally, for *two-stage pooled* we can support more than 6.9 million devices per km².

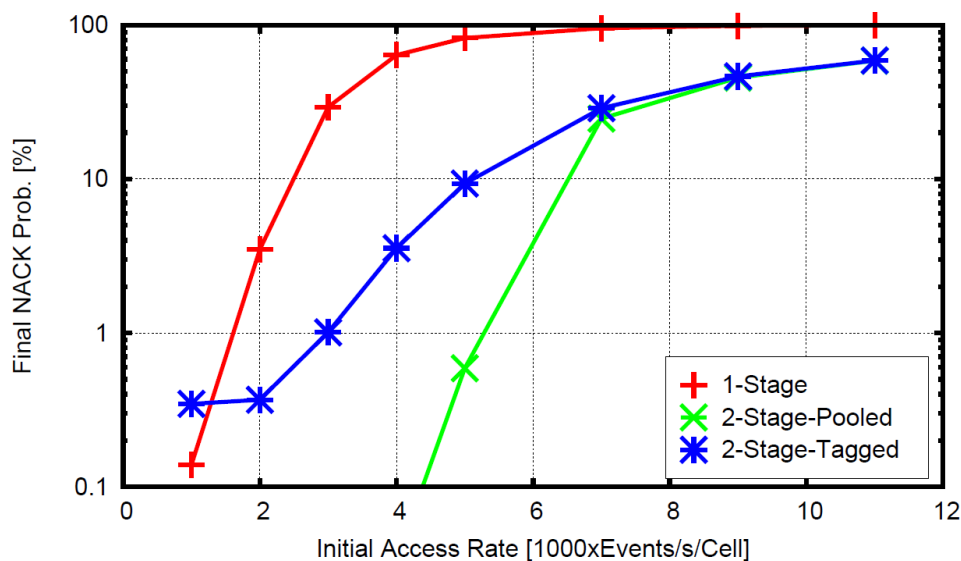


Figure 3-11. Residual failure rate after four failed trials shown over the initial access rate of new requests per sector.

3.3.5 UC5 – Connected Cars

The Connected cars UC completes the set of 5G UCs proposed by METIS-II. This UC addresses the use case families uMTC and xMBB. Concerning uMTC, the focus is on the provision of ultra-reliable data exchange between vehicles and their surroundings to achieve more efficient, safer, and more comfortable journeys. This communication allows the car to avoid accidents, but also traffic jam queues and thus minimizes fuel consumption. Such kind of communication is challenging, as reliability of the transmission can be impacted by the availability of radio resources (possible concentration of a high number of vehicles in a single cell) and high velocity (frequent cell change and challenging transmission conditions caused by the high Doppler shift). With regard to xMBB, the focus is on the support of a real-time remote computing services for highly mobile users, e.g. on-the-way workers as well as leisured people while driving in cars or using public transportation. In this section, the focus is on traffic efficiency and safety, i.e., the support of uMTC family.

The basis for the performance evaluation presented in this section is in [MII16-D21]. Three relevant scenarios are envisioned in [MII16-D21] and used in this assessment: an urban realistic scenario, also known as Madrid Grid scenario, an urban synthetic scenario, that will be referred to as 3GPP Grid in this evaluation, and a Highway scenario. For the sake of completeness, Table 3-9 presents the main parameters of the simulations conducted. Most of the parameters have the same values for the three scenarios. Concerning the density of vehicles, the 3GPP Grid and Highway scenarios present a fixed value, due to the specific UE dropping model in [MII16-D21]. In the Madrid Grid, we have considered a set of densities from 100 to 1000 vehicles/km², 1000 being the maximum vehicle density envisioned for urban environments in [MII16-D21]. The definition of the traffic model is another element of paramount importance. We have used exactly

the traffic model defined in [MII16-D21]. It is worth noting that, at the time of writing, 3GPP has not yet defined the parameters of the traffic model in its evaluation framework [3GPP16-38913]. Note that carrier frequency and bandwidth values are provided for the sidelink, i.e. the direct D2D link between devices.

Table 3-9. Main simulation parameters for UC5.

Attributes	Madrid Grid	3GPP Grid	Highway
Carrier frequency (sidelink)	6 GHz		
Carrier bandwidth (sidelink)	10, 20, 30, 40, 50 and 100 MHz		
UE TX power	23 dBm		
UE antenna gain	3 dBi		
Noise figure	9 dB		
Number of TX antennas	1		
Number of RX antennas	2		
Density of vehicles	100, 250, 500, 750 and 1000 vehicles/km ²	595 vehicles/km ²	10.25 vehicles per lane and km
Speed	60 km/h	60 km/h	140 km/h
Traffic model	Constant bit rate: packets of 1600 bytes, 100 ms periodicity		

The technical solution assessed in this section is based on the use of D2D communication between the vehicles, i.e. only sidelink is used for V2V communication. It is assumed that a dedicated pool of resources of certain bandwidth is available for V2V. The resources of the pool can be allocated in a semi-persistent way to V2V users. The presence of a central controller that aims at minimizing the interference among users is also considered. The central controller modifies the resource allocation to a user whenever this user significantly changes its position. The controller knows the periodicity of the traffic generated by the vehicles to allocate the resources in a semi-persistent manner.

The main KPI in this assessment is the PRR that measures the reliability in the reception of transmitted packets for different ranges of distance with respect to the transmitter of the packet.

The latency requirement set by [MII16-D11] for UC5 traffic safety packets is 5 ms to be achieved with reliability of 99.999%. This reliability should be valid within the specified communication range that is 50 m in urban scenarios, 500 m in rural scenarios and 1 km in highway scenarios according to [MII16-D11].

PRR curves for Madrid Grid with different bandwidths and vehicle densities are shown from Figure 3-12 to Figure 3-14. The PRR curves have been obtained with a granularity of 5 m., i.e., each point represents the PRR for a range of distances $[x-5, x]$ being x the value of the abscissa. Figure 3-12 shows the PRR when the system bandwidth is 10 MHz. It can be seen how the performance degrades as the density increases, due to the higher level of interference. A PRR higher than 99.999% has been achieved with 10 MHz for a range of 50 m and the lower user density (100 vehicles/km²), although those requirements have not been achieved for higher densities. Nevertheless, for the following user density considered, i.e. 250 vehicles/km², we have reached the 99.999% reliability for a shorter range of 45 m.

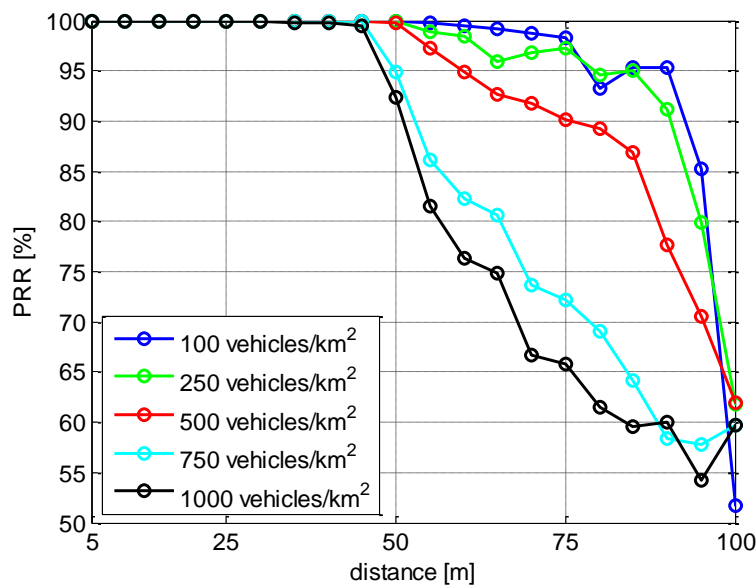


Figure 3-12. PRR in Madrid Grid with 10 MHz bandwidth for different vehicle densities.

The same behaviour is observed for higher densities for which we have achieved the 99.999% reliability level for 45 m, but just 99.9% for 50 m. To get these reliability levels, we have used 20 MHz for densities of 500 and 750 vehicles/km², and 30 MHz for 1000 vehicles/km². Figure 3-13 presents the PRR curves for a bandwidth of 20 MHz, where a clear improvement with regard to the 10 MHz bandwidth can be observed. The improvement is not so clear for the higher bandwidths considered, as can be seen in Figure 3-14 that shows the PRR curves for a density of 1000 vehicles/km² and different system bandwidths. In this figure, the curves for bandwidths between 20 and 100 MHz are overlapping. Nevertheless, some improvement is obtained concerning the coverage range supported with 99.999% reliability. For a bandwidth of 30 MHz the range achieved is 45 m, but for 20 MHz the range is 5 m. It is worth to note that the high

variation of some curves, that show local increases of PRR with the distance, which is due to the specific geometry of the scenario and the distribution of users that may improve/worsen the reception of packets for specific distances. The main conclusion of this part of the assessment is that the 5G requirements are not fulfilled with the system considered although the system performance is very close to that objective. Further research is needed to improve the achieved performance.

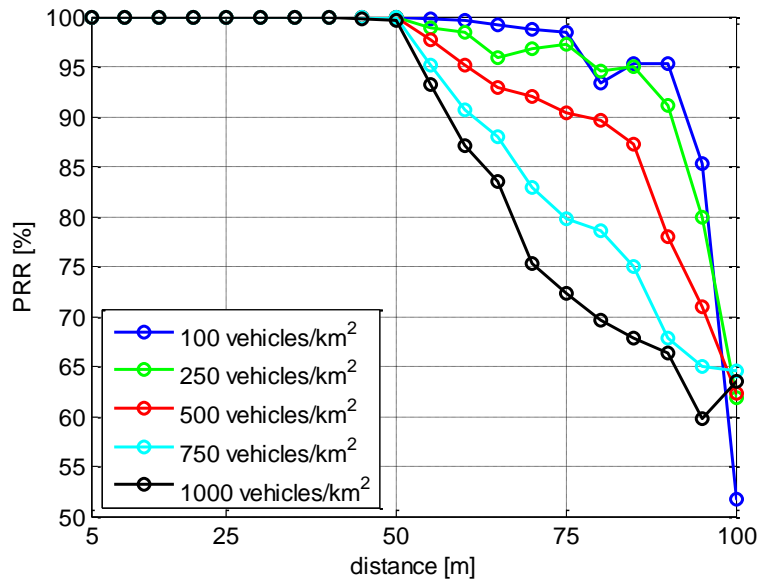


Figure 3-13. PRR in Madrid Grid with 20 MHz bandwidth for different vehicle densities.

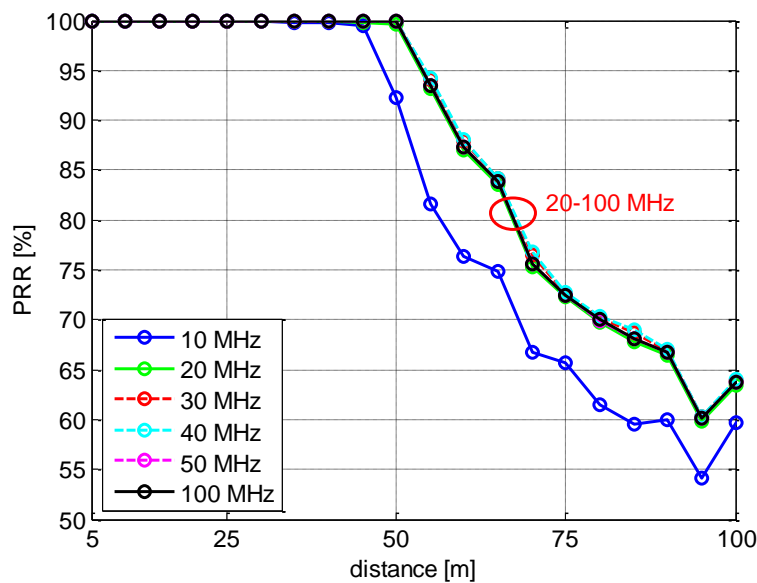


Figure 3-14. PRR in Madrid Grid with 1000 vehicles/km²

The PRR curves for 3GPP Grid are shown in Figure 3-15. The results indicate that the evaluated system is not able to fulfil the reliability requirements with the system bandwidths considered. In fact, even with 100 MHz bandwidth, the PRR for a distance of 50 m is approximately 99%. A 99.999% PRR has been achieved for a shorter distance of 45 m. As in the previous scenario, further research is needed to improve the achieved performance. It is worth noting that, in the 3GPP Grid, the length of roads per unit of area is higher than in the Madrid Grid. Therefore, having a lower vehicle density does not imply having a lower number of vehicles per kilometre of road. In fact, the density of 595 vehicles/km² in the 3GPP Grid is equivalent to 24 vehicles/km in each lane, while the 1000 vehicles/km² in the Madrid Grid is equivalent to 25 vehicles/km in each lane. Another important difference between both scenarios is the mobility model that in the 3GPP Grid case allows cars to overlap. This characteristic, together with the fact that in the 3GPP Grid all the streets have 4 lanes while in Madrid Grid most of them have 2 lanes, results in a higher probability of having a high number of vehicles in the close vicinity of any vehicle in the 3GPP Grid. This fact has a clear impact on the lower PRR values for short distances.

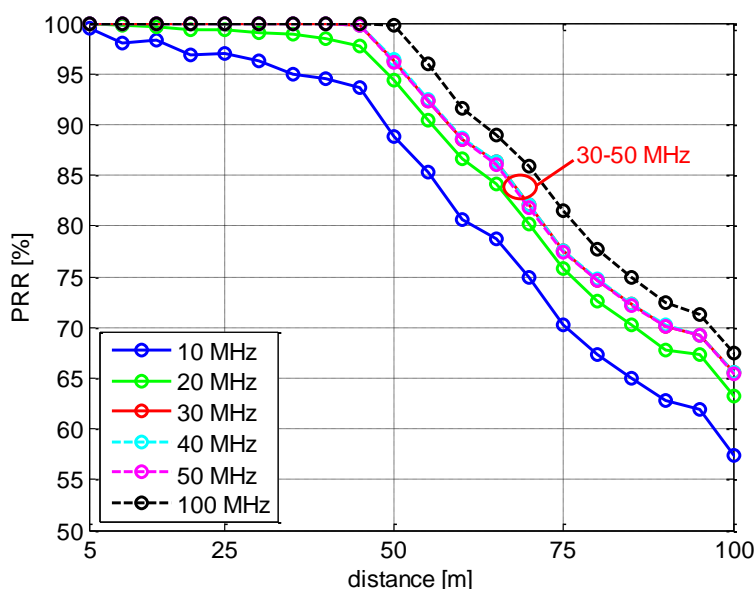


Figure 3-15. PRR in 3GPP Grid.

The PRR curves for the Highway scenario are shown in Figure 3-16. The results indicate that the evaluated system is not able to fulfil the reliability requirements with the system bandwidths considered. In fact, it seems unfeasible to get a high PRR for 1000 m that is the required coverage range for this scenario due to lack of improvement when increasing the bandwidth from 20 MHz to 100 MHz (see overlapping curves in Figure 3-16). Further evaluations are needed to determine whether the currently achieved performance could be improved. Otherwise, the requirements should be revised to reduce the required coverage range.

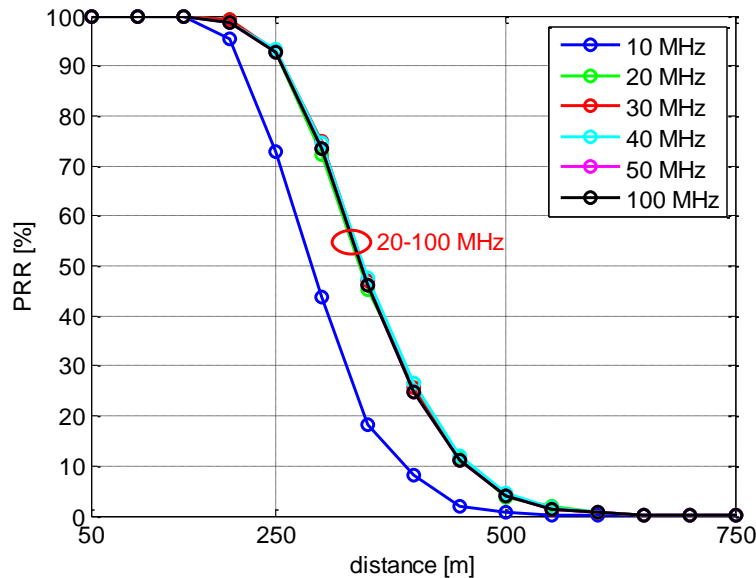


Figure 3-16. PRR in Highway.

3.3.6 RAN energy efficiency

Defined RAN energy efficiency evaluation method assumes evaluation of at least UC1 and UC3 deployments to obtain final energy efficiency values. In calculations below only UC1 data is processed.

Step 1. Calculate traffic volume density for a 5G dense urban deployment according to procedure defined in [MII16-D21], and estimate corresponding packet inter-arrival time (IAT)

According to UC1 evaluation from Section 3.3.1, miniIAT when experience user data rate of 300 Mbps is achievable is equal to 0.05 s = 20 s at the traffic volume density of 4.93 Tbps (cf. Figure 3-2 and Figure 3-3 and bandwidth scaling factor of 10).

Step 2. Scale obtained IAT to calculate different load levels for 5G.

Reusing [EAR10-D23] traffic profiles, averaged IAT for following periods were obtained:

- 17:00 – 0:59 = $\text{minIAT} * 16/14.25 = 0.056 \text{ s}$ ($\lambda = 17.9$)
- 1:00 – 1:59 and 10:00-16:59 = $\text{minIAT} * 16/10.25 = 0.078 \text{ s}$ ($\lambda = 12.8$)
- 2:00 – 9:59 = $\text{minIAT} * 16/3.875 = 0.206 \text{ s}$ ($\lambda = 4.85$)

Step 3. Repeat Step 1 and 2 to calculate IAT for rural 5G network deployments taking into account different experienced user throughput KPIs.

Skipped



Step 4. Use calculated IATs/load points to obtain the total radio network power consumption at given load via simulations.

As energy efficiency data was already available (cf. Section 3.3.1), calculations of total radio network power consumption at three loads were skipped. Instead, IAT calculated in Step 2 were used to calculate averaged RAN energy efficiency improvement gains in given time periods. Curve fitting and value approximation was used.

- 17:00 – 0:59 = 521.2
- 1:00 – 1:59 and 10:00-16:59 = 543.8
- 2:00 – 9:59 = minIAT * 16/3.875 = 658.9

Step 5. Redo Steps 1-4 for baseline 4G.

Skipped for dense urban scenario

Step 6. Integrate results obtained with above-mentioned setups with different weights to calculate overall energy efficiency improvements of the network.

As weight α are equal to 1/3, RAN energy efficiency for dense urban scenarios is equal to

$$EE_{dense\ urban} = \frac{1}{3} * (521.2 + 543.8 + 658.9) = 574.6 \text{ a.u.}$$

4 Performance of selected METIS-II 5G RAN components

METIS-II tackles 5G challenges through different TeCs developed to address spectrum considerations [MII16-D31], UP [MII-D41], as well as synchronous [MII16-D51] and asynchronous [MII16-D61] CP designs. All these solutions contribute to the first version of the overall 5G RAN design concept proposed by METIS-II in [MII16-D22]. This section shows performance evaluation results for selected TeCs compared to legacy solutions such as LTE-A. The focus is to provide numerical evaluation results that address 5G KPIs as defined in [MII16-D11].

Each subsection dedicated to an individual TeC with evaluation results is used for a short elaboration on a specific problem space, and assessment of performance improvements and implications to the overall 5G RAN design. Further information on the concepts can be found either in Annex C and/or in indicated METIS-II deliverables.

TeCs have been grouped according to the 5G generic services, depending on the service that is most related to the concept. This could be xMBB, mMTC and uMTC. In addition, a fourth group of TeCs that enable handling more than one service is presented.

Table 4-1. Overview of TeCs captured in Section 4.

Service family	Section	Functional description	Key highlights and 5G RAN design implications
xMBB	4.1.1	Integration of LTE-A and 5G using Dual Connectivity	Common LTE-A and 5G interface between core network (CN) and RAN (S1*) for smooth introduction of 5G
	4.1.2	Intercell interference management using Frequency Quadrature Amplitude Modulation (FQAM)	Data rates of edge users can be improved by FQAM operations with info exchange between neighbouring BSs (X2* or multi-connectivity signalling)
	4.1.3	Interference management using joint transmission based on zero forcing precoding	To achieve maximum gains in terms of data rates, BSs need to obtain information on symbols, gains and phases of transmitting radio links in proximity
	4.1.4	RRM enhancements via context awareness	For proactive scheduling, acquisition and signalling of context messages between UEs and BSs is needed
	4.1.5	RRM in networks enhanced by nomadic nodes	Interference management and backhaul link measurements have a

			strong impact on performance of dense networks consisting of nomadic nodes
	4.1.6	Dynamic cell switch off for energy efficiency	Centralized RAN architecture and channel quality assessment for switched-off BSs benefit network energy efficiency
	4.1.7	Optimization of handovers for D2D	Enhancement to X2* interface, addition of D2D link measurement and mode-switching mechanism are required to address D2D mobility issue for maximizing D2D benefit in spectrum efficiency improvement
	4.1.8	Clustering of radio nodes for mmW operations	Geometrical position and antenna model of all the mmW transmitting/receiving nodes of the cellular network should be known by the network at any time.
mMTC	4.2.1	FQAM-FBMC operations for mMTC spectral efficiency improvements	Prototype filter design with better performance than legacy solutions
	4.2.2	Cluster head operations for mMTC access	Group based system access outperforms individual access solutions for massive number of devices in a cell. The implications to the RAN design relate to the grouping functionalities and the group coordination for the collection of the RACH requests.
	4.2.3	RRC state handling improvements	For low mobility devices, CP latencies in initial access can be improved by keeping context information in the BS
	4.2.4	Context awareness enhancements for mMTC data transmissions	Context aware device grouping can improve the averaged battery lifetime for mMTC
uMTC	4.3.1	V2V communication enhancements with harmonized centimetre and millimetre wave bands	Uses efficiently the available spectrum to support at the same time very frequent short-range and less frequent long-range V2V communications with reliability. Requires means to map



			packets with different QoS requirements to different AIVs
Service mix	4.4.1	RACH multiplexing for prioritization of initial access	RACH preamble multiplexing can be used to differentiate performance of initial access in mixed service scenarios
	4.4.2	Considerations on the guard band allocations in time-frequency resource grid	Well localized time-frequency resource grid reduces signalling and improves link level performance
	4.4.3	Dynamic TTI configurations for handling different services	Dynamic TTI configurations improves latency and data rates in service mix scenarios with different physical layer numerologies
	4.4.4	Dynamic traffic steering	For efficient traffic steering dynamic QoS virtual functions in the RAN higher layer are beneficial
	4.4.5	Network slicing	Network slicing enables efficient sharing of pooled resources to meet individual QoS policies

4.1 xMBB

4.1.1 Tight integration of 5G with LTE-A

The handover between third generation (3G) and 4G is an inter-AI hard handover (HH) that causes a transmission interruption in the order of 50 ms [STB11], but the interruption can be much longer in some cases. In the initial phase of 5G and due to the exploitation of high frequency bands, the 5G networks may experience coverage holes. In order to fulfil the extremely high requirements foreseen for 5G, such as ultra-reliable communication or availability of high data rates transmission everywhere [MII16-D11], a solution similar to Dual Connectivity (DC) [3GPP14-36842] is proposed between evolved LTE and 5G using the Packet Data Convergence Protocol (PDCP) as an aggregation layer, thus allowing a tight integration between evolved LTE and 5G.

Different realizations of tight integration have been evaluated using a system-level simulator with an LTE system operating at 2 GHz and a 5G AI at 15 GHz. Concepts that are compared are the HH, fast switch (FS) of the UP, and DC [MII16-D61] (cf. the details of the simulation setup in Annex C.1.1). Figure 4-1 shows 10%-ile DL user throughput vs. cell load for DC, HH and FS. Performance of stand-alone 5G AI is used for comparison. Based on evaluation results, tight integration of 5G and LTE using DC provides best performance in terms of user throughput out of all considered integration methods, and outperforms standalone 5G deployments in considered

scenario. The main reason is that the DC utilizes resources from two AIVs (i.e. LTE and 5G) and thus doubles the available resources (20+20 MHz). In addition, there is a diversity gain by using DC approach.

The possible 5G RAN design implications of this technique are a common LTE-A and 5G interface between CN and RAN (denoted as S1* in [MII16-D22]), new signalling for AIV (cf. [MII16-D22]) quality metric, and a fast and lightweight addition/deletion of new CP connection to a user in order to support ultra-reliability requirements.

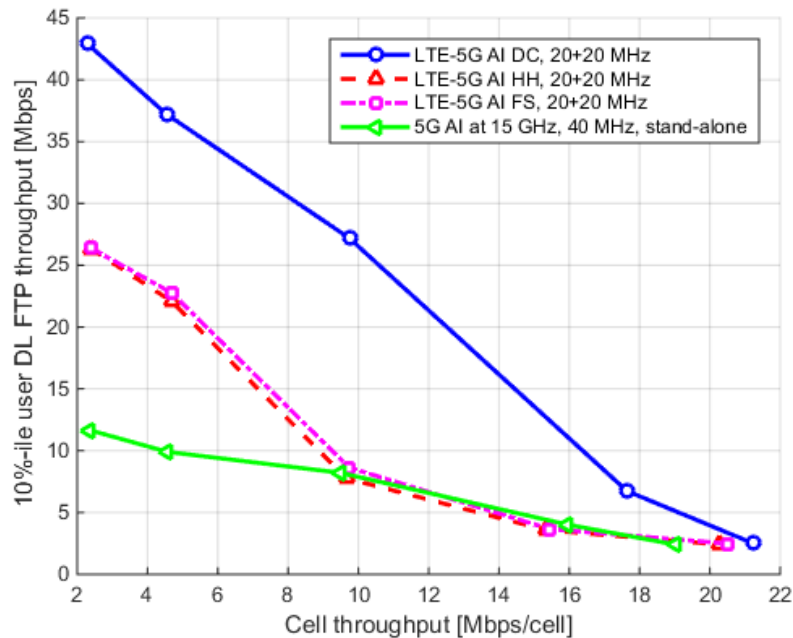


Figure 4-1. 10%-ile user throughput vs. cell load for DC, HH and FS.

4.1.2 Flexible interference management for 5G AIVs

Conventional interference management approaches assume interference follows a Gaussian distribution. It is known that the worst-case additive noise in wireless networks, in the sense of the channel capacity, has a Gaussian distribution. In practice, the distribution of Inter-cell Interference (ICI) depends on the modulation schemes of the interfering BSs. Therefore, an active interference design improving channel capacity in the presence of interference, particularly in the low Signal-to-Interference and Noise Ratio (SINR) regime, can be achieved by applying a new type of modulation called FQAM [MII16-D41].

In this TeC, a resource partitioning scheme to support FQAM in high interference scenarios is evaluated. The proposed scheme partitions radio resources into orthogonal parts for QAM and FQAM along extended radio resource dimensions, namely space, time and frequency. This can be achieved by incorporating advanced beamforming algorithms, revising already established time-based procedures (e.g. almost blank sub-frames), or performing a frequency-based split of FQAM resources to effectively improve the data rate of the edge users experiencing heavy

interference. The details of this approach can be found in [MII16-D51]. Evaluation results focusing on the spatial dimension are presented here.

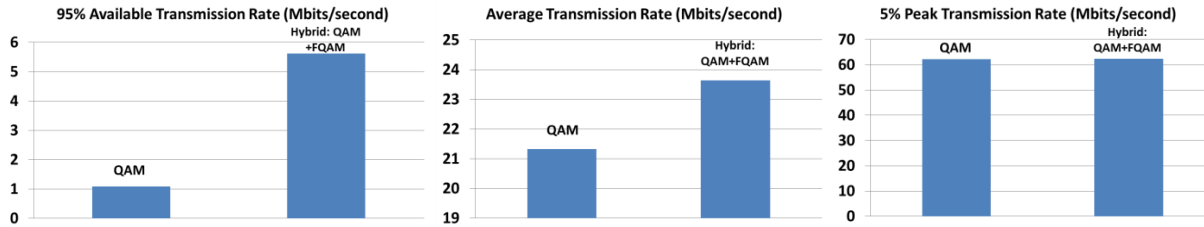


Figure 4-2. 5%-ile UE throughput, average UE throughput, and 95%-ile UE throughput.

Figure 4-2 (left-most) shows that the cell edge UE throughput can be significantly improved by applying FQAM to those UEs experiencing high level of interferences. Figure 4-2 (centre, right) shows also the average and peak UE throughput and, as observed, if the hybrid scheme is applied to all beams, the average throughput is still higher than QAM. However, for peak UE throughput applying the hybrid scheme only cause negligible improvement since peak rate is normally achieved by those UEs experiencing low level of interferences and thus QAM should be used.

The degree of signalling coordination required for this TeC can be dynamically adjusted as required, as outlined in [MII16-D51]. When using the frequency-based FQAM method, coordination can be done by simple exchange of information, such as LTE-A X2 relative narrowband transmit power [3GPP16-36213] or any X2AP messages [3GPP16-36423] in general. In space-based or time-based FQAM, signalling information exchange among BSs is required to determine the beams or the sub-frames where FQAM should be applied, where this exchange can be implemented using either a distributed or a centralized approach. The necessary notification between adjacent cells can be on X2* or can be facilitated by multi-connectivity (e.g., using low frequency AIV), in particular, if one leg of multi-connectivity can achieve a higher visibility of interference pattern per contending zone via UE reports.

4.1.3 Joint transmission with dummy symbols for dynamic TDD

Dynamic TDD is considered a promising technology for handling fast-changing traffic, especially in short-range indoor deployments where transmit powers for UL and DL are similar. At the same time, it generates new interferences (UE-to-UE and BS-to-BS) in addition to the existing ones (BS-to-UE and UE-to-BS). In ultra-dense networks (UDNs), where chances of LoS between a UE and its interferers increase, combating these interferences becomes even more important.

This TeC evaluates a novel way to mitigate BS-to-BS interference by means of network-wide joint transmission (JT) where single-antenna BSs cooperate to construct one large spatially distributed antenna array in the DL. JT is facilitated using zero forcing transmit precoding in order to null BS-to-UE interference. UEs equipped with single antennas are unable to perform transmit precoding in the same way and transmit independently. To deal with BS-to-BS interference, it is proposed to include UL BSs in the precoder design. Since DL BSs are not aware of which symbols UL UEs will transmit beforehand, dummy symbols are transmitted virtually with zero power. The proposed

scheme denoted as joint transmission with dummy symbols (JT-DS) relies on both DL and UL traffic for its implementation. Number of UL BSs that can participate in the precoding is also constrained by the number of cooperating DL BS antennas. For the selection of UL BSs, we consider those serving UEs with worst UL rates calculated according to our baseline [CS15].

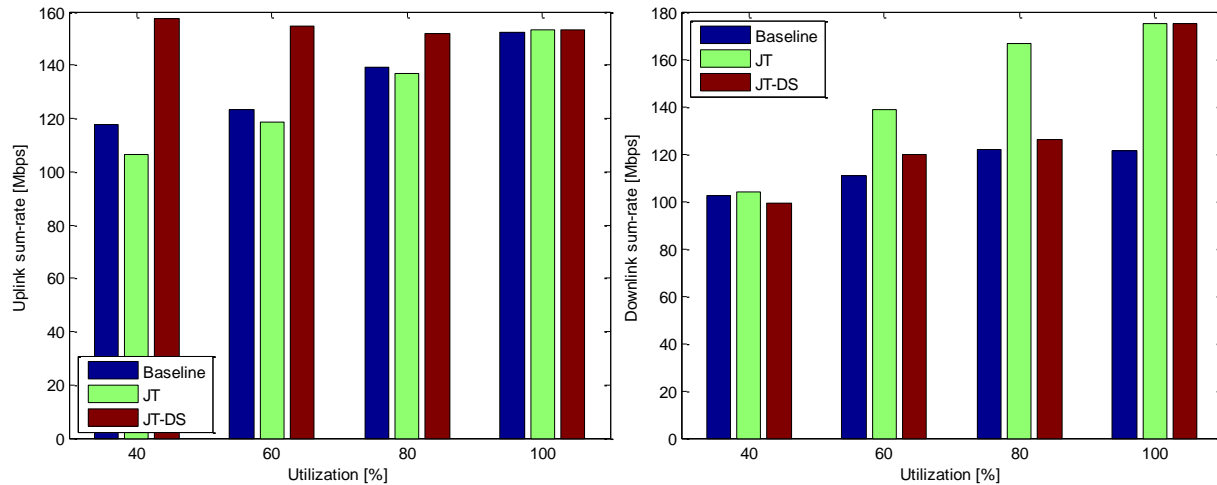


Figure 4-3. Average UL (left) and DL (right) sum-rate.

Figure 4-3 shows the average UL and DL sum-rate, respectively, as a function of system utilization defined here as the ratio between number of scheduled UEs and number of deployed BSs. For UL, JT-DS significantly improves performance thanks to the mitigation of BS-to-BS interference, but uncontrolled UE-to-BS interferences limit further gains. The number of UL BSs that can participate also decreases with utilization as DL traffic increases. In comparison, JT which only nulls inter-user interference between DL UEs will have marginal effect on UL performance. For DL, nulling BS-to-UE interferences will significantly improve performance with JT, except for at very low utilizations where the already low interference is further reduced by walls. The limited gains of JT-DS are attributed to a more ill-conditioned precoder compared to JT due to the inclusion of UL BSs, resulting in lower DL transmit powers in order to not violate the BS power constraint. In addition, transmission of dummy symbols will not contribute to the DL sum-rate. DL performance is also constrained by UE-to-UE interferences. At full (100%) utilization, UL BSs can no longer participate in the precoding. Based on the results, the best transmission scheme depends on the utilization percentage and the preference for UL or DL sum-rate maximization.

For successful implementation, all symbols, gain and phase of all links should be known to BSs.

4.1.4 Diurnal mobility prediction to assist context aware RRM

Regarding the mobility behaviour of users, it is not random but rather direction oriented and a significant portion of mobile users follows diurnal mobility. They traverse within a limited set of trajectories, comprising of specific landmarks (e.g., person travelling to office, commuter in a public transport, etc.), on a regular basis. It means that mobility can be predicted in many cases.

In proposed TeC mobility prediction accuracy of a user is enhanced by extracting/exploiting the context information about user's origin and destination (Markov chain based prediction). Enhanced route prediction is used in tandem with resource allocation to enable best service quality. To exemplify, if a user avails a streaming media service and route prediction anticipates that such a user would run into a coverage hole, then the user is allocated with more resources before entering the coverage hole and data is buffered in his device. The buffered data is used in coverage holes so that users experience uninterrupted and uniform QoE (cf. Annex C.1.2).

This TeC makes use of [MII16-D21] as evaluation methodology basis. Madrid Grid test environment is used as the evaluation scenario. There are 6 coverage holes present in the simulation scenario at different roads as shown in Annex C.1.2, where the achievable throughput is zero. The UE is allocated originally with one PRB and as soon as a coverage hole is anticipated via route prediction, two or three PRBs can be allocated and data buffered. User is assumed to follow diurnal mobility and would traverse among 10 known trajectories with different probabilities. Context information about origin, destination of users, roadmaps with coverage holes is assumed to be known. More explanation on considered set up and mobility model could be found in [KZS16]. With the proposed approach the accuracy of next serving cell and next route prediction in the considered scenario is increased to 85% and 90%, respectively, as opposed to 40% and 60% accuracy with simple Markov model. Figure 4-4 shows that this TeC improves the throughput in the routes with coverage holes. In the left part of the figure, results are shown for the allocation of 2 PRBs, while the right part of the figure shows the results for the allocation of 3 PRBs.

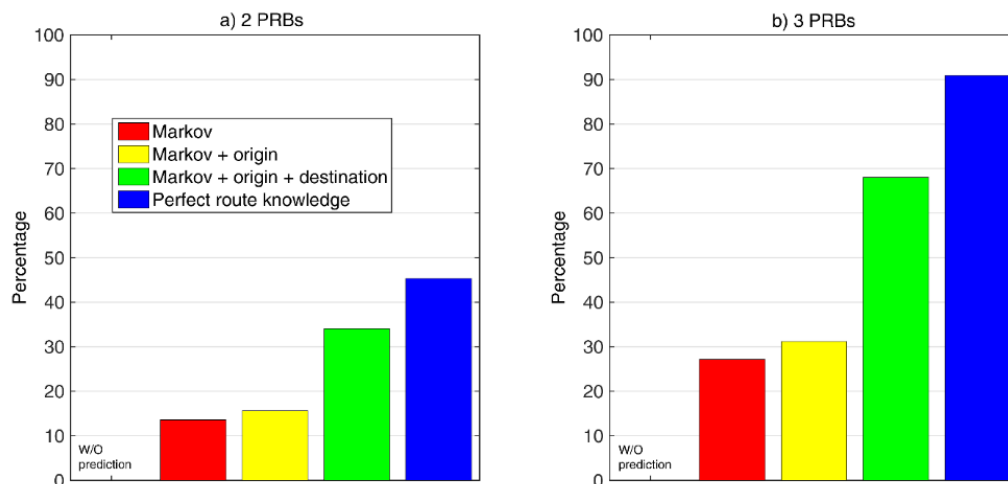


Figure 4-4. Throughput improvement in routes with coverage hole.

To enable context aware resource management schemes, acquisition of context information from several entities (e.g. UE, vehicular infrastructure, etc.) and appropriate signalling of context messages among UEs, BSs and vehicular infrastructures are required. More information about signalling and interfaces required are found in [KS16].

4.1.5 5G user-centric interference management in UDNs

The concept of this TeC is to provide a UE-centric interference management in heterogeneous UDNs by means of selecting appropriate access nodes. Here, two case studies for a hotspot area and a 5G RAN consisting of nomadic nodes (NNs), also known as vehicular NNs (VNNs), under a macro BS coverage are evaluated.

In the first case study, a dense NN deployment is considered, where NNs are mounted on cars that are parked along a road side (see Annex C.1.3). To overcome increased interference among NNs due to close proximity, coordinated resource allocation and JT are applied adaptively based on backhaul conditions (i.e., between access node and serving BS), load constraints and service type. Evaluation results are depicted in Figure 4-5-left for the first case study. The blue bar indicates the baseline, where all the users are attached to the macro BS only. The red bar represents user throughput gain from activation of a number of NNs that results in traffic offloading from the macro (RAN moderation). Finally, the green bar shows the gains when we also employ interference management between the activated NNs on the access links [MII16-D51]. Evaluation results show that, up to 50% higher mean user throughput can be achieved in case of one active NN. However, the achievable gain decreases when more NNs are activated, which is due to interference from neighbouring NNs. Thus, interference management is crucial, particularly when the network density increases in dynamic radio topologies.

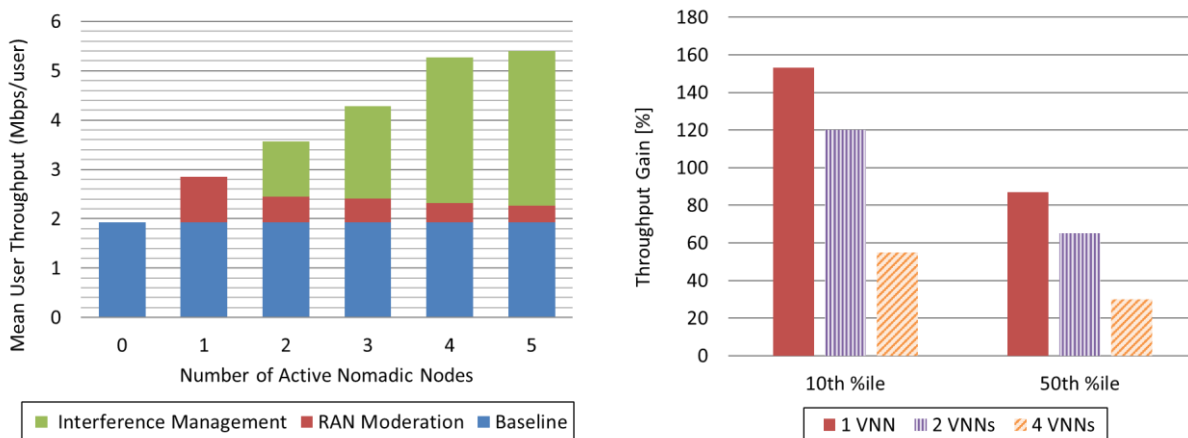


Figure 4-5. Mean user throughput for different number of activated NN in dense NN deployment (case study 1 - left) and downlink throughput gain of the NN deployments compared to picocell deployments (case study 2 - right).

In the second case study, the flexibility of NNs is exploited by selecting the closest NNs to a hotspot area and the performance of such dynamic radio topology is compared with that of a fixed picocell deployment. In this case, to reduce the impact of interference among selected NNs and to increase the spatial diversity, a minimum distance of 50 m is set between active NNs. In this case study, there are 20 randomly located and inactive, parked NNs, present at each macrocell, in average (see Annex C.1.3). A specific number (1, 2, or 4 NNs) of the closest NNs to the centre of each hotspot are activated by the network [SBS+17]. UEs attach to the node with the largest

Reference Signal Receive Power (RSRP) value. For comparison, the same number of picocells is considered, where due to dynamicity of the hotspot (e.g., a street event), from hotspot perspective picocells are randomly located. The downlink throughput gains at 10%-ile and 50%-ile user throughput with respect to picocell deployment are shown in Figure 4-5-right. It can be seen, for example, by activating one NN closest to the hotspot, 10%-ile throughput gain is around 150% compared to one picocell.

In order to benefit from NN operations new inter-cell resource management schemes are needed for the coordination of the access nodes in dynamic radio topology. Also, the backhaul link measurements and activation commands may possibly imply new signalling elements on the wireless backhaul link.

4.1.6 Dynamic cell switch off

Contemporary cellular networks are dimensioned to cater for the traffic at peak hours. However, when the active traffic is not at its peak, certain cells could be switched off to reduce the overall network energy consumption. In this TeC, a centralized entity dynamically selects which transmission nodes should remain active, based on traffic requests. Cooperation schemes among the selected nodes, such as JT and dynamic point selection/blanking (DPS/DPB), are exploited in order to switch off more nodes than possible without such multipoint coordination [MII16-D51].

Simulation results were obtained in a Manhattan-like urban scenario. Power consumption of BSs in the considered scenario was achieved using power models specified in METIS-II for 2010 and 2020 equipment [MII16-D21]. In Figure 4-6 results are shown for three configurations: no coordination with 2010 or 2020 equipment, and the TeC here proposed (denoted as EE JT). Different traffic load conditions were considered by assuming Constant Bit Rate (CBR) traffic sources for each user. Note that in the bar representing the overall power consumption different colours are used to highlight the dynamic (related to power amplifier operations and baseband processing and then load dependent) and static portions of BS power consumption as defined in [MII16-D61]. The higher energy efficiency of 2020 equipment reflects in a drastic reduction of the power consumption, both with and without the centralized entity for coordination. The 2020 equipment can be switched on and off more dynamically comparing to equipment foreseen for 2010 (cf. e.g. lean design solutions in [MII16-D61]), which is effectively exploited by the proposed solution. As a consequence, for 2020 networks and for low to medium traffic loads, an additional 51% power consumption reduction can be achieved using the EE JT, compared to a non-coordinated solution. See more details about this evaluation in Annex C.1.4.

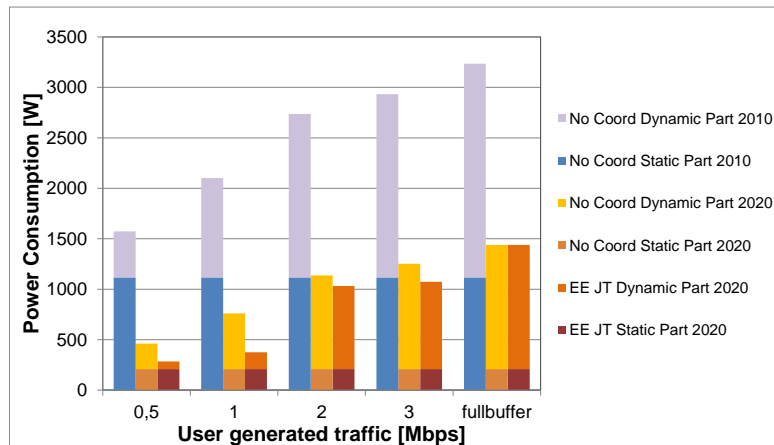


Figure 4-6. Comparison of power consumption with and without coordination for 2010 and 2020 radio networks with METIS-II BS power consumption models.

As the proposed solution operates in the MAC layer, a centralized-RAN architecture is preferred, where the scheduling is performed in a central unit that controls resource allocation for a large number of nodes. Additionally, a mechanism is needed to assess channel quality also for the nodes that are switched off (e.g., through the transmission of periodic beacons as suggested in [MET14-D32]).

4.1.7 Mobility management framework for D2D communication

D2D communication is highly expected to improve spectrum efficiency of a 5G network. However, mobility impacts the reliability of D2D links [MII16-D21]. In a legacy network (i.e., LTE or LTE-A), when two moving UEs (e.g. vehicles) connect to different serving BSs, D2D communication between the vehicles in UP is disrupted, e.g., due to different D2D resource allocations in different CPs. Data packets are dropped during the disruption time. Therefore, considering a mobility management framework which jointly tackles the mobility management of a D2D pair is required to reduce possible D2D communication disruption time due to handover.

Simulations were conducted in the Madrid Grid scenario, where a device pair circulated along the greenfield (see Figure 4-7 (a)). From the simulation results shown in Figure 4-7 (b), we observe that the joint mobility management method proposed in [MII16-D22] and [MII16-D61] guarantees a better reliability (up to 95%) than the legacy solution does when inter-device distance is smaller than 40 m. This is because the two UEs can jointly hand over to a target BS to which both measures “acceptable” signal strength. Among the three factors, inter-device distance is the most significant factor that impacts reliability. In contrast, handover delay brings a minor impact to reliability, where it matters only in cases with high device velocity. The impact of device velocity is “method-dependent” and can be more complicated if Doppler effect takes place in very high device velocity situations. See more detail discussion for the simulation results in Annex C.1.5.

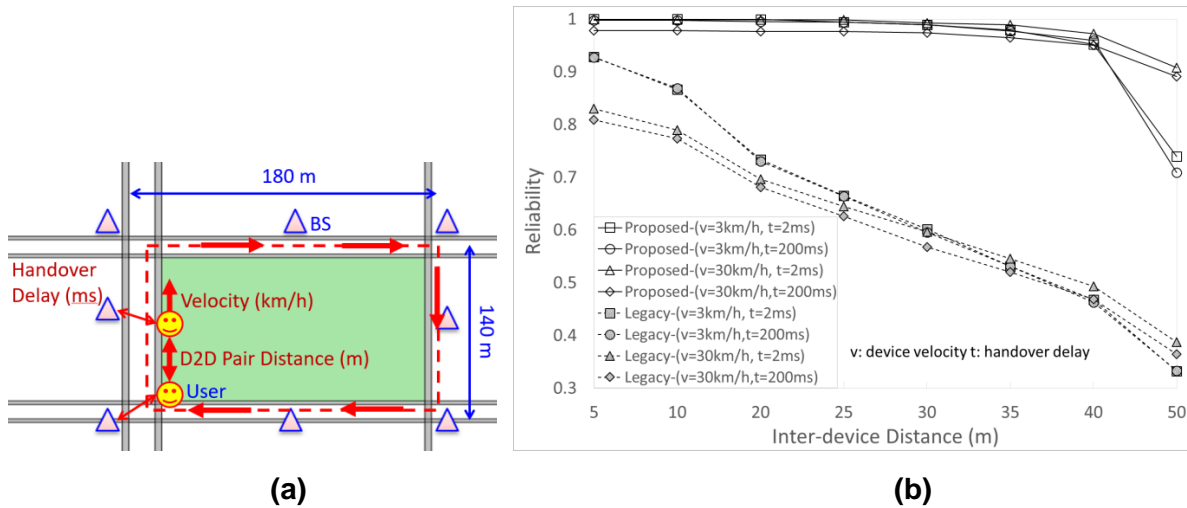


Figure 4-7. (a) One pair D2D simulation environment where the D2D device pair circulates along the greenfield, (b) Simulation result of one pair D2D scenario

According to lesson we learned from above observations, to realize a joint mobility management framework for D2D, enhancements to X2 interface (denoted as X2* in [MII16-D22]) are required to support D2D service continuity, e.g., cooperative mobility management signalling between serving and target BSs [MII16-D61]. In addition, multi-AIV signal measurement and D2D link measurement are necessary as a part of overall mobility management procedures. Furthermore, inter-device distance and device velocity should be further investigated to tackle two questions: when should the two devices communicate through D2D and when should they switch back to cellular. As a result, a smart mode-switching mechanism in 5G RAN is required, which is able to determine a suitable mode (i.e., D2D or cellular mode) at a right moment.

4.1.8 Resource management and traffic steering in heterogeneous environments

In a heterogeneous environment where systems operating at mmW and traditional bands co-exist, a proper mechanism to manage resources and cope with interference in mmW bands is under investigation. This TeC focuses on a Pre-emptive Geometric-based Interference Analysis (PGIA) [MII16-D51] that is able to determine, prior to the establishment of a new transmission link, a set of possibly interfering mmW transmission links in a resource sharing cluster (RSC). In RSC incumbent and new links are grouped allowing the network to implement a suitable resource partitioning mechanism at scheduler level, or to take other alternative measures at higher levels, e.g., traffic steering through establishment of transmission links on a different cell layer. In particular, the considered TeC allows to limit interferences and reduces the subsequent signalling overhead for the evaluated scheme.

Results depicted in Figure 4-8 (left) show that the PGIA coupled with a simple resource sharing mechanism can significantly reduce the number of interfered links. Without PGIA, the average percentage of interfered mmW links rises over 95% as the number of concurrent links in 1 km²

grows to 200, while using PGIA and resource sharing mechanism the average percentage of interfered mmW links is capped around 2.5%.

In Figure 4-8 (right) the average throughput per link in the different considered scenarios is depicted. It should be noted that the PGIA mechanism not only keeps the number of interference links very low, but also, in doing so, achieves a better average throughput per link with a consistent gain in scenarios with many concurrent links.

See the details of the simulation setup in Annex C.1.6 where complementary results can be also found.

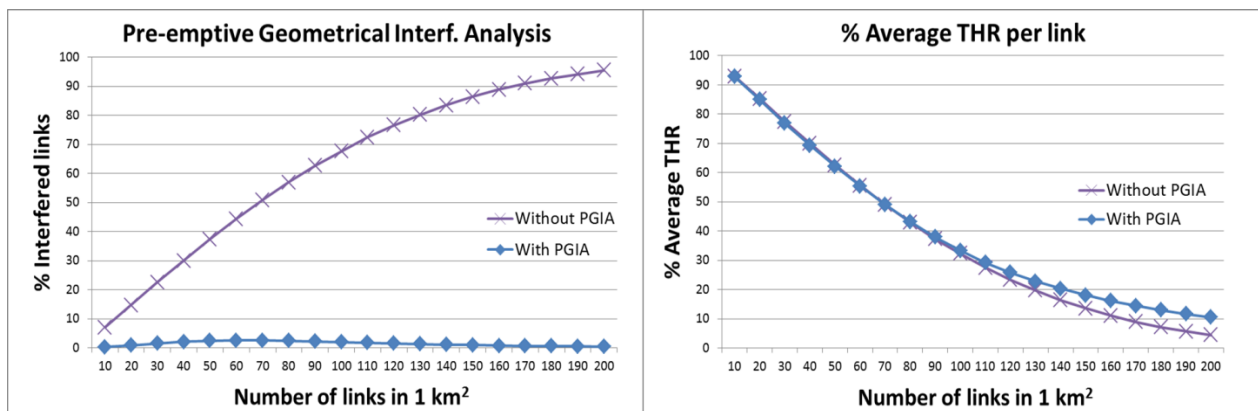


Figure 4-8. Impact of PGIA on: average percentage of interfered links normalized by total number of links (left), and average throughput (THR) per link normalized by total throughput without any resource sharing (right).

A prerequisite is that the geometrical position of all the mmW transmitting/receiving nodes of the cellular network should be known by the network at any time regardless of their mobility. A model of the antenna of each mmW node (e.g., at least the main beam angle and the FBR) is needed for the analysis.

4.2 mMTC

4.2.1 FQAM-FBMC design and its application to mMTC

We propose a novel design which efficiently combines two air interface components: FQAM as a novel modulation scheme and QAM-Filter Bank Multicarrier (QAM-FBMC) as a new waveform [NCK+14], [YKK+15] and [KYK+15].

There are three existing QAM-FBMC solutions with different prototype filter design: 1) PHYDYAS filter and its block interleaved variant are used for odd- and even-numbered subcarriers, respectively [NCK+14], 2) Type-I filter is used for both odd- and even-numbered subcarriers [YKK+15] and 3) two different Type-II filters are used for odd- and even-numbered subcarriers, respectively [KYK+15]. In contrast to the current QAM-FBMC implementations, in the proposed

FQAM-FBMC solution, the same PHYDYAS prototype filters for odd- and even-numbered subcarriers is used to reduce implementation complexity [BRR+10] [MII16-D41]. In particular, as the level of self-interference depends on the spacing between two active subcarriers carrying QAM symbols, two approaches based on FQAM-FBMC are proposed to eliminate self-interference [YM16]. In the Approach 1, Amplitude Shift Keying (ASK) is applied as long as an active subcarrier may generate self-interference. In Approach 2, the spacing between adjacent active subcarriers are taken into consideration and QAM or ASK modulation is opportunistically applied. By doing this, the rate loss can be further reduced.

We evaluated the three current solutions and the two approaches proposed in [YM16] and [MII16-D41]. The results are shown in Figure 4-9. The Proposed Approach 1 requires a similar SINR as Solution 1 to achieve target experienced throughput of 1.5 kbps. The Proposed Approach 2 requires the same level of SINR as Solution 3 in Additive White Gaussian Noise (AWGN) channel. However, in Extended Vehicular A (EVA) channel, the required SINR is almost the same for all approaches except Solution 2. The proposed approaches have lower complexity and much better spectrum confinement. They provide three benefits: high bandwidth scalability, low energy consumption and lower SINR for target experienced throughput making this TeC suitable to support multiple services/applications in 5G.

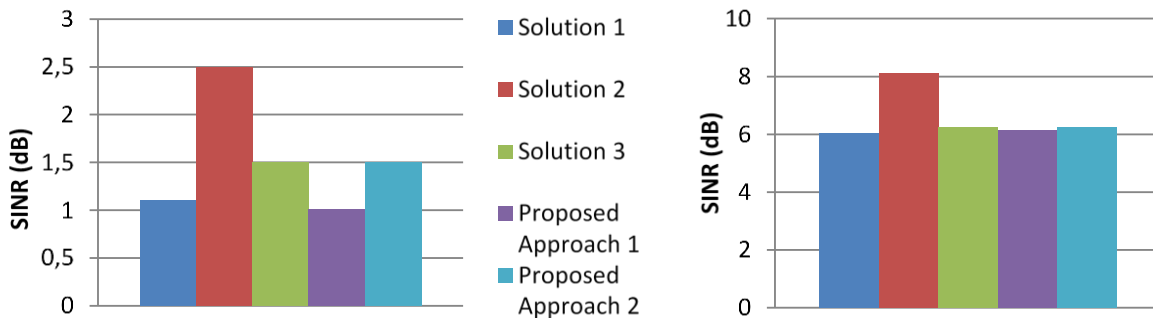


Figure 4-9. Required SINR for experienced throughput of 1.5 kbps for AWGN channel (left) and EVA channel (right).

Switching between the two approaches or even to rollback QAM-FBMC can be configured flexibly and such configuration should be signaled explicitly or implicitly to the receiver.

4.2.2 Group based system access

Random access of a large number of devices introduces new challenges to the 5G RAN design. One potential approach for radio access for devices that are static or semi-static is to group them and perform group based initial access [MII16-D61]. Grouping and cluster head selection should take place using various criteria such as system access periodicity and device location/mobility pattern. Group head uses Uu interface for communication with the 5G RAN. In this case, instead of having all the group members to proceed in random access, the transmission requests could be aggregated, and only one device (i.e., the group head) performs the random access request. The latter is plausible since during the initial attach of the UE to the network, the network is aware

of the groups and informs the UEs about the group head that they should associate to. Then, given that the network (eNB) is aware of the groups it may provide uplink resource to the UEs (for details please refer to the Annex C.2.2. and [MII16-D61]). In the evaluation, a single BS deployment is considered and the devices that are trying to access the network are static or semi-static. The devices that are accessing the medium may have either periodic or totally random transmission attempts.

In the simulation analysis, the devices are accessing the system simultaneously using one out of the 64 available preambles. In case a collision occurs, the devices proceed in retransmissions considering the service requirements (depending on the urgency of the accessed service more retransmissions are allowed). The periodic system access and the limited mobility of the devices enable the allocation of devices to stable groups. From the evaluation results depicted in Figure 4-10 (a) it is observed that using the group system access reduces the collision rate significantly. Additionally, the average initial access delay (i.e., random access, random access response, terminal identification, and contention resolution) is reduced, as shown in Figure 4-10 (b), since the devices are accessing the system with fewer collisions and thus experience fewer retransmissions. Number of collisions and delay on a per service basis is presented in the Annex C.2.2.

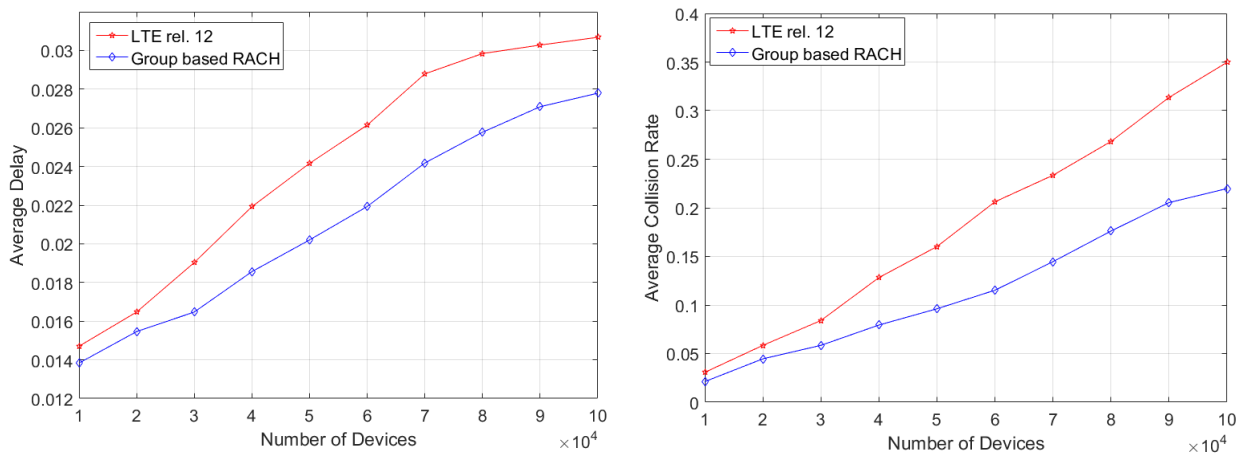


Figure 4-10. (a) Number of collisions and (b) average initial access delay of successful system accesses for the Group Based System Access compared with LTE-A.

Group based system access has an impact on 5G RAN design since special control mechanisms are required for the grouping of devices on the one hand, and combined RACH process is required on the other. These updates require enhancements in the initial access process which in the current LTE-A is designed for xMBSB services where each UE individually accesses the network.

4.2.3 RRC state handling improvements – Connected Inactive

As highlighted in Section 2.2.2, device energy efficiency is an important performance metric in 4G, as it increases the operational time of handhelds between the charges. However, in 5G, along with the proliferation of IoT, energy efficiency will become a critical KPI for mMTC devices, as these are expected to operate on a single battery for 10 years or longer [MII16-D11]. To tailor 5G

operations for IoT services METIS-II investigates a new RRC state, called RRC Connected Inactive that limits the signalling exchange between devices and the infrastructure, and allows fast accessibility [MII16-D61]. This is achieved through keeping context information (e.g., security data, UE capability information, etc.) in the RAN when UE goes into RRC Idle mode. In 4G moving out of the RRC Connected state means flushing such information in a serving BS. However, keeping it in the access infrastructure, as proposed for RRC Connected Inactive, reduces mobility related signalling when UE moves within a configured tracking area, minimizes the latency for the initial packet transmission and at the same time allows UE to benefit from DRX operations. These gains are expected for other services, such as low mobility xMBB, but are most evident for mMTC UCs. To exemplify, in mMTC a data transfer (e.g. a sensor report) can be comparable in terms of volume, or even smaller than the signalling that network needs to exchange with the mMTC device for connection establishment. Therefore, reduction of signalling will lead to noticeable improvements of battery lifetime.

Assessment of new RRC Connected Inactive state, by means of analytical evaluation of CP latency reduction, is done in Section 3.2.1.

4.2.4 Context-aware D2D communication for mMTC

Two critical challenges in the context of exploiting cellular networks for IoT are the availability of the mMTC service and battery life of sensor devices. mMTC devices can be located everywhere, even in the deep indoor placements. To overcome the propagation constraints in mMTC communication and related power dissipation challenge at device side, METIS-II studied the exploitation of context-aware D2D communication for mMTC [MII16-D61] that could provide further improvements to the scheme proposed in Section 3.2.3. In this particular research, certain UEs are selected by the network to act as relay UEs for mMTC devices located in cell border or in deep indoor. More details of this technology and the methodology used to evaluate it can be found in Annex C.2.4.

In Figure 4-11, cumulative CDF of served days for mMTC UEs is shown. In the *Distance plus CSI based D2D clustering* scheme, both location information and cellular channel state information (CSI) of sensors are used to efficiently form D2D clusters and select transmission modes for D2D UEs. As a baseline scheme, the performance of LTE system is also drawn. In this work, if a radio link experiences a very bad SNR value, no data transmission is possible on this link and the user is in network outage. As can be seen from Figure 4-11, 16% of mMTC UEs are in outage and cannot be served by LTE network. The steps appeared in the figure is due to the fixed MCS. By applying our proposed scheme, 99% of UEs can be served by either cellular or D2D link. Additional results shown in Annex C.2.4 demonstrate that the outage improvement does not come with poorer performance for UEs in LTE coverage. Additionally, in that figure, it can be observed that 70% of UEs can meet the battery life requirement of 10 years in LTE system, while this value has been improved to 90% by using our D2D scheme.

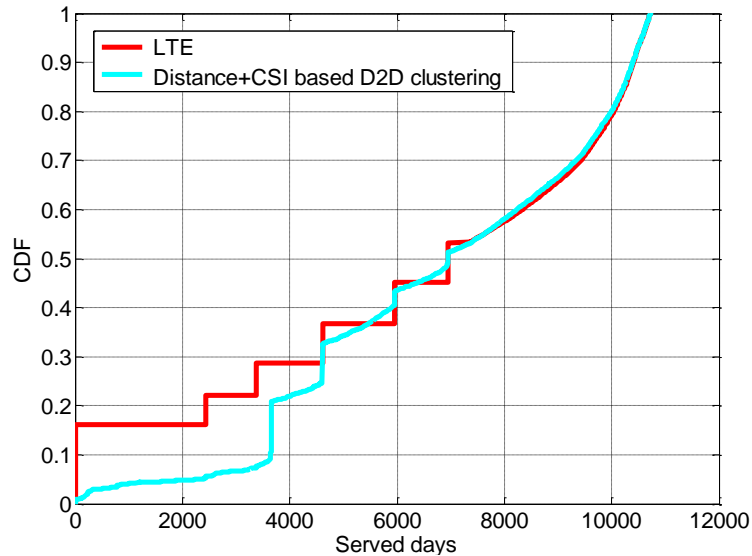


Figure 4-11. CDF plot for served days of mMTC UEs.

To support this TeC, the BS of the 5G system should implement a smart transmission mode selection taking into account the context information (e.g. channel quality between BS and UEs, location and battery level information of UEs). Decisions made by the selection algorithm should be signalled to the UEs. Therefore, signalling should include both the transmission of context information and decisions. Support of mobile relaying based on D2D communications is also a must.

4.3 uMTC

4.3.1 AIV harmonization for V2V communication

In cooperative intelligent transportation systems (C-ITS), vehicles broadcast status packets to send information to their neighbours. For traffic safety applications, 100 ms is the typical periodicity of these packets, while we envision that, for autonomous driving, the periodicity will be reduced down to 10 ms while the packet size will be increased. In urban scenarios, traffic safety related packets typically require a high PRR for distances of 50 m with maximum E2E delays of 100 ms. Autonomous driving related packets may require a high PRR for shorter distances, about 10 m, with maximum E2E delays of 10 ms. According to our results (see Annex C.3.1), the simultaneous fulfilment of both sets of requirements is very difficult, if not impossible, when the transmission uses an AIV over a single frequency band in an urban scenario due to both technical and regulatory issues. The proposed technique is based on the joint use of two harmonized AIVs: one in cmW band (with larger communication range) and the other in mmW band (with more spectrum available). In the considered scenario, 1 out of 10 transmitted packets is sent over 10 MHz in the cmW AIV, and used for both traffic safety and autonomous driving. The remaining 9 packets are sent over 100 MHz in the mmW AIV, and cater for autonomous driving. Such

approach enables the simultaneous fulfilment of the requirements set for the two type of packets, as depicted in Figure 4-12. See Annex C.3.1 for more details about the analysis of this technique.

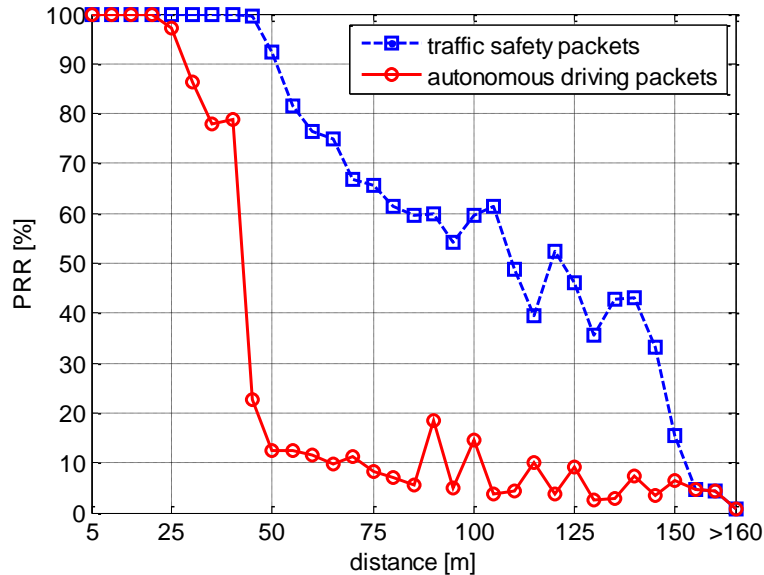


Figure 4-12. PRR vs distance between vehicles.

In order to support this TeC the 5G system architecture should provide means to integrate two AIVs, each one using different frequency bands, including mmW band, and allowing DC of both AIVs. There should be means to separate packets with different QoS requirements (e.g. traffic safety packets and autonomous driving packets) in traffic flows through different AIVs.

4.4 TeCs addressing mixed services

4.4.1 RACH multiplexing in support to diverse access requirements

In order to prioritize uMTC applications in the system access handling multiple 5G services, several schemes have been proposed in the literature including access class barring, resource split, etc.,. These approaches however, are not in-line with the expectations for the 5G on its flexibility. As the ratio of uMTC and mMTC or xMTC devices (and hence the ratio of RACH resources reserved for different services) may fluctuate, new divisions of RACH resources need to be communicated inside the given cell, also for the mMTC devices that rely on long DTX periods. A much more flexible solution is based on assigning a set (e.g. 2 or more) of orthogonal RACH preamble signatures for delay sensitive services [MII16-D61]. This approach assigns requests with more restricted delay requirements with a higher priority, since combinations of preambles have higher probability of correct detection by the receiver. The combination of preambles may take place in time, frequency, or both domains, and results in higher priority access requests experiencing fewer collisions and retransmissions.

Evaluation of this approach has been done for METIS-II UC4 [MII16-D21]. The devices were abstracted to the number of random access attempts per second ranging from 10,000 to 50,000. 10% of these attempts were associated with delay sensitive services (e.g. uMTC) and remaining ones were caused by services with no strict delay requirements. Three approaches for use of RACH preambles were analysed. In the first one, all devices (high and low priority ones) are accessing the system using one preamble (denoted in the figures as *LTE with full resource pool*). In the second one, RACH requests coming from delay sensitive services (high priority transmissions) were given a fixed number of 20 out of 50 available preambles (we assume that a number of preambles is used for contention free RACH), while remaining 30 were shared between delay-tolerant applications (low priority transmissions); this is denoted as *LTE with resource split*. In the third approach the proposed scheme is applied (denoted as *Preamble Coding*), where two preambles are used for high priority initial access and one for low priority initial access.

As depicted in Figure 4-13 (a) for high priority initial access assessment, the *preamble coding* outperforms the other two approaches, since the combination of preambles reduces the probability of having a collision when accessing the system. Collisions in high priority transmissions will occur only if two low priority devices select the same preambles as the combination dedicated for a high priority device that attempts to access the system at the same time. For the low priority requests the *LTE without resource split* scheme outperforms both the proposed scheme and the *LTE with resource split* scheme, as shown in Figure 4-13 (b), since there is no differentiation among the service requests and all the preambles are used for the low priority requests as well. It should be noted though that the *preamble coding* scheme performs significantly better than the *LTE with resource split* scheme because all the available preambles are used.

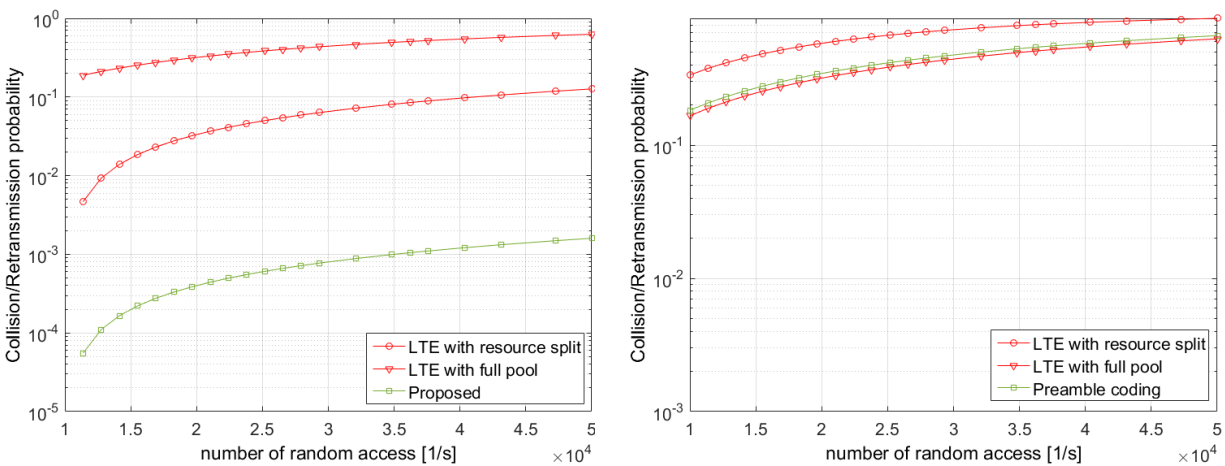


Figure 4-13. Comparison of (a) collision/retransmission probability for high priority request, and (b) collision/retransmission probability for low priority request.

4.4.2 Regular resource grid for new waveform

To enable multiplexing diverse service types in 5G with mixed numerologies and possibly also asynchronous access, the resulting interference level between services has to be kept sufficiently low. That may be realized by e.g., applying filtering or windowing to the conventional OFDM

transmission per sub-band basis, and some additional guard band needs to be inserted. If sub-bands are simply shifted to add guard bands, the conventional regularity of the resource grid will be destroyed (cf. Figure 4-14 (a)). A more efficient approach allocating guard bands within the regular resource grid as shown in Figure 4-14 (c) is proposed.

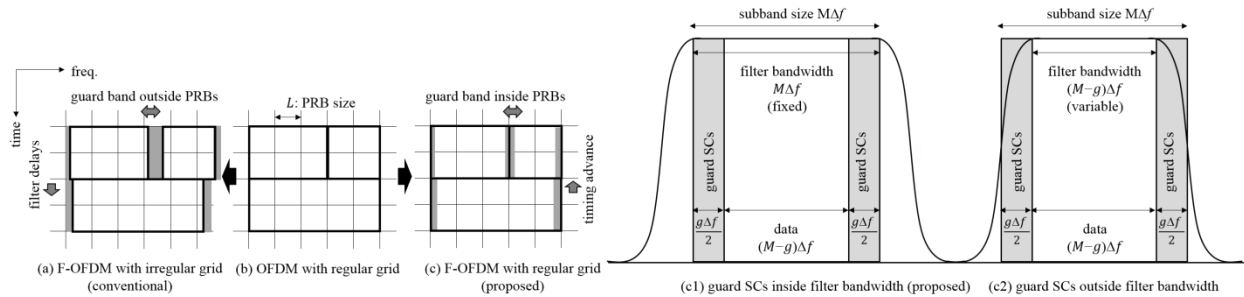


Figure 4-14. Different approaches for inserting guard bands (left), and different filter bandwidth allocation (right): guard Sub-carriers (SCs) (c1) inside passband and (c2) outside passband.

One way of implementing (c) is to define filters; each optimized for different guard bandwidth (cf. Figure 4-14 (c2)), but this is rather complex. (c1) is a much simpler option as it keeps the filter bandwidth constant [WBK+16] [WBK+16_2] [MII16-D41]. The options (c1) and (c2) have been evaluated in an UL asynchronous scenario with two UEs having frequency resources allocated next to each other (separated by $g=2$ guard SCs) with the UE's power ratio ΔP . Figure 4-15 shows that the proposed (c1) results in a similar or even better performance than (c2) despite its simpler design except for extremely high interference levels (40 dB higher). More detailed analysis and setup can be found in [WBK+16] and [WBK+16_2].

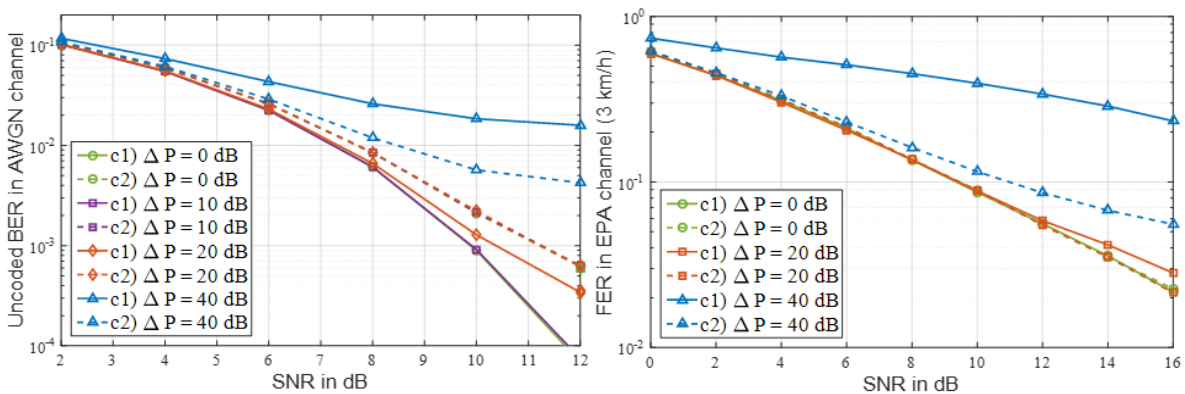


Figure 4-15. Performance for guard SCs inside (c1) and outside (c2) filter bandwidth.

It is also worth mentioning that both options (c1) and (c2) (cf. Figure 4-14 (c)) can keep the regular grid with significantly lower signalling overhead compared to the violated resource grid (cf. Figure 4-14 (a)). The later would require to signal the shifted sub-band locations in the entire resource space. Furthermore, the proposed option (c1) is much simpler than option (c2) as less filters would

have to be signalled. This reduced signalling overhead will lead to improvements measured in system KPIs such as enhanced experienced user throughput as more resources would be available for data transmission, lower E2E latency and RAN energy consumption.

4.4.3 Flexible multi-service scheduling framework

This TeC evaluates a flexible scheduling framework that is able to simultaneously accommodate UEs with very diverse service types and performance requirements. It is based on a flexible frame structure with variable TTI size configuration that allows scheduling each UE according to its corresponding optimization target. It is fully flexible in the sense that it does not require separation and reservation of resources for different services, adapting dynamically to the traffic demands.

Presented system-level simulation results compare performance of several TTI size configurations (fixed per simulation at this point) to estimate the most suitable TTI size that should be dynamically chosen per UE depending on service requirements, traffic type, radio channel quality and system load. The evaluation is performed in a 3GPP Urban Macro scenario with 7 BSs, each having 3 sectors, 500 m ISD and using 10 MHz band [3GPP10-36814]. In-resource control channel (CCH) scheduling grants with link adaptation are assumed, which allows to model different degrees of CCH overhead (i.e. aggregation levels or number of resource elements) depending on the UE radio conditions [PBF+16] [PNS+16].

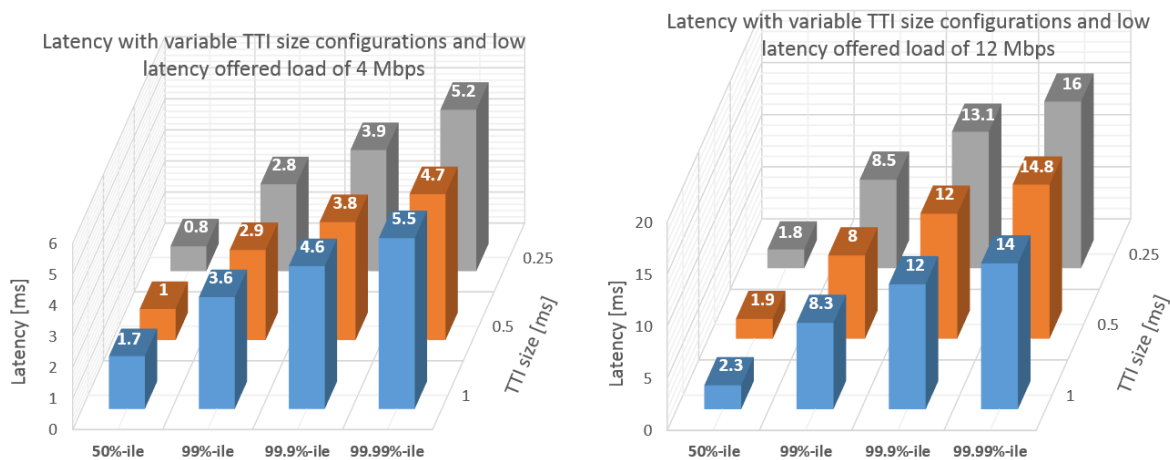


Figure 4-16. Latency values from packet latency CDF with variable TTI configurations and offered loads for a mix of xMBB and uMTC traffic.

The packet latency (i.e. MAC layer one-way UP latency) for different TTI sizes and system loads with a mix of xMBB and uMTC services. xMBB traffic is modelled with a single user full buffer download, whereas higher priority uMTC low-latency traffic follows a Poisson arrival process with 1 kB payload and varying total cell offered load. More details can be found in [PPS+16]. As depicted in Figure 4-16, at low system loads, using a short TTI is in general a more attractive solution to achieve low latency communications. However, looking at the tail values (99.9%-ile and above), a 0.5 ms TTI size offers better latency than the 0.25 ms TTI, even for low loads.

As the load increases, longer TTI configurations with lower relative CCH overhead (and therefore higher spectral efficiency) provide better performance as these better cope with the non-negligible queuing delay. The 1 ms TTI configuration is beneficial from a latency point of view for high loads and above the 99.9%-ile, due to queuing delay. As the offered load increases or as we consider UEs with the worst channel conditions, the queuing delay becomes the most dominant component of the total latency, therefore it is beneficial to increase the spectral efficiency of the transmissions (by using a longer TTI) in order to reduce the experienced delay in the queue. The observed trends are relevant for uMTC use cases, which require latency guarantees of a few milliseconds with reliability levels up to 99.999%.

The results presented above and detailed in [MII16-D51], as well as related studies performed in [PNS+16] and summarized in Annex C.4.2, indicate that the optimum TTI size varies depending on multiple factors. Therefore, it is beneficial to be able to dynamically adjust the TTI size per user's service requirements and scheduling instance, rather than operating the system with a fixed TTI.

4.4.4 Multi-AI traffic steering framework

The resource management framework captured in Section 4.4.3 assumes that individual access nodes are capable of handling multiple service types. However, for the 5G it cannot be precluded that access nodes will support only a subset of AIVs depending on their physical properties, such as maximal TX power or operating frequencies. For example, wide area nodes at low frequencies could be used for mMTC services while ultra-densely deployed small cells operating at mmW frequencies would be more suitable for xMBB. Therefore, efficient handling of multiple services in 5G could be achieved using multi-connectivity, i.e. ability of UE to simultaneously connect to multiple access nodes. Such approach is evaluated in multi-AI dynamic traffic steering framework described in [MII16-D51]. The considered solution takes real-time feedback from multiple access nodes serving UEs via different AIVs, in order to adjust the traffic flows on a synchronous timeframe. This allows the introduction of centralized outer loop traffic moderation, optimizing data flow for more than one access node.

An overview of the dynamic multi-AI traffic steering mechanism is explained in the Annex C.4.3 based on the framework described in [MII16-D51] and [PME+16], with the possible virtual functions within the access network – outer (AN-O) layer explicitly defined, as well as the possible control information exchange required with the access network – inner (AN-I) layer. The possible performance gains using ultra-dense deployments, in terms of packet delivery delay normalized to the maximum delay are also shown in Figure 4-17. The parameters used for throughput calculation and related evaluations are based on the ones used in [MII16-D51 and] [PME+16], with increased user and 5G radio nodes density. The detailed simulation parameters are described in Annex C.4.3. The performance results indicate the significant gains that 5G RAN can achieve with the help of dynamic QoS virtual function in the AN-O, tightly interworking with the traffic steering function, taking real-time UE link quality into account.

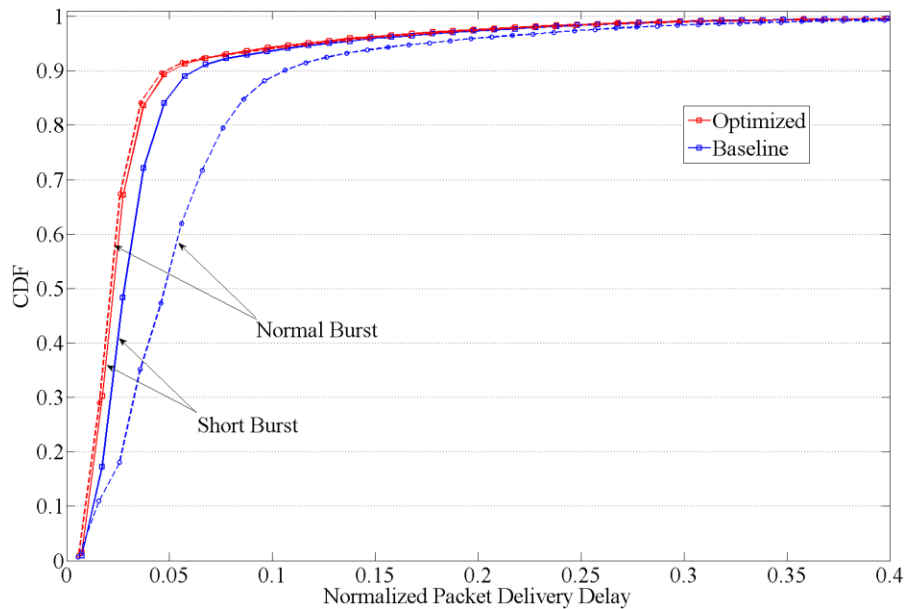


Figure 4-17. Normalized packet delivery distribution for normal and short burst packets.

The evaluations indicate that enabling a dynamic 5G RAN through enhanced virtual functions implemented in the access-agnostic AN-O layer, with assistance information from AN-I layer in the form of quantized AIV-independent information, can provide significant gains. Such enhanced capabilities in the 5G RAN is also a key enabler for achieving the diverse set of requirements imposed due to the support for mixed services.

4.4.5 RRM for network slicing

Network slicing is a new 5G concept in which multiple logical networks run as virtually independent business operations on a common physical infrastructure. In contrast to the operation of dedicated physical networks, sharing of available resources on a dynamic base allows exploitation of pooling gains, similarly as described in Section 4.4.3. With respect to the RAN, an efficient sharing of scarce radio resources among the network slices is the key challenge, which is achieved by RRM for network slicing outlined in [MII16-D51]. It is realized by introducing a logical entity in the RAN, called AIV-agnostic slice enabler (AaSE) that is responsible for monitoring and enforcing service level agreements (SLAs) for individual slices by means of traffic steering and resource management. AaSE maps the abstract slice specific SLA definition to the QoS policies.

The simulation results in Figure 4-18 show a comparison of two RANs (subnetworks) in terms of user throughput. In the first case (red curves), two dedicated networks with 10 MHz system bandwidth are operated for independent businesses. The dedicated network 1 serves hundred users with a low demand, such that a low load in the network occurs. In contrast, the dedicated network 2 serves 710 users causing a fully loaded system with lower performance per user. In the second case (blue curves), a common RAN for both networks is operated on 20 MHz system bandwidth. The pooling of resources enables a gain in user throughput shown when looking at all users in total. By means of an SLA, it is targeted that users of the virtual network 1 (network

slice 1) reach a similar capacity as in the case of dedicated networks. As the dedicated network 1 reached a mean network throughput (averaged over time) of 218 Mbps, an SLA was used to a guaranteed network capacity of 220 Mbps. Network slice 1 achieves a network throughput of 209 Mbps. This is slightly below the guaranteed capacity due to variations in the traffic pattern that cause a demand of less than 220 Mbps at some time instances.

The simulation results show that network slicing can achieve performance gains due to pooling of resources while protecting the performance of individual network slices.

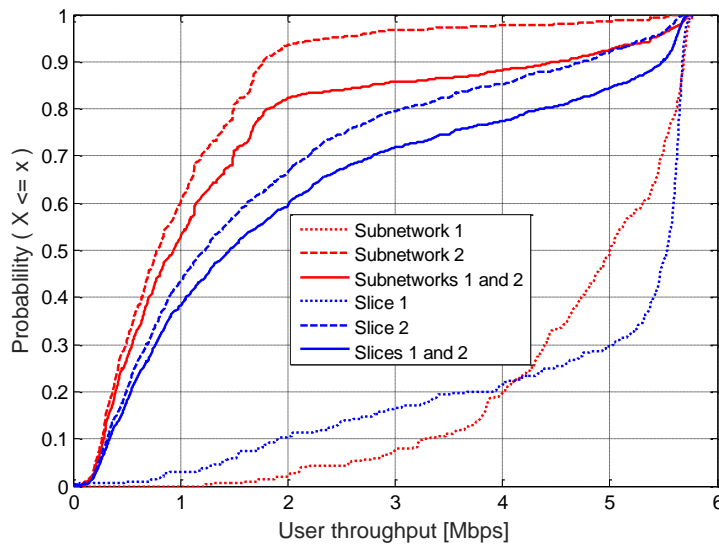


Figure 4-18. Simulation results of RRM for network slicing.

5 Conclusions

Deliverable D2.3 has presented the final METIS-II **performance evaluation framework**. The most novel feature and one of the major achievements of this framework is the final version of the RAN energy efficiency evaluation methodology.

A set of **inspection KPIs** was evaluated positively, confirming that the METIS-II technology proposals for 5G RAN design in [MII16-D22], [MII16-D31], [MII16-D41], [MII16-D51] and [MII16-D61] enable the fulfilment of the 5G system requirements.

Analytical **evaluation of KPIs** concluded the ability of the 5G RAN designed by METIS-II to fulfil the 5G system requirements. Evaluation results indicate that 5G RAN can deliver peak data rates at the order of 21 Gbps in DL and 12 Gbps in UL. Comparing to 4G operations, 5G RAN designed in METIS-II will also enable significant reduction of UP and CP latencies, down to 0.763 ms and 7.125 ms, respectively. In UP, it is of paramount importance the reduction of the sub-frame length to 0.125 ms. CP latency reduction was enabled by new RRC Connected Inactive state. It was also proved that for mMTC operations a single battery life time exceeding 10 years is possible for devices that sporadically upload the data to network.

Simulation-based evaluation for the five METIS-II 5G UCs has been conducted based on METIS-II and 3GPP performance evaluation framework. In those UCs, most of the METIS-II KPI requirements for 5G [MII16-D11] have been fulfilled using a subset of the TeCs proposed in the project, while some feasible solutions are envisaged for those requirements not met. In UC1, for dense urban environment and HetNet deployment, users can expect data rates above 300 Mbps and operators can support traffic volumes greater than 750 Gbps/km². In this UC, significant energy efficiency gains have been demonstrated as well. In UC2, high frequency bands and massive antenna systems enable Gbps data rates indoors, reaching up 7.85 Gbps (that is above the 5 Gbps target). In UC3, traffic volumes of 700 Mbps and 650 Mbps are supported in DL and UL for the required user data rates of 50 Mbps and 25 Mbps, considering an LTE system at 800 MHz with beamforming capabilities. With 3.5 GHz, UC3 required data rates can be supported with 10 times higher load. In addition, energy efficiency analysis shows that the system with beamforming consumes half the energy of the system without beamforming, when sleeping capabilities are considered. In UC4, it is shown that, depending on the traffic profile, 5G will cater for more than 1 million devices per km². For devices transmitting once every 100 s, proposed access scheme support more than 6.9 million devices per km². In UC5, reliability provided in urban scenarios for 5 ms end-to-end latency is close to 99.999% for the required range of 50 m. However, in the highway scenario, the required coverage range of 1000 m is far from the approximately 150 m obtained in this assessment.

From the isolated analysis of TeCs, some **key concepts** could be highlighted. The tight integration of 5G with LTE-A has proved to be useful in initial deployment phases. The new roles of infrastructure and user devices such as nomadic nodes, mobile relays, cluster heads etc., have demonstrated their ability to increase system performance (throughput, energy efficiency, etc.). The dynamic cell switch off is a powerful tool to increase energy efficiency when traffic load is not



high. Random access optimizations (based on grouping of accesses, preamble multiplexing, etc.) allow to increase the number of supported mMTC devices and to differentiate services appropriately. The AI flexibility, with regard to e.g. granularity of resources in frequency (bandwidths) or time (subframe durations), improves network and user performance in terms of e.g. data rates or latency, when handling different services at the same time. Traffic steering and network slicing enable tailored QoS support of different services. Harmonization of AIs is needed to facilitate an optimal RRM across different AIs. New waveforms that provide improved spectrum confinement, flexibility and better coverage (operating at lower SINR values for a given block error rate (BLER)) enable active interference design for additional ICI reduction. Finally, the RRC Connected Inactive state provides CP latency reduction and mMTC energy consumption improvements.

6 References

- [3GPP10-36814] 3GPP TR 36.814, "Further advancements for E-UTRA physical layer aspects (Release 9)", V9.0.0, Mar. 2010.
- [3GPP13-132030] 3GPP R1-132030. "Channel models for D2D performance evaluation", May 2013.
- [3GPP13-132394] 3GPP R2-132394, "Text proposal on UE power consumptions model for UEPCOP", Aug. 2013.
- [3GPP13-36872] 3GPP TR 36.872, "Small cell enhancements for E-UTRAN – Physical layer aspects (Release 12)", V12.1.0, Dec. 2013.
- [3GPP14-36843] 3GPP TR 36.843, "Study on LTE Device to Device Proximity Services (Release 12)", V12.0.1, Mar. 2014.
- [3GPP14-36866] 3GPP TR 36.866, "Study on Network-Assisted Interference Cancellation (NAIC) for LTE (Release 12)", V12.0.1, Mar. 2014.
- [3GPP15-150073] 3GPP RWS-150073, "RAN workshop on 5G: Chairman Summary", Sep. 2015.
- [3GPP15-152129] 3GPP RP-152129, "NGMN requirement metrics and deployment scenarios for 5G", Dec. 2015.
- [3GPP15-154981] 3GPP R1-154981, "Updated offline discussion summary on V2X evaluation assumptions", Aug. 2015.
- [3GPP15-36873] 3GPP TR 36.873, "Study on 3D channel model for LTE (Release 12)", V12.2.0, Jun. 2015.
- [3GPP15-36897] 3GPP TR 36.897, "Study on elevation beamforming / Full-Dimension (FD) Multiple Input Multiple Output (MIMO) for LTE (Release13)", V13.0.0, Jun. 2015.
- [3GPP15-36912] 3GPP TR 36.912, "Further Advancements for E-UTRA (LTE-Advanced) (Release 13)", V13.0.0, Dec. 2015.
- [3GPP15-45820] 3GPP TR 45.820. "Cellular system support for ultra-low complexity and low throughput Internet of Things (CloT) (Release 13)", V13.1.0, Nov. 2015.
- [3GPP16-165538] 3GPP Tdoc R2-165538, "State transition and small data transmissions for inactive UEs", Aug. 2016.
- [3GPP16-165850] 3GPP R1-165850, "WF on antenna placement in Indoor scenarios", May 2016.
- [3GPP16-23060] 3GPP TS 23.060, "General Packet Radio Service (GPRS); Service description; Stage 2 (Release13)", V13.8.0, Sep. 2016.



- [3GPP16-23401] 3GPP TS 23.401, "General Packet Radio Service (GPRS) enhancements for Evolved Universal Terrestrial Radio Access Network (E-UTRAN) access (Release 13)", V13.9.0, Dec. 2016.
- [3GPP16-24301] 3GPP TS 24.301, "Non-Access-Stratum (NAS) protocol for Evolved Packet System (EPS); Stage 3 (Release 13)", V13.6.1, Jun. 2016.
- [3GPP16-36104] 3GPP TR 36.104, "Base Station (BS) radio transmission and reception (Release 8)", V14.0.0, Jun. 2016.
- [3GPP16-36211] 3GPP TR 36.211, "Physical channel and modulation (Release 13)", V13.3.0, Sep. 2016
- [3GPP16-36213] 3GPP TS 36.213, "Evolved Universal Terrestrial Radio Access (E-UTRA); Physical Layer Procedure (Release 13)", V13.1.1, Mar. 2016.
- [3GPP16-36304] 3GPP TR 36.304, "User Equipment (UE) procedures in idle mode (Release 14)", V14.1.0, Dec. 2016.
- [3GPP16-36321] 3GPP TR 36.321, "Medium Access Control (MAC) protocol specification (Release 13)", V13.4.0, Dec. 2016.
- [3GPP16-36331] 3GPP TS 36.331, "Radio Resource Control (RRC); Protocol specification (Release 13)", V13.2.0, Jun. 2016.
- [3GPP16-36423] 3GPP TS 36.423, "X2 application protocol (X2AP) (Release 14)", V14.0.0, Sep. 2016.
- [3GPP16-36885] 3GPP TR 36.885, "Study on LTE-based V2X services (Release 13)", V14.0.0, Jun. 2016.
- [3GPP16-38900] 3GPP TR 38.900, "Study on channel model for frequency spectrum above 6 GHz (Release 14)", V14.1.0, Sep. 2016.
- [3GPP16-38913] 3GPP TR 38.913, "Study on Scenarios and Requirements for Next Generation Access Technologies (Release 14)", V14.0.0, Oct. 2016.
- [3GPP17-1700294] 3GPP, R1-1700294, "NR SS burst set periodicity", Jan. 2017.
- [3GPP17-1700309] 3GPP, R2-1700309, "Minimum system information", Jan. 2017.
- [3GPP17-1700329] 3GPP, R1-1700329, "Periodicity of synchronization signals", Jan. 2017.
- [5GCM15] "5G Channel Model for bands up to 100 GHz", White Paper, Dec. 6, 2015, <http://www.5gworkshops.com/5GCM.html>.
- [BRR+10] M. Bellanger, et al., "FBMC physical layer: a primer," PHYDAS, Jan. 2010.
- [CS15] H. Celik and K. W. Sung, "On the Feasibility of Blind Dynamic TDD in Ultra-Dense Wireless Networks," in IEEE VTC (Spring), pp.1-5, 11-14 May 2015.
- [ECC16-PT1083] ECC PT1 (16)083_A31, "Liaison Statement from ECC PT1 to ETSI ERM and 3GPP RAN on IMT 2020/ 5G spectrum in Europe", Apr. 2016.



- [ETSI-125951] ETSI Technical Report “Universal Mobile Telecommunications Systems (UMTS); FDD Base Station (BS) classification (3GPP TR 25.951 version 10.0.0 Release 10)”, May 2011.
- [FCL00] Y. Fang, I. Chlamtac and Y. Lin, "Portable movement modeling for PCS networks." IEEE Transactions on Vehicular Technology Vol. 49, no. 4, pp. 1356-1363, 2000.
- [HSL+14] S. Hong et al., “Frequency and Quadrature- Amplitude Modulation for Downlink Cellular OFDMA Networks,” IEEE Journal on Selected Areas in Communication, vol. 32, no. 6, pp.1256-1267, Jun. 2014.
- [ITUR08-M2135] ITU-R M.2135 “Guidelines for evaluation of radio interface technologies for IMT-Advanced”, 2008.
- [ITUR13-M2290] ITU-R M.2290-0 “Future spectrum requirements estimate for terrestrial IMT”, Dec. 2013.
- [ITUR15-M2083] ITU-R M.2083 “IMT Vision – Framework and overall objectives of the future development of IMT for 2020 and beyond”, Sep. 2015.
- [ITUR15-WP5D] ITU-R WP5D working document “Spectrum needs for the terrestrial component of IMT in the frequency range between 24.25 GHz and 86 GHz”, 2015.
- [ITUR17-C508] ITU-R WP5D Contribution 508 “Proposals for preliminary draft new Report ITU-R M.[IMT-2020.TECH PERF REQ], Feb. 2017.
- [ITUT12-G729] ITU-T Recommendation G.729 “Coding of speech at 8 kbit/s using conjugate-structure algebraic-code-excited linear prediction (CS-ACELP)”, Jun. 2012.
- [KS16] N. P. Kuruvatti, H. D. Schotten, “Framework to Support Mobility Context Awareness in Cellular Networks”, Vehicular Technology Conference Spring (VTC-Spring), Nanjing, China, May 2016.
- [KYK+15] K. Kim, Y. H. Yun, C. Kim, Z. Ho, Y. Cho, and J. Seol, “Pre-processing based soft-demapper for per-tone MIMO operation in QAM-FBMC systems,” in Proc. of 2015 IEEE 26th Annual International Symposium on Personal, Indoor, and Mobile Radio Communications (PIMRC), pp. 507-511, Hong Kong, China, Aug. 2015.
- [KZS16] N. P. Kuruvatti, W. Zhou and H. D. Schotten, “Mobility Prediction of Diurnal User Mobility for Enabling Context Aware Resource Allocation”, Vehicular Technology Conference Spring (VTC-Spring), Nanjing, China, May 2016.
- [LNS+14] M. Lauridsen, L. Noël, T. B. Sørensen, et al., “An empirical LTE smartphone power model with a view to energy efficiency evolutions”, Intel Technology Journal, vol. 18, no. 1, Mar. 2014.



- [MAG-D11] ICT-671650 mmMAGIC D1.1, "Use case characterization, KPIs and preferred suitable frequency ranges for future 5G systems between 6 GHz and 100 GHz", Nov. 2015.
- [MET13-D61] ICT-317669 METIS D6.1. "Simulation guidelines". ICT-317669 METIS Deliverable 6.1 Version 1, Oct. 2013.
- [MET14-D23] ICT-317669 METIS D23, "Components of a new air interface – building blocks and performance", METIS Deliverable D2.3 Version 1, Apr. 2014.
- [MET14-D32] ICT-317669 METIS D32 "First performance results for multi-node/multi-antenna transmission technologies", METIS Deliverable D3.2 Version 1, Apr. 2014.
- [MII16-D11] ICT-671680 METIS-II D11, "Consolidated scenarios, requirements, use cases and qualitative techno-economic feasibility assessment," METIS-II, Deliverable D1.1 Version 1, Jan. 2016.
- [MII16-D21] ICT-671680 METIS-II D21, "Performance evaluation framework," METIS-II, Deliverable D2.1 Version 1, Jan. 2016.
- [MII16-D22] ICT-671680 METIS-II D22, "Draft overall 5G RAN design," METIS-II, Deliverable D2.2 Version 1, Jun. 2016.
- [MII16-D31] ICT-671680 METIS-II D31, "5G spectrum scenarios, requirements and technical aspects for bands above 6 GHz," METIS-II, Deliverable D3.1 Version 1, May 2016.
- [MII16-D41] ICT-671680 METIS-II D41, "Draft air interface harmonization and user plane design," METIS-II, Deliverable D4.1 Version 1, May 2016.
- [MII16-D51] ICT-671680 METIS-II D51, "Draft Synchronous Control Functions and Resource Abstraction Considerations," METIS-II, Deliverable D5.1 Version 1, May 2016.
- [MII16-D61] ICT-671680 METIS-II D61, "Draft Asynchronous Control Functions and Overall Control Plane Design," METIS-II, Deliverable D6.1 Version 1, Jun. 2016.
- [NCK+14] H. Nam, et al., "A New Filter-Bank Multicarrier System for QAM Signal Transmission and Reception," in Proc. IEEE Intern. Conf. Commun. (ICC'14), Jun. 2014, pp. 5227–5232.
- [PBF+16] K.I. Pedersen, G. Berardinelli, F. Frederiksen, et al., "A Flexible 5G Frame Structure Design for Frequency-Division Duplex Cases", in IEEE Communications Magazine, pp. 53-59, Mar. 2016.
- [PFT+00] J. Padhye, V. Firoiu, D. F. Towsley, et al., "Modeling TCP Reno Performance: A Simple Model and Its Empirical Validation", in IEEE/ACM Trans. on Networking, Vol. 8, No. 2, pp. 133-145, Apr. 2000.



- [PME+16] A. Prasad, F.S. Moya, M. Ericson, R. Fantini, Ö. Bulakci, "Enabling RAN Moderation and Traffic Steering in 5G Radio Access Networks," 84th IEEE Vehicular Technology Conference, Montreal, Sep. 2016.
- [PNS+16] K.I. Pedersen, M. Niparko, J. Steiner, et al., "System Level Analysis of Dynamic User-centric Scheduling for a Flexible 5G Design", GLOBECOM, Dec., 2016.
- [PPS+16] G. Pocovi, et al., "On the Impact of Multi User Traffic Dynamics on Low Latency Communications", ISWCS, Sep. 2016.
- [RVX+16] A. Rico-Alvarino, M. Vajapeyam, H. Xu et al. "An overview of 3GPP enhancements on machine to machine communications", IEEE Communication Magazine, vol: 54, no. 6, Jun 2016.
- [SBS+17] T. Sahin, Ö. Bulakci, P. Spapis, et al., "Nomadic Nodes for Dynamic Radio Topology in 5G Wireless Networks: System-level Performance Evaluation," accepted to VTC 2017- Spring, Sydney, Australia.
- [SKM09] S. Singh, M Sathish Kumar, and H. S. Mruthyunjaya, "Effect of Peak-to-Average Power Ratio Reduction on the Multicarrier Communication System Performance Parameters," World Academy of Science, Engineering and Technology International Journal of Electrical, Computer, Energetic, Electronic and Communication Engineering, vol 3, no. 4, 2009.
- [SPE16-D51] ICT-671705 Speed 5G, "MAC approaches with FBMC and simulation results," Speed 5G, Deliverable D5.1 Version 1, Jun. 2016.
- [STB11] S. Sesia, I. Toufik and M. Baker, "LTE - The UMTS Long Term Evolution", second edition, Wiley, 2011.
- [SWS15] S. Saur, A. Weber and G. Schreiber, "Radio Access Protocols and Preamble Design for Machine Type Communications in 5G", in Proc. Forty-Ninth Asilomar Conference on Signals, Systems and Computers, Pacific Grove, California, pp. 8-12, Nov. 2015.
- [TLS+13] T. Tirronen, A. Larmo, J. Sachs et al., "Machine-to-machine communication with Long - term evolution with reduced device energy consumption", Trans. Emerging Tel. Tech., 2013.
- [WBK+16] P. Weitkemper, J. Bazzi, K. Kusume, A. Benjebbour and Y. Kishiyama, "On Regular Resource Grid for Filtered OFDM," in IEEE Communications Letters, May 2016.
- [WBK+16_2] P. Weitkemper, J. Bazzi, K. Kusume, A. Benjebbour and Y. Kishiyama, "Adaptive Filtered OFDM with Regular Resource Grid," in Proc. IEEE International Conference on Communications (ICC 2016) Workshop on 5G RAN Design, (Kuala Lumpur, Malaysia), May 2016.



- [WEB1] http://www.dlr.de/ts/en/desktopdefault.aspx/tabid-9883/16931_read-41000/
- [WEB2] https://www.metis2020.com/confluence/download/attachments/9667464/simplifiedTC2_Ped_sim180s_step0.1s_90peds_withAngles_bin.zip?version=1&modificationDate=1454021424000&api=v2
- [WIN10-D53] CELTIC CP5-026 WINNER+ Deliverable D5.3, "Final channel models", Version 1.0, Jun. 2010.
- [YKK+15] Y. Yun, C. Kim, K. Kim, Z. Ho, B. Lee, and J. Seol, "A new waveform enabling enhanced QAM-FBMC systems," in Proc. of 2015 IEEE 16th International Workshop on Signal Processing Advances in Wireless Communications (SPAWC), pp.116-120, Stockholm, Sweden, Jun. 2015.
- [YM16] Y. Qi, M. Tesanovic, "FQAM-FBMC Design and Its Application to Machine Type Communication," PIMRC, Sep. 2016.
- [ZN13] K. Zhou, N. Nikaein, "Packet aggregation for machine type communications in LTE with random access channel," in Wireless Communications and Networking Conference (WCNC), 2013 IEEE, pp.262-267, Apr. 2013.

A Annex: Final METIS-II 5G performance evaluation framework

A.1 Simulation KPIs

A.1.1 Detailed RAN energy efficiency evaluation procedure

Following assumptions are taken:

- Three different radio network load levels are evaluated to account for a temporal traffic variations during 24 hours.
- Two evaluation scenarios (e.g. Dense Urban and Rural) are evaluated to account for spatial traffic variations across the network (in line with 3GPP assumptions from [3GPP16-38913]).
- Radio network element goes immediately to the sleep mode when no resources are used for UL or DL data transmission.
- Power consumption during sleep mode is not related to duration of sleep cycle.
- Radio network element goes out of sleeping mode exactly in the TTI when its radio resources will be used for data transmission.
- RAN energy efficiency calculations are done jointly with simulations for evaluation of experienced user throughputs and traffic volume density.
- For 5G deployments either [MII16-D21] or [3GPP16-38913] settings should be used.
- For 4G deployments IMT-A evaluation assumptions [ITUR08-M2135] should be used and 3GPP Rel10 features.

Following steps should be done for calculation of 5G RAN energy efficiency improvements.

Step 1. Calculate traffic volume density for a 5G dense urban deployment according to procedure defined in [MII16-D21], and estimate corresponding packet inter-arrival time (IAT)

File size S is fixed to 3.5 MB, and load is increased by decreasing the packet IAT down from the arbitrary value. Traffic volume density is calculated using minimum IAT when network is able to maintain experienced user throughput at the minimum level of 300 Mbps in DL and 50 Mbps in UL with 95 % availability and retainability as defined in [MII16-D11]. Such IAT is denoted as minIAT

Step 2. Scale obtained IAT to calculate different load levels for 5G.

Two options are possible:

- Reuse [ES-202706] assumptions and calculate three load points by increasing miniIAT by 10, 3.333 and 2 with a_i load weights of 1/3, 5/12 and 1/4 respectively (cf. Step 6).
- Reuse [EAR10-D23] traffic profiles (cf. Figure A-1) and use calculated miniIAT as a setting for traffic profile at rush hour on 21:00 or 22:00 (16%). Calculate three load points with the weights of 1/3, 1/3 and 1/3.
 - Averaged traffic profile from 17:00 - 0:59 h = $(12+13+14+15+16+16+15+13)\%/8=14,25\%$. If 16% equals to miniIAT, then for calculation of RAN energy consumption at this load point use $IAT = \text{miniIAT} * 16 / 14.25$.
 - Averaged traffic profile from 1:00 – 1:59 h and 10:00-16:59 h equals to 10.25%. IAT for this load point is $\text{miniIAT} * 16 / 10.25$.
 - Averaged traffic profile from 2:00-9:59 h equals to 4.875%. IAT for this load point is $\text{miniIAT} * 16 / 4.875$.

Step 3. Repeat Step 1 and 2 to calculate IAT for rural 5G network deployments taking into account different experienced user throughput KPIs.

In step 1) experienced user throughput equals to 50 Mbps and 25 Mbps in DL/UL for rural.

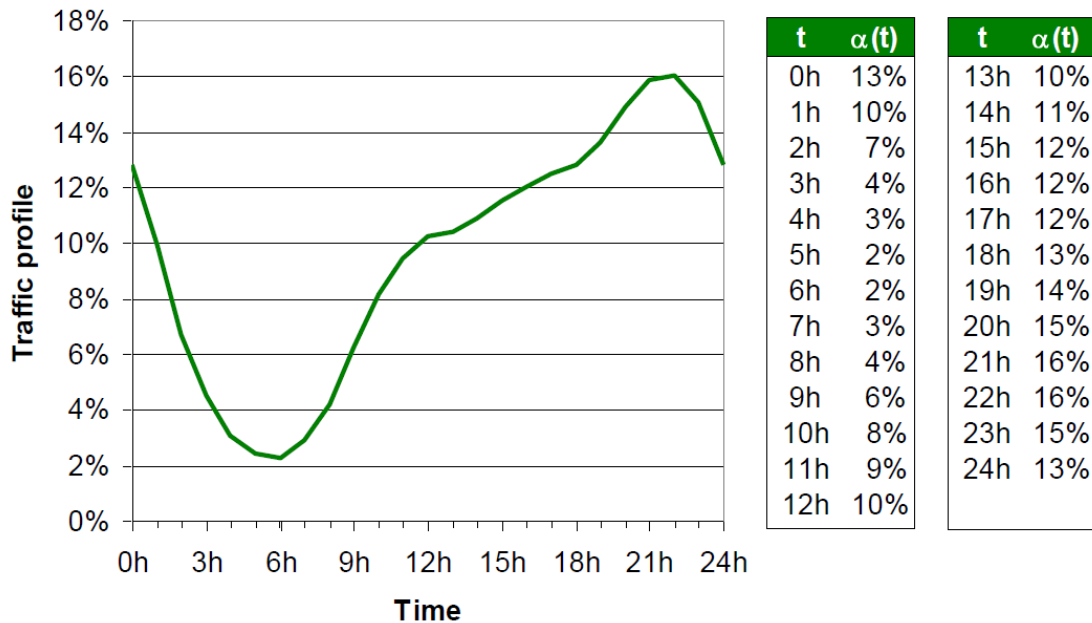


Figure A-1. Averaged daily traffic profile [EAR10-D23].

Step 4. Use calculated IATs/load points to obtain the total radio network power consumption at given load via simulations.

The overall power consumption behaviour of a BS is denoted as

$$P_{in} = \begin{cases} N_{sec}(P_0 + \Delta_p P_{max} \lambda \alpha_{PSD} + P_1 \lambda), & 0 < \lambda < 1 \\ N_{sec} P_{sleep}, & \lambda = 0 \end{cases}$$

where BS's energy consumption (EC) is proportional to the bandwidth load level λ . P_{max} is the maximum radio unit output power, while P_0 is the power consumption at the minimum non-zero output power due to load independent operation, P_{sleep} denotes BS power consumption in a sleep mode, α_{PSD} (power spectrum density ratio) is defined as the ratio of the actual power spectrum density to the one with maximum transmit power averaged on the whole bandwidth, N_{sec} is the number of sectors in the BS, Δ_p is the slope of the load dependent power consumption largely determined by the radio unit efficiency, P_1 is the baseband processing related power consumption. Use values from Table A-1.

Table A-1. Key parameters of BS power consumption model.

Name	Unit	5G Macro	5G Pico / small cell
P_{max}	W	46.0	21.0
P_0	W	44.7	3.2
Δ_p	a.u. (ratio)	3.5	2.2
P_1	W	2.2	0.3
P_{sleep}	W	27.1	2.2

As result of the simulation, following data should be obtained:

Table A-2. RAN energy consumption for a specific load and test environment in 5G.

Deployment scenario and load level	IAT (for calculation of exchanged bits)	RAN energy consumption EC_i [joules or watts * simulation time]
5G_Rural_IAT_for_load_1		
5G_Rural_IAT_for_load_2		
5G_Rural_IAT_for_load_3		



5G_Dense_urban_IAT_for_load_1		
5G_Dense_urban_IAT_for_load_2		
5G_Dense_urban_IAT_for_load_3		

Step 5. Redo Steps 1-4 for baseline 4G.

Use RMa (rural) and UMi (dense urban) environment as defined for IMT-A evaluation process. Use same parameter settings as in [ITUR08-M2135] for spectral efficiency calculations. The only difference is traffic (bursty traffic instead of full buffer).

Traffic for baseline is scaled as follows:

- Rural (RMa):

Traffic should be 1000 lower so for rural environment in 4G reduce the packet size to 350 kB (3.5 MB / 10) and $IAT_{4G_Rural_x} = IAT_{5G_IAT} * 100$.

- Dense urban (UMi):

There may be a different number of users in 5G and 4G deployment scenarios (in 4G UMi there are no small cells with users as in 5G Dense Urban). This has to be taken into account when scaling IAT/load level. Example below assumes that in 5G we have 4x as many users as in dense urban 4G deployment scenario (hexagonal macro layer is complemented with 3 outdoor small cells per macro sector, each cell has 10 users).

Traffic should be 1000 lower, so for dense urban environment in 4G reduce the packet size to 350 kB (3.5 MB / 10) and $4G_Rural_IAT_for_load_1 = 5G_Rural_IAT_for_load_1 * 100 * 4$.

As result of the simulation, following data should be obtained:

Table A-3. RAN energy consumption for a specific load and test environment in 4G.

Deployment scenario and load level	IAT (for calculation of exchanged bits)	RAN energy consumption EC_t [joules or watts * simulation time]
4G_Rural_IAT_for_load_1		
4G_Rural_IAT_for_load_2		
4G_Rural_IAT_for_load_3		
4G_Dense_urban_IAT_for_load_1		
4G_Dense_urban_IAT_for_load_2		

4G_Dense_urban_IAT_for_load_3

Step 6. Integrate results obtained with above-mentioned setups with different weights to calculate overall energy efficiency improvements of the network.

$$EE_{scenario} = \sum_{load\ level=i} a_i \frac{V_i}{EC_i}$$

$$EE_{global} = \sum_{scenario\ j} b_j EE_{scenario}$$

where a_i is a weight for load level i , b_j denotes the weight for deployment scenario j , V_i is aggregated throughput served in the simulated area for a load level i and EC_i is the power consumption of all RAN nodes in the simulated area for a load level i .

It should be noted that values of a_i and b_j are not yet defined and are subject of further discussion in METIS-II.

A.2 Simulation parameters for deployment scenarios

A.2.1 Synthetic deployment scenarios

Table A-4 contains general information on proposed synthetic deployments: InH, HetNet (consisting of UMa and Outdoor Small Cells (OSC)), UMa and RMa.

Table A-4. Simulation parameters for synthetic deployment scenarios in system level simulations.

Deployment scenario	InH	UMa	HetNet OSC	RMa
BS antenna height	3 m, mounted on ceiling	25 m, above rooftop	10 m on the lamppost / below the rooftop	35 m, above rooftop
Number of BS antenna elements (TX/RX)	Up to 256/256 >6 GHz Up to 16/16 <6 GHz	Up to 32/32	Up to 256/256 >6 GHz Up to 16/16 <6 GHz	Up to 32/32
Number of BS antenna ports	Up to 8	Up to 16	Up to 8 < 6GHz	Up to 8

BS antenna gain	5 dBi (per element)	17 dBi	5 dBi (per element)	17 dBi
Maximum BS TX power	40 dBm EIRP for >6 GHz (in 1 GHz), 21 dBm for <6 GHz (in 20 MHz)	49 dBm per band (in 20 MHz)	40 dBm EIRP for >6 GHz (in 1 GHz), 30 dBm <6 GHz (in 20 MHz)	49 dBm per band (in 30 MHz)
BS noise figure	5 dB	5 dB	5 dB	5 dB
Carrier bandwidth for evaluation (per BS)⁴	100 MHz at 3.5 GHz and 1 GHz at 70 GHz	Up to 10 MHz at 2 GHz for UC4 and UC5 Up to 100 MHz at 3.5 GHz for UC1	1 GHz at 25 GHz in UC1 10 MHz at 5.9 GHz for RSU in UC5	30 MHz at 800 MHz, assuming Carrier Aggregation with other bands

Indoor hotspot

The InH scenario consists of one floor of a building. The height of the floor is 3 m. The floor contains 16 rooms of 15 m x 15 m and a long hall of 120 m x 20 m.

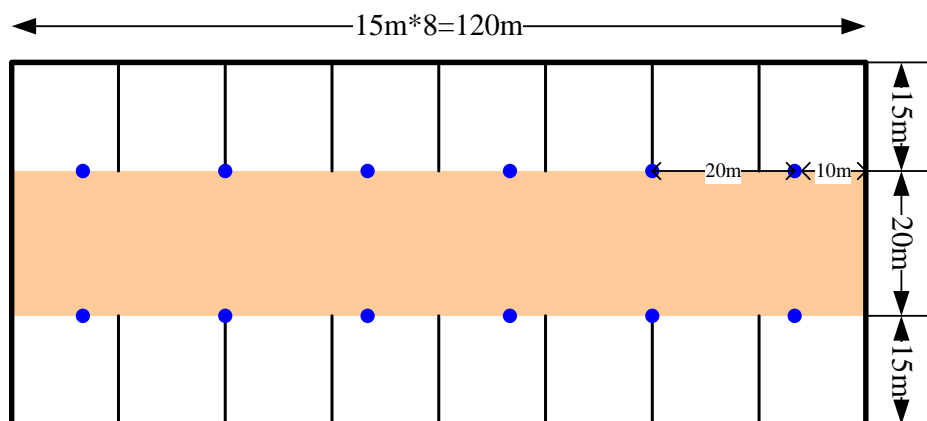


Figure A-2. Sketch of InH deployment.

⁴ The spectrum information used in this document on carrier center frequencies and carrier bandwidth sizes per each base station and access point are given as examples to be used only for 5G radio technology performance evaluation purposes. The amount of spectrum needed for 5G and what spectrum bands would be used for 5G are still under study.

Proposed BS network layout consists of small cells placed in the corridor, 6 along one long edge and 6 more along the other long edge, with the first site placed at 10 m with respect to the left side of the building (cf. Figure A-2).

Urban/Rural macro

UMa BSs are deployed in a regular, hexagonal grid as depicted in Figure A-3. BSs are connected to a set of 3 sector antennas, whose characteristics are defined in Annex A.2.2.

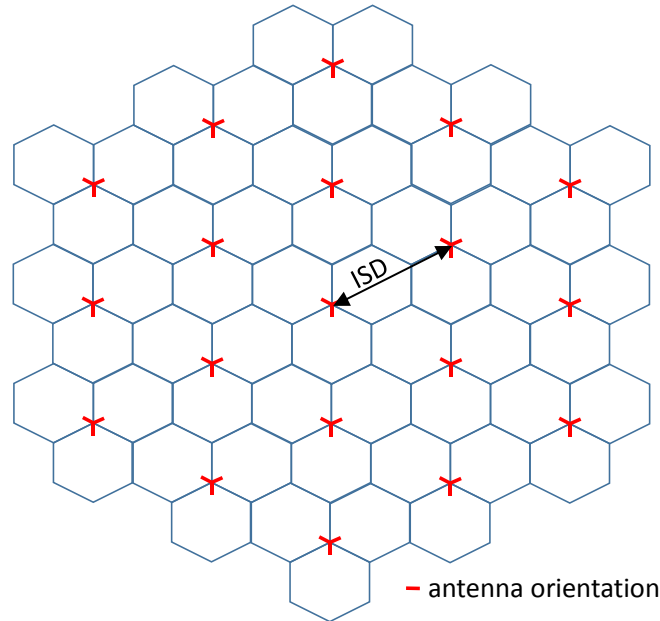


Figure A-3. UMa and RMa BS deployment and antenna orientation.

HetNet / Outdoor small cells

The HetNet scenario consists of two layers: UMa BSs and OSC. OSCs are deployed as outdoor BSs and are only considered as a part of HetNet deployment scenario. For UC1 each UMa cell is complemented with 8 OSCs randomly placed in the coverage area of the UMa sector. The constraint for the OSC deployment is that the distance between the OSC and the UMa BS must be greater than 55 m and the distance between the OSC (inter and intra UMa cells) shouldn't be smaller than 20 m (as OSCs are deployed as outdoor BSs, most likely by mobile network operators, it is very likely that similar limitations could be enforced by the operator). Number and deployment of OSCs configured in UC5 is for future studies. Each OSCs is equipped with omnidirectional antenna

A.2.2 BS antenna pattern

For UMa and RMa BS sector, the horizontal antenna pattern is specified as:

$$A(\theta) = -\min \left[12 \left(\frac{\theta}{\theta_{3dB}} \right)^2, A_{mh} \right]$$

Where $A(\theta)$ is the relative antenna gain in horizontal direction (dB), θ is the horizontal angle, θ_{3dB} is the 3 dB beamwidth and A_{mh} is the maximum attenuation of the antenna in the horizontal plane. For system level simulations in UMa values of $\theta_{3dB}=65^\circ$ and $A_{mh}=30$ dB shall be used [3GPP15-36897], whereas for RMa $\theta_{3dB}=70^\circ$ and $A_{mh}=25$ dB [3GPP10-36814].

For elevation angle antenna pattern is defined as:

$$A_e(\phi) = -\min \left[12 \left(\frac{\phi - \phi_{tilt}}{\phi_{3dB}} \right)^2, A_{mv} \right]$$

where $A_e(\phi)$ is the relative antenna gain in the elevation direction (dB), ϕ is the elevation angle, ϕ_{3dB} is the elevation 3 dB beamwidth, A_{mv} is the maximum attenuation of the antenna in the vertical plane and ϕ_{tilt} is the tilt angle that can be adjusted in each deployment scenario. For system level simulations in UMa values of $\phi_{3dB}=65^\circ$ and $A_{mv}=30$ dB shall be used [3GPP15-36897], whereas for RMa $\phi_{3dB}=10^\circ$ and $A_{mv}=20$ dB [3GPP10-36814].

The combined antenna pattern is computed as:

$$-\min[-(A(\theta) + A_e(\phi)), A_m]$$

where A_m is a maximum attenuation of the antenna equal to 30 dB for UMa and 25 dB for RMa.

For the InH and OSCs, the antenna pattern is assumed omnidirectional.

A.2.3 Realistic deployment scenarios

Indoor office

A realistic office environmental model is attained by explicitly considering walls, screens, desks, chairs and people. The environmental model geometry is given by the dimensions of the rooms, cubicle offices and tables. The width and depth of these objects are illustrated in the (3D sketch shown in Figure A-4, and the 2-dimensional (2D) sketch shown in Figure A-5.

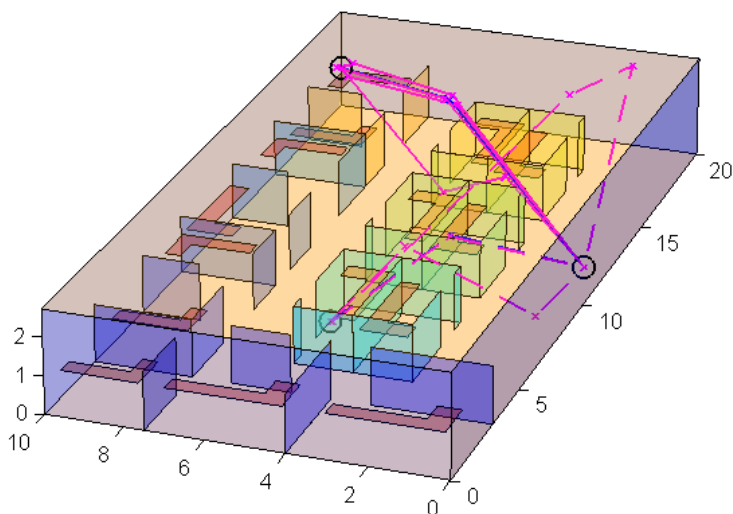


Figure A-4. 3D sketch of the realistic indoor office.

BSs have up to 256 antenna elements in above 6 GHz bands and up to 16 in below 6 GHz. Indoor office can be used for evaluation of UC2. Further information on the model can be found in Annex A.3.2.

Madrid Grid

Madrid Grid is a realistic extension of a popular Manhattan Grid model [ETSI-125951]. Its basic elements are regular, multi-storied blocks of different sizes and heights, park area, roads and pavements. This environment was developed in METIS project [MET13-D61] for the purpose of capturing dynamic traffic variations (in both space and time) in a typical European dense urban environment. Madrid Grid can be used for evaluation of UC1, UC4 and UC5. More details can be found in Annex A.3.1.

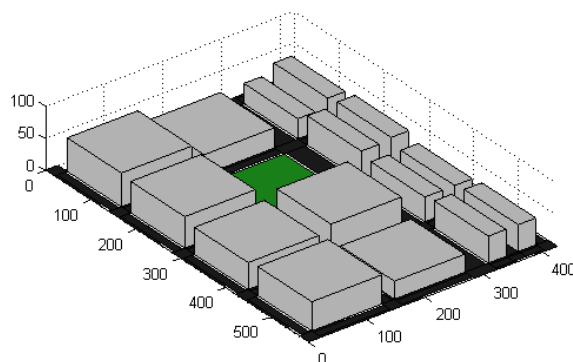


Figure A-5. 3D visualization of the Madrid grid.

Suburban and rural realistic scenarios

Past experience has shown that in congested scenarios system performance evaluated under real conditions can differ significantly from synthetic scenarios. This has motivated the adoption of real scenarios for xMBB UC1 and UC2. However, there is not a clear need for such realistic considerations in suburban or rural scenarios where coverage is the main challenge rather than the management of interferences. In this sense, METIS-II has not focused on the development of a realistic model for the equivalent of the RMa deployment. For interested readers, the closest model used in 5G-PPP (with some differences related to focus on suburban environment instead of rural one) is the Extended Suburban model developed in SPEED 5G project [SPE16-D51].

A.3 Models for individual use cases

In each individual UC, both synthetic and realistic deployment scenarios are considered. Therefore, simulations models are described in this section for both types of deployment scenarios. If not stated explicitly in the section below, following parameters should be assumed. UE height is considered as 1.5 m. UEs in every UC are equipped in 2D omnidirectional antenna (0 and 3 dBi gain for UC1-4 and UC5, respectively). UE noise figure is 9 dB. For all UCs apart from UC5 and evaluations in Madrid Grid, UE position is fixed and doesn't change throughout the simulation drop. In synthetic deployment scenarios for frequencies below 6 GHz ad 3D channel model from [3GPP15-36873] is recommended for macro UEs in UC1 and UC4, a 2D [3GPP10-36814] channel model for InH are used for UC2 (with 3D distances) and RMa for UC3.

For frequencies above 6 GHz, which corresponds to small cells, UMi extensions of ITU-R models provided in [5GCM15] are selected. For D2D transmissions [3GPP14-36843] models are recommended for frequencies below 6 GHz.

For realistic deployment scenarios ray-tracing based pathloss traces are recommended [MET13-D61]. Concerning small scale parameters characterization, this should be added on top of ray-tracing based pathloss traces. The models for small scale are the same of the synthetic case, that is [5GCM15] for above 6 GHz and [3GPP15-36873] for below.

Table A-5 provides info on system level simulation parameters that should be used for evaluation of individual UCs. Additional details and the models can be found in remaining part of this section.

Table A-5. System level simulation parameters for synthetic deployment scenarios.

Use case	UC1	UC2	UC3	UC4	UC5
Number of UE antenna elements (TX/RX)	16/16	16/16	8/8	2/2	2/4
Number of UE antenna ports (TX/RX)	8/8 for <6 GHz 4/4 for >6 GHz	8/8 for <6 GHz 4/4 for >6 GHz	4/4	1/1	1/2

UE maximum TX power	24 dBm	24 dBm	24 dBm	21 dBm	23 dBm
Min 2D UE-BS distance	10 m for OSC BS and 35 m for UMa BS	10 m	35 m	35 m	35 m

A.3.1 Dense Urban Information Society

User deployment

In synthetic deployment scenarios UEs (xMBB devices) are uniformly distributed across the cells. There are 10 UEs per macro cell and 5 UEs in OSC. Indoor UEs are uniformly distributed with the height of:

$$h_{UT} = 3(n_{fl} - 1) + 1.5$$

In equation above n_{fl} denotes the number of floors with uniform distribution between 1 and N_{fl} , where N_{fl} is the maximum floor number uniformly distributed between 4 and 8.

For realistic deployment scenario, the environment model defines a minimal layout of 0.25 km². Considering global user density of 200 000 users/km², the total number of UEs to simulate on such minimal layout is 50 000 users (total for outdoor and indoor).

Traffic model

For evaluation of capacity, full buffer traffic model in the synthetic deployment is used, in which an infinite amount of data is awaiting for transmission in the buffers. For evaluation of traffic volume density, experienced user throughput, latency and reliability, real traffic models are recommended, in particular the 3GPP FTP Model 3 [3GPP13-36872] depicted in Figure A-6. 3GPP FTP Model 3 defines bursty traffic where packets of fixed file size S arrive to the same source (UE, BS) according to a Poisson process with mean inter-arrival time D . Start of packet transmission is counted since the time it arrives at the queue.

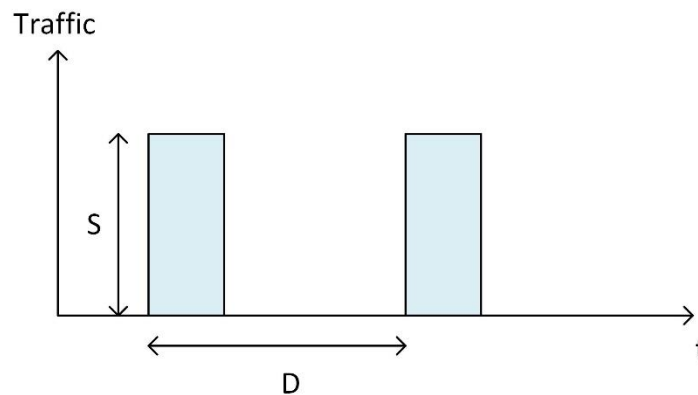


Figure A-6. Traffic generation of 3GPP FTP Model 3.

To calculate supported traffic volume density, file size S is fixed to 3.5 MB, and load is increased by decreasing the packet inter-arrival time, D , down from the arbitrary value. Traffic volume density is calculated using maximum packet inter-arrival time when experienced user throughput of devices at the level of 300 Mbps in DL and 50 Mbps in UL (or higher) and 95 % availability and retainability as defined in [MII16-D11]. For evaluation of latency and reliability it is assumed that once a file of 3.5 MB is generated, it reaches the radio access network as a burst of IP packets of 1518 B, assuming for those packets a data rate transmission over the backhaul of 10 Gbps.

Up to 10% of traffic can be transmitted using a D2D link.

A.3.2 Virtual Reality Office

User deployment

According to the mean user density required in [MII16-D11] ($1/10$ users/m²) and the area of the scenario (200 m² in realistic scenario and 6000 m² in synthetic scenario), 20 and 600 UEs (xMBB devices) should be generated in the scenario, respectively. However, in synthetic deployments in order to reduce the simulation complexity 10 UEs per cell could be used (120 per total simulation area). In realistic scenario, all rooms are occupied by 1 user except rooms R4 (2 users), R8 (2 users), and R12 (4 users). See the numbering of the rooms in Figure A-7.

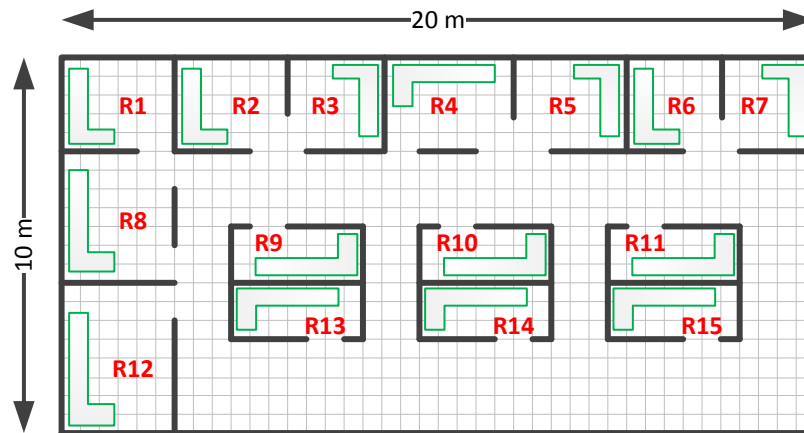


Figure A-7. Room numbering in realistic indoor office scenario.

Traffic model

Traffic is defined as in Annex A.3.1 with exception that experienced data rate for DL and UL as well as availability and retainability values are taken from Table 2-1 for this UC. To reach supported traffic volume of 0.1 Gbps/m² defined in [MII16-D11], average packet inter-arrival time for UL and DL should be equal to 29.3 ms for each 600 UEs in synthetic deployment scenario or 20 UEs in realistic deployment scenario.

Realistic scenario

For the simulation of indoor propagation, a real layout of the walls and materials used within the building is needed to compute the real losses with ray-tracing.

In order to perform the ray-tracing, a maximum number of reflections, as well as distance dependencies of free-space loss and material constants for penetration and reflection losses needs to be specified. Such information is provided in [MET13-D61].

A.3.3 Massive Distribution of Sensors and Actuators

User deployment

UEs (mMTC devices) are uniformly distributed across the UMa cell. Such cell cover the area of $\sim 0.072 \text{ km}^2$ and assuming a typical case of 3 operators per such area, 24 000 mMTC devices per single operator and cell are considered. Outdoor UEs are deployed at the height of 1.5 m.

Indoor UEs are uniformly distributed with the height

$$h_{UT} = 3(n_{fl} - 1) + 1.5$$

In equation above n_{fl} denotes the number of floors with uniform distribution between 1 and N_{fl} , where N_{fl} is the maximum floor number uniformly distributed between 4 and 8. Minimum distance between BS and UE is equal to 35 m.

Traffic model

Devices upload 125 B every 100 second. Uniform time offset between 0 and 1 sec is assumed at the beginning of the simulation to ensure even random traffic distribution in time.

Channel models

For indoor UEs O2I penetration losses is added for each link, modelled as $20 \text{ dB} + 0.5 * x \text{ [dB]}$, where x is an independent uniform random value between 0 and 25.

A.3.4 Connected Cars

The Connected Cars UC considers two different scenarios: an urban scenario and a highway scenario. In the urban scenario, both synthetic and realistic options are considered while only a synthetic case is defined in the highway scenario. The realistic scenario considers three types of vehicles: cars, buses and pedestrians. On the other hand, the synthetic scenarios only consider cars.

Deployment scenario

In the urban synthetic scenario, BSs are dropped according to synthetic deployment of HetNet configuration from Annex A.2.1.

In the urban realistic scenario, the base stations are placed according to the Madrid Grid realistic model described in Annex A.2.3

In the highway (synthetic) scenario, BSs are dropped according to synthetic deployment of RMa configuration from Annex A.2.1.

User deployment

In the urban synthetic scenario vehicles are dropped in roads in urban environment. Considered road configuration is shown in the Figure A-8 and has been defined according to the 3GPP model captured in [3GPP16-36885] for urban environment. Every road between the buildings contains two lanes per each direction (3.5 m width). Vehicles are dropped on roads according to a spatial Poisson process with an average inter-vehicle distance of 41.67 m (distance covered in 2.5 s at a speed of 60 km/h) in the middle of each lane. The number of vehicles is determined by the total length of roads and the mentioned average inter-vehicle distance. The total road length within the 433x250 m area formed by 1 building, its surrounding sidewalk and rings of lanes, is equal to 2684 m. Therefore, in each of these areas, 64.4 cars should be placed in average which is equivalent to 595 vehicles per km² in considered scenario. It is worth noting that [MII16-D11] foresees user vehicular densities in urban environments up to 1000 users per km². Therefore, the number used in this scenario is within the range set by [MII16-D11].

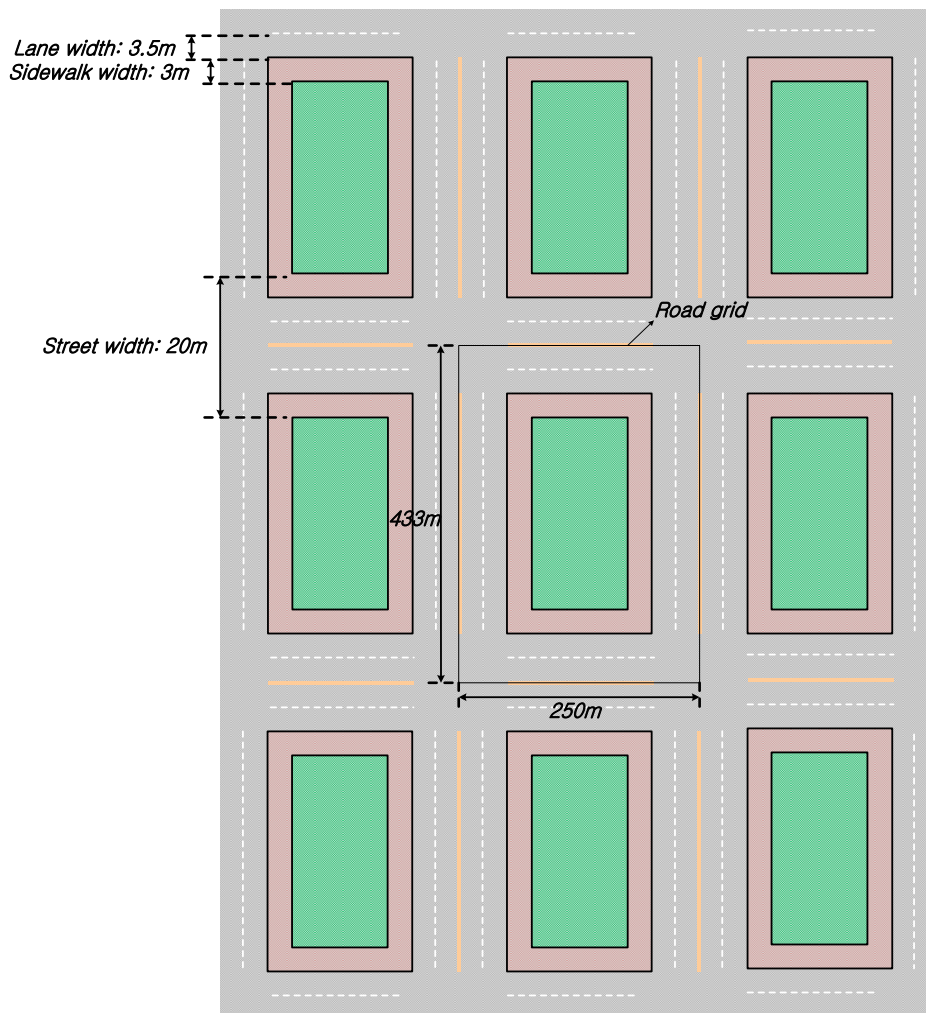


Figure A-8. Road configuration for urban traffic efficiency and safety evaluation [3GPP16-36885].

In the urban realistic scenario, cars are dropped in the roads of the Madrid Grid uniformly and placing the same number of users in each lane segment, where a lane segment is the part of a lane between two contiguous street crossings. Concerning the buses, one bus is dropped initially in the road segment of each bus stop. Finally, pedestrians are uniformly dropped in the sidewalks. The number of buses is determined by the number of stops in the Madrid Grid, i.e. 8, but the number of cars and pedestrians is configurable.

In the highway synthetic scenario, vehicles are dropped in the lanes of a highway deployment from [3GPP16-36885] illustrated in the Figure A-9. The depicted highway presents 3 lanes in each direction, with a lane width of 4 m. It is required to have a highway length of at least 2 km. Vehicles are dropped in the roads according to a spatial Poisson process with an average inter-vehicle distance of 97.22 m (distance covered in 2.5 s at a speed of 140 km/h). Therefore, 61.72 vehicles will be placed in average per each kilometre of highway. This value is in consonance with the values reflected in [MII16-D11].

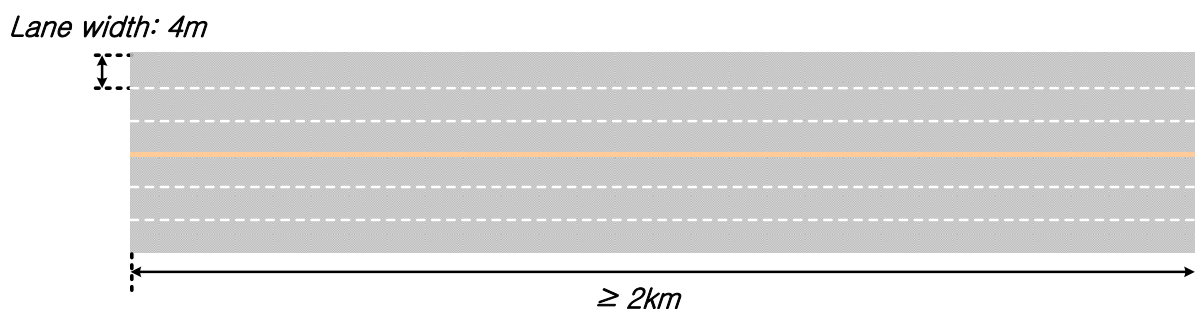


Figure A-9. Road configuration for highway traffic efficiency and safety evaluation [3GPP16-36885].

Figure A-10 depicts the exact location of the highway with respect to the Rural macro deployment scenario described in Annex A.2.1.

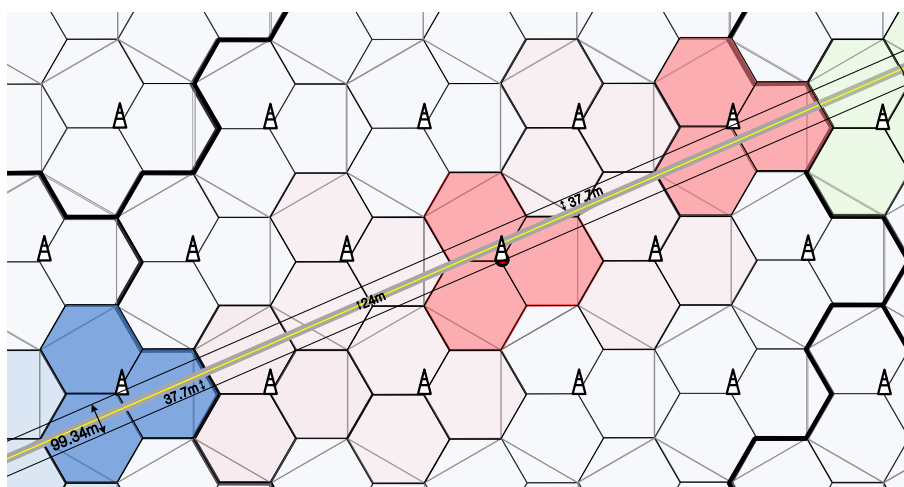


Figure A-10. Location of the highway in the deployment scenario [3GPP16-36885].



Mobility model

In the urban synthetic deployment scenario, vehicles move along the streets at 60 km/h. At the intersections, vehicles have 50% probability to go straight and 25% probability of turning left or right. Vehicle position is updated every 100 ms on the simulation.

In the urban realistic scenario, cars, buses, and pedestrians are dropped and move within the Madrid Grid according to car mobility models and traces described in [MII16-D21].

In the highway (synthetic) scenario, vehicles move along the lanes of the highway at 140 km/h. Vehicle position is updated every 100 ms of the simulation.

Traffic model

[MII16-D11] considers, for traffic safety applications, the following models:

- Periodic broadcast traffic consisting of at least 1600 B payload (for transmission of information related to 10 detected objects resulting from local environment perception and the information related to the actual vehicle) with repetition rate of at least 5-10 Hz.
- Event-driven broadcast traffic consisting of at least 1600 payload with repetition rate of at least 5-10 Hz (for transmission of information related to 10 detected objects resulting from local environment perception and the information related to the actual vehicle).

In 3GPP [3GPP16-36885] following assumptions are used:

- Periodic broadcast traffic consists of one 300 B payload followed by four 190 B messages. Message generation period is equal to 100 ms and the time instance of 300 B size message is randomized among the vehicles.
- Event-triggered traffic is triggered by event following Poisson process with varying arrival rate (up to individual choice). Each event generates 6 messages, 800 B each, with space of 100 ms

Channel models

In this section both the vehicle-to-vehicle channel and the vehicle-to-macrocell channel is considered. In addition, channel models have to be specified for the three considered scenarios.

In the urban synthetic scenario, for the vehicle-to-vehicle channel model, WINNER+ B1 Manhattan Grid layout model [WIN10-D53] shall be used for pathloss calculation. Pathloss at 3 m is used if the distance is less than 3 m. Shadowing should be lognormal with 3 dB standard deviation for LOS and 4 dB for NLOS. Shadowing should be spatially correlated according to the process defined in [3GPP16-36885] with correlation distance of 10 m. Fast fading should be implemented according to NLOS in Annex A.2.1.2.1.1 or A.2.1.2.1.2 in [3GPP14-36843] with fixed large scale parameters during the simulation. Channel is updated every 100 ms (after location update). The updating process is explained in [3GPP14-36843].

In the urban synthetic scenario, for the vehicle-to-macrocell channel model, UMa model in [3GPP15-36873] is used.



In the urban realistic scenario, for the vehicle-to-vehicle channel model, the default model for UMi in Manhattan scenarios [ITUR08-M2135] can be still applicable, with lower transmitter height plus 10 additional dB of attenuation in case of having other cars in the middle of the communication channel.

In the urban realistic scenario, for the vehicle-to-macrocell channel model, pathloss traces are available [MII16-D21]). Concerning small scale parameters characterization, this should be added on top of ray-tracing based pathloss traces.

In the highway scenario, for the vehicle-to-vehicle channel model, WINNER+ B1 LOS [WIN10-D53] shall be used for pathloss calculation with antenna height of 1.5 m. Pathloss at 3 m is used if the distance is less than 3 m. Shadowing should be lognormal with 3 dB standard deviation. Shadowing should be spatially correlated according to the process defined in [3GPP15-36885] with correlation distance of 25 m. Fast fading should be implemented according to NLOS in Annex A.2.1.2.1.1 or A.2.1.2.1.2 in [3GPP14-36843] with fixed large scale parameters during the simulation. Channel is updated every 100 ms (after location update). The updating process is explained in [3GPP14-36843].

In the highway scenario, for the vehicle-to-macrocell channel model, 3GPP RMa model defined in [3GPP10-36814] with 3D distances is recommended.

B Annex: METIS-II 5G evaluation

B.1 Control plane latency

Table B-1 shows assessment of CP delay for transition from RRC Idle to RRC Connected mode that was done by 3GPP for Rel 10 LTE-A and captured in [3GPP15-36912].

Table B-1. CP delay components of transition from RRC Idle to RRC Connected mode for LTE-A Rel 10 [3GPP15-36912].

Component	Description	Time (ms)
1	Average delay due to RACH scheduling period (1 ms RACH cycle)	0.5
2	RACH preamble	1
3-4	Preamble detection and transmission of RA response (time between the end RACH transmission and UE's reception of scheduling grant and timing adjustment)	3
5	UE processing delay (decoding of scheduling grant, timing alignment and Cell Radio Network Temporary Identifier assignment + L1 encoding of RRC CONNECTION REQUEST)	5
6	Transmission of RRC and Non-Access Stratum (NAS) Request	1
7	Processing delay in enhanced eNB (L2 and RRC)	4
8	Transmission of RRC CONNECTION SETUP (and UL grant)	1
9	Processing delay in the UE (L2 and RRC)	12
10	Transmission of RRC CONNECTION SETUP COMPLETE	1
11	Processing delay in eNB (Uu → S1-C)	
12	S1-C Transfer delay	
13	MME Processing Delay (including UE context retrieval of 10ms)	
14	S1-C Transfer delay	
15	Processing delay in eNB (S1-C → Uu)	4
16	Transmission of SECURITY MODE COMMAND and RRC CONNECTION RECONFIGURATION (+TTI alignment)	1.5
17	Processing delay in UE (L2 and RRC)	16
	Total delay	50

Components from Table B-1 were mapped into the CP latency evaluation procedure proposed for 5G in [MII16-D21] as depicted in Table B-2. Respective components for LTE-A approach

are mentioned in brackets (x), where x denotes respective component number. This procedure is equivalent to IMT-A evaluation method for CP latency captured in [ITUR08-M2135].

Table B-2. Evaluation of LTE-A and 5G CP latency for transition from RRC Idle to RRC Connected.

Step	Description	LTE-A delay components and latency	5G delay components and latency
0	UE wakeup time	Implementation dependent and neglected in further calculation 0 ms	Implementation dependent and neglected in further calculation 0 ms
1	DL scanning and synchronization + broadcast channel acquisition	UE in RRC Idle mode keeps listening to broadcast channel so delays related to DL scanning and broadcast channel acquisition are neglected in further calculations 0 ms	UE in RRC Idle mode keeps listening to broadcast channel so delays related to DL scanning and broadcast channel acquisition are neglected in further calculations 0 ms
2	Random access procedure	Assuming 1 ms scheduling request periodicity (cf. Table 10.1.5-1 in [3GPP16-36213]) it takes 0.5 ms for step (1), 1 ms sub-frame for transmission of (2), RA response is transmitted not sooner than after 3 sub-frames (cf. Section 5.1.4 in [3GPP16-36321]) (3,4), UE processing delay for (5) is 5 ms 9.5 ms	Shortening of a 5G sub-frame down to 0.25 ms result in (1), (2) and (3, 4) equal to 0.125, 0.25, 0.75 ms respectively. Assuming faster UE processing of step (5) is assumed to be to 1.25 ms 2.375 ms
3	UL synchronization	After RA procedures UL synchronization is achieved 0 ms	After RA procedures UL synchronization is achieved 0 ms
4	Capability negotiation + HARQ retransmission probability	1 sub-frame for transmission of RRC/NAS request in (6), 4 ms for L2 and RRC processing in eNB (7), 1 sub-frame for transmission of RRC CONNECTION SETUP and UL grant in (8), 12 ms of processing delay in the UE (9) (in Section 11.2 of [3GPP16-36331])	Shortening of a 5G sub-frame down to 0.25 ms can result in (6) and (8) equal to 0.25 ms, assuming faster processing of BS and UE, delay associated with components (7) and (9) result in latencies of 1 and 3 ms, respectively

		the maximum delay of this step is 15 sub-frames) 18 ms	4.5 ms
5	Authorization and authentication/ key exchange + HARQ retransmission probability	Components (11-14) in LTE-A done in parallel to step 4 0 ms	Components (11-14) done in parallel to step 4 0 ms
6	Registration with the BS + HARQ retransmission probability	1 sub-frame for transmission of (10) and 4 ms for (15) 5 ms	Assuming 0.25 ms sub-frame give 0.25 ms for (10) and with faster processing in BS (15) is shortened to 1 ms 1.25 ms
7	RRC connection establishment/ resume + HARQ retransmission probability	1 sub-frame for transmission of (16) and 0.5 sub-frame for TTI alignment and 16 ms for (17). In Section 11.2 of [3GPP16-36331] maximum delay for (17) is equal to 20 sub-frames 17.5 ms	Assuming 0.25 ms sub-frame we can reduce (16) to 0.375 ms and with better UE processing capability (17) as short as 4 ms is assumed 4.375 ms
	Total delay	50.0 ms	12.5 ms

Based on given calculations total CP latency for LTE-A Rel 10, when going from RRC Idle to RRC Connected, is equal to 50 ms and for 5G it can be as low as 12.5 ms.

B.2 UC2

UC2 evaluation based on Section 3.3.2 assumptions but with carrier frequency of 30 GHz is given in Figure B-1 and Figure B-2.

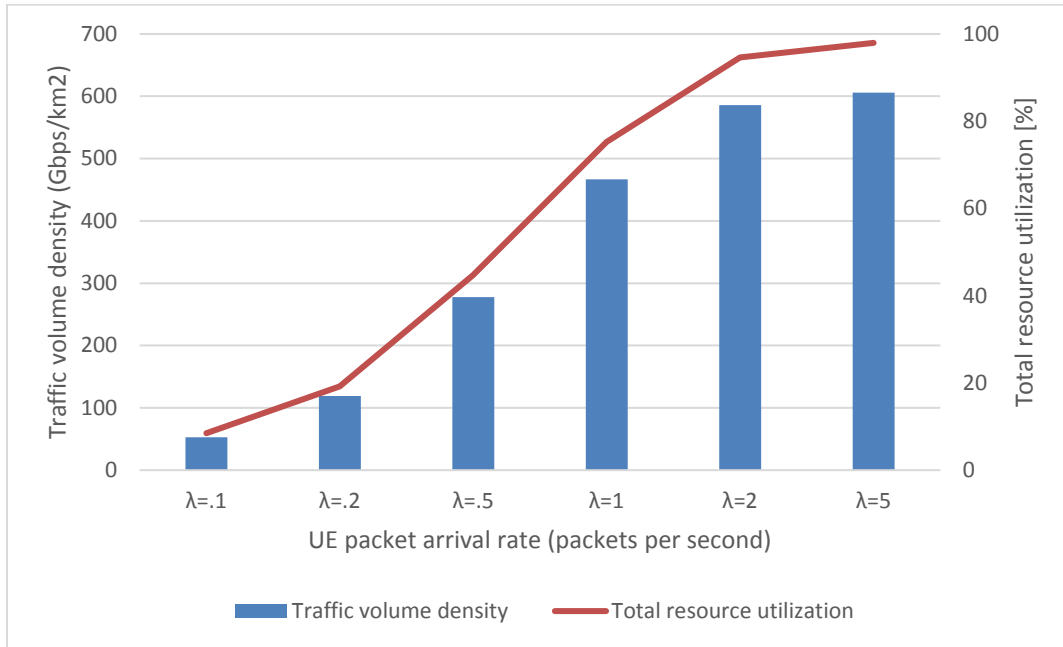


Figure B-1. Traffic volume density and resource usage in UC2 for carrier frequency of 30 GHz.

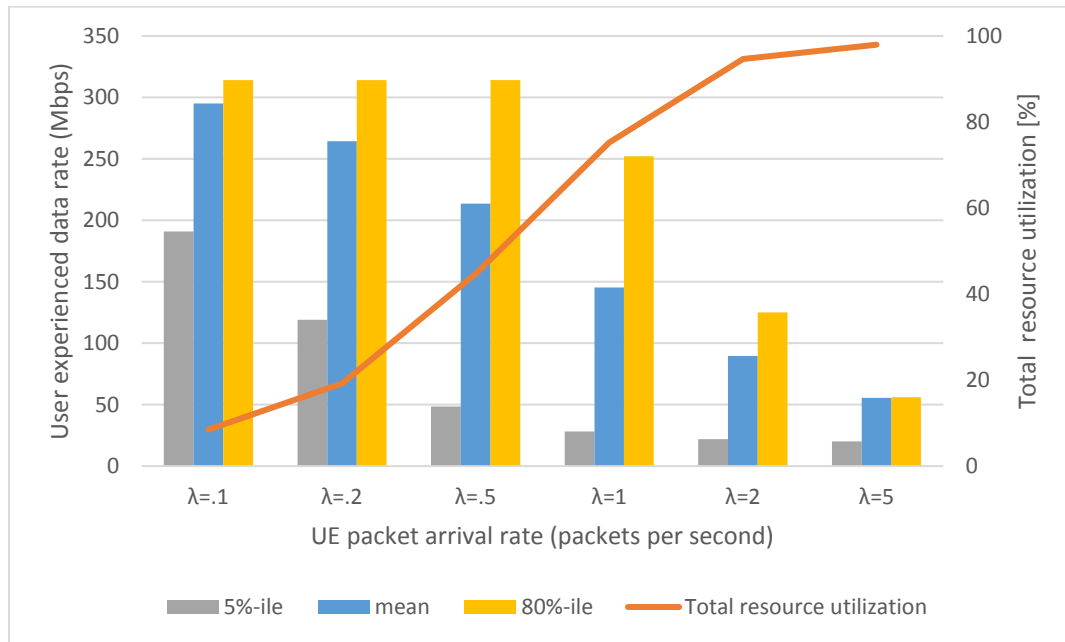


Figure B-2. User experienced data rate and resource usage in UC2 for carrier frequency of 30 GHz.

B.3 UC4

This study evaluates the UL direction of a 5G RAN carrying IoT sensor or actuator traffic. 10 MHz of bandwidth is assumed and an LTE resource structure, i.e. 50 PRBs, each consisting of 12 subcarriers and 14 OFDM symbols (3 out of 14 OFDM symbols are used for pilots and sounding leaving $11 \times 12 = 132$ resource elements per PRB for mMTC data transmission). 48 PRBs are used for small packet access. 2 PRBs are reserved for further UL signalling, e.g. for handover signalling, which is not considered in this study. The PRBs in one sub-frame are subdivided into a number of SPBs as depicted in Figure B-3. In our study one SPB of size 6 PRBs is dedicated to resource requests ($M_R = 1$), while 6 SPBs of size 7 PRBs each are dedicated to data transmission ($M_D = 6$).

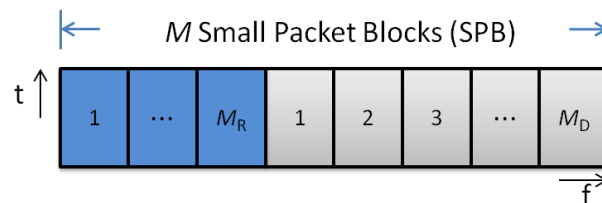


Figure B-3. One TTI with M SPBs used for resource requests and data transfer.

A short packet from mMTC device consist of 840 data bits and is sent using QPSK modulation scheme with a code rate of 0.45. The request message is a Zadoff Chu preamble [3GPP16-36211] and does not contain any further information about the requesting UE. The UE randomly chooses one out of the (at maximum) 64 preambles. The BS is able to detect that a certain

preamble is used, but it cannot detect if there is a collision on that preamble. The capturing effect is considered, i.e. in some cases it is possible that a collided data transmission is received correctly, but any parallel transmission using same resources is lost.

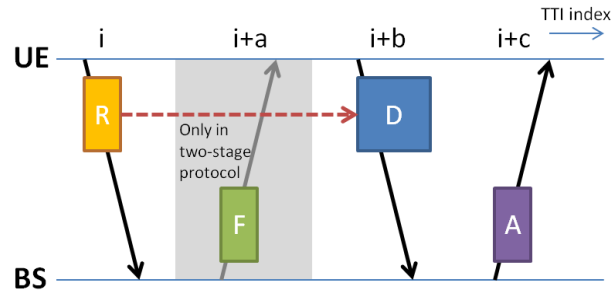


Figure B-4. Basic message flow of one-stage and two-stage radio access protocols.

Three basic access procedures were assessed, namely one-stage access, two-stage access with tagged resources, and two-stage access with pooled resources. In case of one-stage access, the request is transmitted in the same sub-frame as the data resources. Hence in this case, as depicted in Figure B-4 the feedback message (F) is omitted and the delay b is equal to 0. In contrast to this, in case of two-stage access, the UE sends a scheduling request (R), i.e. a randomly chosen preamble, waits “ a ” sub-frames for a feedback message and, after a further predefined delay transmits the data (D). In both cases transmission is finalized by an acknowledgement (A). In case of “tagged” resources, a unique set of preambles point to one unique data resource. In case of “pooled” resources an arbitrary resource may be assigned to a successful preamble. Consequently, in a “tagged” protocol, the mobile applies for a certain data resource. In a “pooled” protocol, a scheduler decides about data resource assignment. For further details please refer to [SWS15].

C Annex: Performance of METIS-II key 5G RAN components

C.1 xMBB

C.1.1 Tight integration of 5G with LTE-A

Different realizations of tight integration have been evaluated using a system-level simulator. The concepts that are compared are the HH, fast switch (FS) of the UP, and DC [MII16-D61]. In the simulation environment there are 7 BSs with 3 sectors each and the ISD is 500 m. LTE and 5G radio nodes are co-sited, and each one operates using 20 MHz bandwidth. The 5G AI utilizes 0.2 ms TTI and 20 sub-bands (which corresponds to an LTE RB) per 20 MHz, while LTE utilizes 100 sub-bands and a TTI of 1 ms. The radio channel model is the 3GPP Case 1 UMa channel model [3GPP10-36814] where the attenuation constant is modified according to the carrier frequency (cf. Table C-1). Signalling is assumed ideal, i.e., all RRC messages are always received correctly, therefore there are no handover failures. Remaining parameters used in simulations are captured in Table C-1.

Table C-1. Simulation parameters for evaluation of tight integration of 5G and LTE.

Parameter	LTE	5G AI
Carrier frequency	2 GHz	15 GHz
Attenuation constant	-15.3 dB	-33.7 dB
BS TX power (equivalent isotropical radiated power)	40 W	40 W
Traffic model	FTP download of one 10 MB packet per UE	
UE velocity	10 m/s	
Backhaul	Ideal	
AIV selection	Best RSRP	
DC selection	Best reference signal received quality	

C.1.2 Diurnal mobility prediction to assist context aware RRM

The scenario considered in Section 4.1.4 is shown in left part of Figure C-1. The scenario has 25 crossroads and 7 landmarks (pinpoints). There are 6 coverage holes present in the simulation scenario at different roads shown as tunnels in the figure.

Right part of Figure C-1 shows an example of the application of this TeC where a vehicle is predicted to traverse a coverage hole.

In the simulations conducted for this TeC, there were 12 micro BSs with LTE-A technology (bandwidth of 10 MHz, 50 PRBs at 2 GHz carrier frequency). See more details in [KS16].

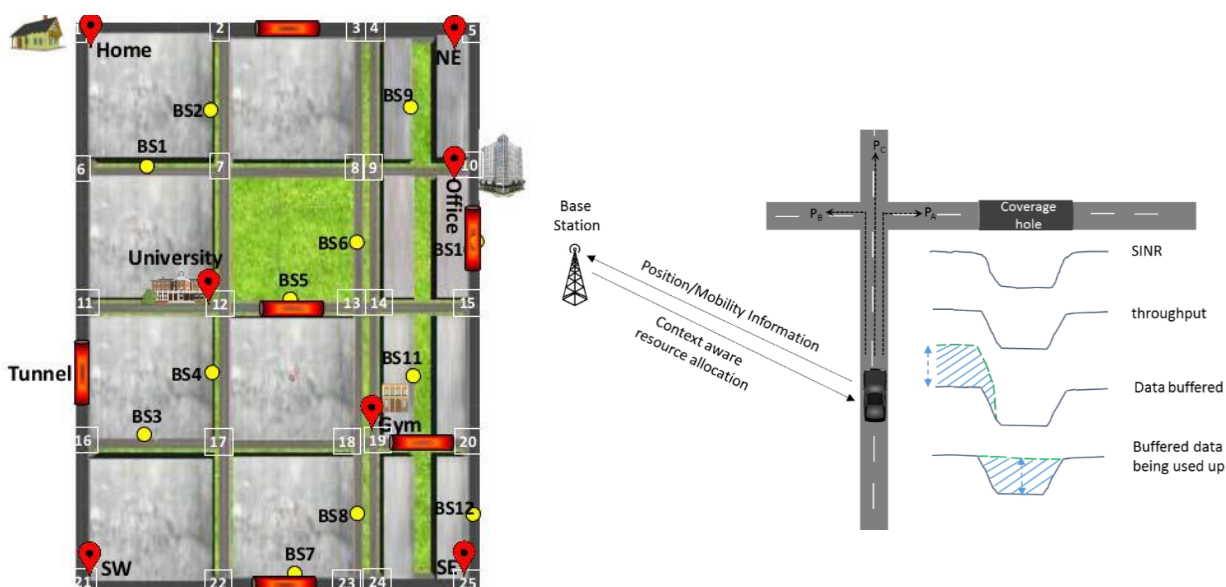


Figure C-1. Considered scenario with landmarks and coverage holes (left), and context aware radio RRM (right).

C.1.3 5G user-centric interference management in UDNs

In the first case study, the key interference management mechanisms applied are JT between the access links of NNs (i.e., between NNs and UEs) when it is possible. The selection of candidate UE for JT is based on the difference of RSRP measurements from serving and neighbouring NNs. Given the number of UEs experiencing low channel quality, a number of RBs is reserved for JT, and resource allocation between different NNs is done. For remaining UEs, interference management is applied, where dynamic frequency partitioning or muting of resources for some NNs is performed [MII16-D51].

For the first case study as described in Section 4.1.5, system-level Monte Carlo simulations were performed to evaluate the performance in proposed scenario with different number of activated

NNs (1-5) and 25 UEs were randomly dropped in a hotspot area at the edges of the macro BS. For the simulation set-up, we used the Madrid Grid deployment (cf. visualization shown in Figure C-2) and radio channel models from 3GPP [3GPP10-36814] (UMa for macro BS and UMi for NNs). Macro BS operates at 2 GHz carrier frequency, while the NNs utilize spectrum at 3.5 GHz with full frequency re-use. Both access node types operate with 20 MHz bandwidth available. Ideal backhaul is assumed for the NN-macro BS links and Round Robin algorithm is used for scheduling.



Figure C-2. Visualization of user-centric interference management in Madrid Grid deployment considering dynamic radio topology based on NNs.

In the second case study as described in Section 4.1.5, a dynamic system-level HetNet simulator is employed [SBS+17]. Picocells and VNNs are deployed on top of a wrapped-around hexagonal grid consisting of 19 tri-sectored macro BSs. A section of the considered network is shown in Figure C-3. The simulator also features the enhanced inter-cell interference coordination (eICIC). This coordination involves two controllable parameters which are the almost blank subframes (ABS) ratio of the macro BSs and the cell range extension (CRE) bias of the pico BSs or the NNs. ABS ratio is the percentage of muted subframes at the macro BS to reduce the interference on DL and CRE allows the deployed small nodes to extend their coverage by increasing the offset value which increases the attachment probability of the UEs in order to offload macro BSs. The selected parameters for the experiments are provided in Table C-2. Furthermore, the uplink

throughput gains for different number of access node activation are provided in Figure C-3. It can be seen that by activating the NNs, it is possible to provide a high capacity gain of 183% at the lower (10%-ile) of the user throughput CDFs, compared to the picocell deployment.

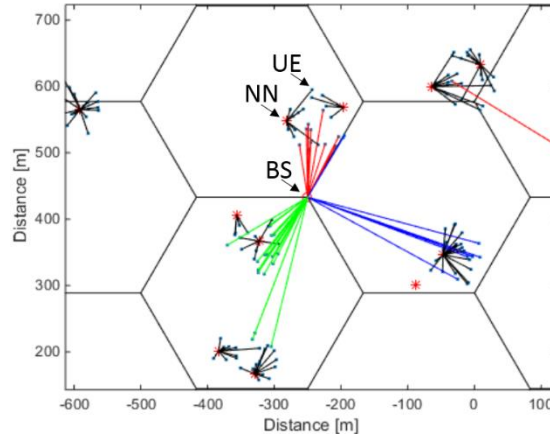


Figure C-3. A section of the network showing the links between the UEs (blue dots) and the NNs (red stars) as black lines, and the links between the UEs and the macro BSs (red circles at the centre of each site) as coloured lines.

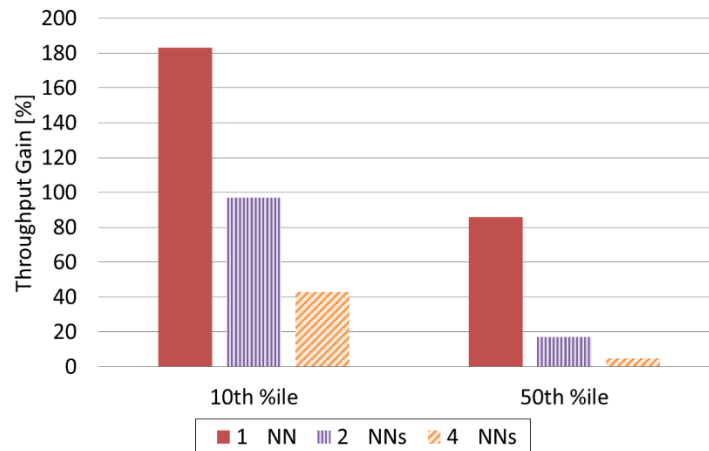


Figure C-4. The uplink throughput gain of the NN deployments compared to picocell deployments in the 10%-ile and the 50%-ile of the CDFs (case study 2).

Table C-2. Simulation parameters for evaluation of user-centric interference management in UDN.

Feature	Implementation
Network topology	Wrapped-around hexagonal grid of 19x3=57 macrocells; randomly placed picocells and VNNs, the latter being 20 per macrocell in average
UE layout and load	Randomly dropped hotspots, 1 per macrocell in average, containing 25 and 50 UEs in UL and DL, respectively; indoor UEs (20 dB penetration loss)
ISD	500 m
System bandwidth	20 MHz and 10 MHz in UL and DL, respectively; centered at 2.6 GHz; FDD
Frequency reuse	1
eICIC parameters	CRE offset of 12 dB and ABS ratio of 25% and 50% in UL and DL, respectively
Traffic type	FTP
Scheduler	Proportional fair
Shadowing	Log-normal shadowing fading with standard deviations 8 dB macro BS to UE, 10 dB pico BS to UE and 7 dB VNN to UE; Shadowing decorrelation distance of 50 m
TX Powers	Macro BS: 46 dBm; Pico BS: 30 dBm; VNN: 30 dBm; UE: max 23, min -40 dBm with UL power control
Antennae	Gains: macro BS 14 dBi, pico BS 5 dBi, VNN 5 dBi and UE 0 dBi; Heights: macro BS 32 m, pico BS 5 m, VNN 1.5 m and UE 1.5 m
Receiver	1x2 Maximal Ratio Combiner
Modulation	QPSK, 16QAM and 64QAM

C.1.4 Dynamic cell switch off

This TeC was evaluated in terms of the overall power consumption of BSs in the considered scenario as a benchmark. This was achieved using power models specified in METIS-II for 2020 equipment [MII16-D21]. According to these power models, the overall energy consumption of a macro or micro BS increases linearly with the total amount of radio resources used for transmission. When no transmission is performed, the BS can enter a sleep-mode that further reduces its consumption.

Simulation results were obtained in the simplified Madrid Grid scenario that was proposed in [MET14-D32]. The scenario reproduces an urban environment with 3 macro and 9 micro BSs, serving 10 outdoor UEs each, and operating in a 10 MHz bandwidth. A simple single input single output transmission scheme is considered. Omni directional antennas are assumed for micro BSs, while directional antennas are used for macro BSs. Large scale fading follows the PS1 and PS3 models as in [MET13-D61], and small scale fading has a time-correlated Rayleigh distribution (velocity of 3 km/h is assumed).

To evaluate the network capability to switch off unnecessary nodes, different traffic load conditions are considered by assuming CBR traffic sources for each user. As a reference, also full-buffer traffic condition has been considered, even if in this case the proposed algorithm cannot switch off any cell, so no gain in energy consumption can be achieved.

The main focus of the proposed scheme is to reduce energy consumption through the reduction of the number of active nodes as already shown in Section 4.1.6. This reduction could be achieved without impacting the delivered data rates as long as the served traffic is not too high, as shown in Figure C-5. The scheduler's metric used in the EE JT scheme favors energy savings over capacity, and prioritize UE transmissions that allows reducing the number of active nodes rather than maximize capacity (or other capacity related metrics as in the Proportional Fair algorithm). However, in full buffer simulations (i.e. in high load conditions), no node can be switched off, since all are needed to cater for the high traffic, and the set of users selected by the EE JT scheduler turns out to be suboptimal. In such cases other scheduling approaches should be exploited.

As the proposed solution operates in the MAC layer, a centralized-RAN architecture is preferred, where the scheduling is performed in a central unit that controls resource allocation for a large number of nodes. Additionally, a mechanism is needed to assess channel quality also for the nodes that are switched off (e.g., through the transmission of periodic beacons as suggested in [MET14-D32]).

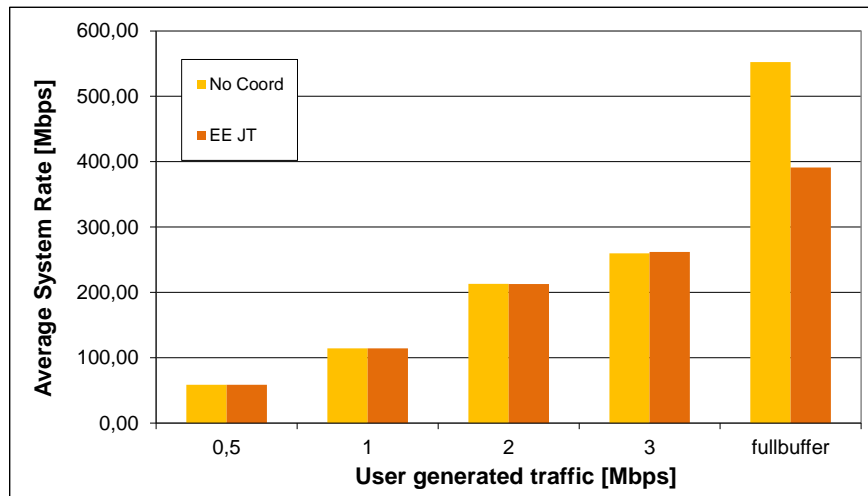


Figure C-5. Average system rate achieved with the coordinate approach.

C.1.5 Mobility management framework for D2D communication

In V2V communication scenarios, mobility impacts the reliability of D2D links. Consider the following scenario in a legacy network (i.e., LTE or LTE-A): two vehicles, connected via D2D and moving in the same direction while keeping a distance apart from each other, hand over their CP connections to a common target BS one after the other at different moments. During the time between the first handover and the second handover communicating vehicles remain in different cells and D2D communication between the vehicles in UP is disrupted, e.g., due to different D2D resource allocations in different CPs. Therefore, data packets are dropped during the disruption time.

Using D2D mobility management approaches proposed in [MII16-D22] and [MII16-D61], possible D2D communication disruption time due to handover can be reduced by enabling two devices to jointly select and switch to the same target BS at the same time. Consequently, the disruption impact of an active D2D communication can be controlled to a lower level. This implies an improvement on reliability of the D2D communication.

We compare the proposed method mentioned above with the legacy method. The legacy method is the one currently specified in 3GPP LTE or LTE-A network [3GPP16-23401], whereas the proposed method is above mentioned joint mobility management method. We assume that the interruption time that device experiences during handover in either of the methods follows an identical handover delay probability distribution, which thus causes D2D communication disruption. Specifically, the handover delay (i.e., interruption time) is defined to be a gamma distribution which is a proper probability distribution to simulate the delay of a series of signalling exchanges of a handover [FCL00]. Specifically, we use a gamma distribution with the scale parameter set to 2 and various shape values so as to simulate signalling delay between base stations and between a base station and a device.

As defined in [MII16-D21], the reliability accounts for the percentage of packets properly received within the given maximum E2E latency (OTT or RTT depending on the service).

To evaluate the performance of proposed solution, Voice over Internet Protocol (VoIP) packet delivery based on G.729 [ITU12-G729] for D2D transmission is simulated. In addition, the maximum E2E latency (i.e. from D2D sender to D2D receiver) is set to 20 ms for VoIP packet freshness. The Madrid Grid [MET13-D61] [WEB2] is used as the simulation environment in which 8 BSs (pico cells) are deployed along the roads surrounding the park area (green colour), as presented in Figure C-6 (a). Precisely, four of them are located at the corners and the other four are at the middle of the four edges.

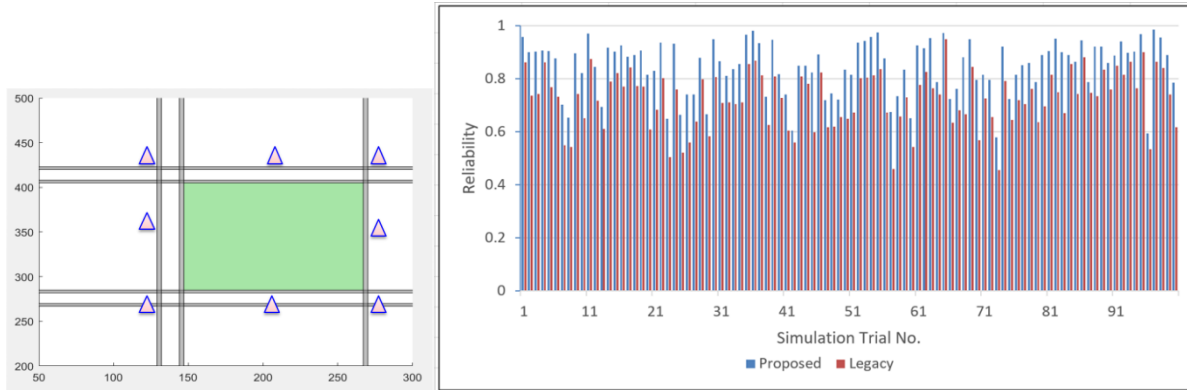


Figure C-6. (a) Considered BS deployment in Madrid grid, (b) D2D packet reception reliability for legacy and joint mobility methods over 100 simulation trials.

We first conducted a simulation with 90 devices. In the beginning of the simulation, 40 device pairs out of the 90 devices are randomly selected and each pair has its connection established. In addition, a pair is set to communicate in D2D mode if their received signal strength is strong enough; otherwise, they communicate in cellular mode, i.e., through infrastructure. During simulation time, each pair dynamically switches between D2D mode and cellular mode based on their received signal strength.

Figure C-6 (b) shows the evaluation results for D2D packet reception reliability in both mobility methods, where the packet reception in cellular mode is omitted in the evaluation. The simulation results indicate a big improved in packet reception reliability for proposed method. The reason is that proposed method enables both devices participating in D2D communication switches to the target base station simultaneously, thus minimizing the D2D link disruption time. Therefore, device pairs in the joint method encounter less packet drop.

To investigate the direct causes that impact reliability, we further conduct a simulation for one-pair D2D scenario in which there is only one pair of devices circulating along the green square in Figure 4-7 (a). Three factors are investigated in the simulation, including device velocity, inter-device distance and handover delay. During the simulation, the two devices keep a fixed inter-device distance at a fixed device velocity while moving along the square, where handover delay still follows an identical gamma distribution during simulation.

Figure 4-7 (b) shows the simulation results where the device velocity is noted as v in kilometre per hour, inter-device distance is in meter (m) and handover delay is noted as t in mini-second.

The legend format for a simulation case is $x-(v=y \text{ km/h}, t=z \text{ ms})$, where x is either the proposed or the legacy methods, y is the value of device velocity v and z is the value of handover delay t . From the simulation results, we observe that the reliability of the proposed method is higher than that of the legacy method. Specifically speaking, the proposed method ensures a reliability more than 95% when inter-device distance is smaller than 40 meters, while the legacy method achieves a reliability 80%~90% only when inter-device distance is within 10 meters. Basically, an increasing inter-device distance results in reliability degradation for all cases. This is because a long inter-device distance makes the two D2D devices easily distributed to different cells. However, the proposed method still maintains a good reliability since the two D2D devices in the proposed method select and switch to the same target base station as long as the signal strength is acceptable. In contrast, in the legacy method the two D2D devices individually select their own target candidates each of which is with strongest signal strength to their corresponding devices. This implies the proposed method entails a robustness to inter-device distance to a certain degree. Reversely, all the cases in the legacy method are sensitive to inter-device distance. In addition, we observe that the device velocity does not impact the reliability significantly in the proposed method for an urban scenario (i.e. a scenario with medium user mobility) unless the inter-device distance is larger than 40 m. The last highlight is that the handover delay, which results from CP mobility management signalling between two BSs through X2* interface or between core network and BS through S1* interface, introduces less impact to the reliability of the both methods. Only when the device velocity is high to a certain level, the reliability gap become obvious between two cases in the same method, where the parameter settings of the two cases are identical except the handover delay. This is because handover occurs more frequently in high-velocity cases, yielding a performance degradation.

C.1.6 Resource management and traffic steering in heterogeneous environments

The simulations for this TeC are performed under the assumptions of a 1 km² flat area with no obstacles and random positioning of transmitting and receiving nodes (here the network is assumed to be highly dynamic and classical distinction between BSs and UEs is blurred due to a widespread use of opportunistic mmW communication/relaying). For receiving nodes omnidirectional antennas are used. Transmitters are equipped with directional antennas characterized with the main lobe of 4 degrees and a front-to-back ratio (FBR) of 30 dB. A maximum range of a mmW radio link is set to 200 m with a carrier-to-interference (C/I) threshold of 12 dB (below this value the transmission throughput of the link is zero). Resource management is ideal resulting in optimal signal power in receiver, equal load sharing in RCS and negligible signalling. Simulations are Monte Carlo with 1000 runs for every studied scenario where a number of mmW links vary from 10 to 200 with a 10 links step

In simulations without PGIA, after the random deployment of nodes in the simulation area (considering maximum range assumption), all receiving nodes with a C/I below the threshold are counted. In simulations with PGIA, every random link is initially member of its own RSC (of size equal to 1). A PGIA is then performed sequentially to determine collisions in the main or secondary

lobes. Collision of at least one of the RSC members with a member of a different RSC results in the merge of the two RSCs. At the end of the process the receiving nodes with a C/I below the C/I threshold are counted. The remaining interfered nodes will be the ones interfered by transmitting links belonging to different RSCs and the impact of each interferer is proportional to the size of its RCS to account for a potential time sharing of the radio resources in RCS. A prerequisite for proposed algorithm is the knowledge of geometrical position of all the mmW transmitting/receiving nodes at the network side, at any time regardless of their mobility. Additionally, a simplified model of the antenna for each mmW node (e.g. the main beam angle and the FBR) is also needed for the geometrical analysis.

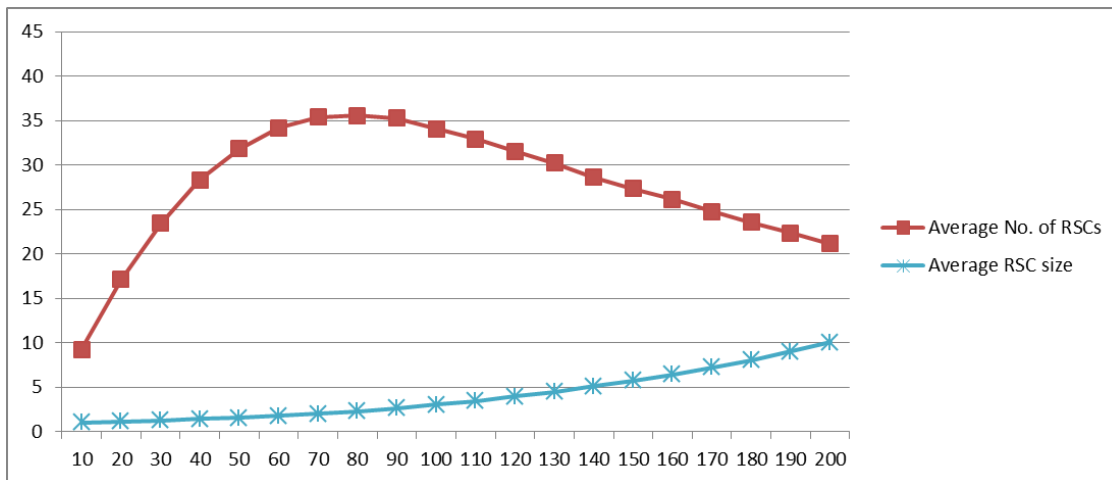


Figure C-7. Average number of RSCs and RSC size (Y axis) as functions of the number of concurrent links (X axis).

Figure C-7 depicts the performance of the RSC clustering mechanism as the number of links increases. The average number of RSCs in considered scenario increases to around 35 and then decreases as the average number of links per cluster (RSC size) increases. This can be explained by the fact that with more links there is a raise in the probability of collisions and subsequently more merges of clusters occur diminishing the average number of clusters and increasing their average size.

C.2 mMTC

C.2.1 FQAM-FBMC design and its application to mMTC

C.2.2 Group based system access

Section 4.2.2 has presented the results of the group based system access. This section provides details on the mechanism for the grouping and the simulation setup. More details can be found in [MII16-D61]. Specifically, grouping and cluster head selection should take place using various criteria such as system access periodicity and device location/mobility pattern. Group head uses

Uu interface for communication with the 5G RAN. In this case, instead of having all the group members to proceed in random access, the transmission requests could be aggregated, and only one device (i.e., the group head) performs the random access request. Thus instead of having all the devices competing for resources, only the group heads will compete. The technique reduces the collision rate in the RACH. The main aspects of this scheme could be summarized as follows:

- The devices are being grouped by the network based on their mobility and communication characteristics (e.g., data to be transmitted, packet delay requirements) during their initial attach to the network. The groups are static since devices with the same transmission periodicity and the same or similar mobility patterns are being grouped, thus facilitating the rare group formation.
- The intra-cluster communication may take place either via a different interface e.g. Institute of Electrical and Electronics Engineers (IEEE) 802.15/Zigbee or IEEE 802.11 or via D2D communication over 5G AIV.

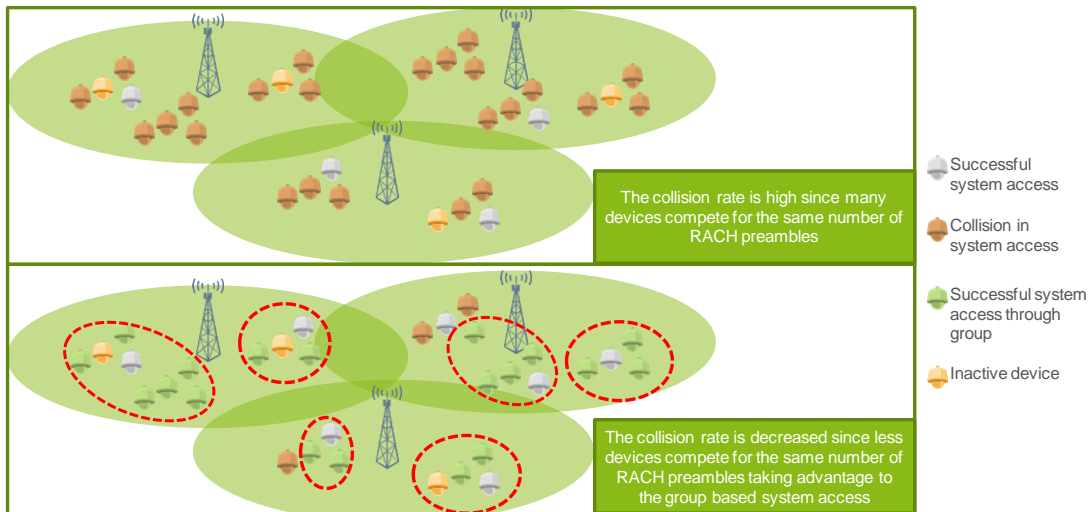


Figure C-8. Schematic representation of the group based cluster-based RACH access.

The presented evaluation considers a single BS deployment and static or semi-static devices that are trying to access the network. The intra-cluster communication is considered to be either scheduled D2D or it is performed via PC-5 interface. The devices that are accessing the medium may have either periodic or totally random transmission attempts. The devices are accessing the system simultaneously. In case a collision occurs the devices proceed in retransmissions considering the service requirements (depending on the urgency of the accessed service more retransmissions are allowed). The devices for their initial access are selecting randomly one out of the 64 available preambles and the retransmission process follows LTE-A approach. The periodic system access and the limited mobility of the devices enable the allocation of devices to groups. The groups are stable since a small number of changes are foreseen for the mMTC devices.

C.2.3 RRC state handling improvements – Connected Inactive

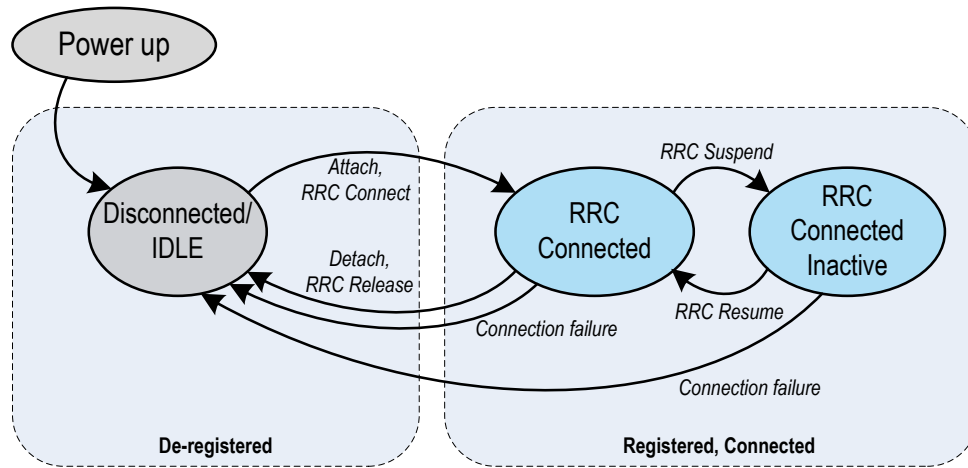


Figure C-9. RRC state transition for RRC Connected Inactive.

C.2.4 Context-aware D2D communication for mMTC

In order to optimize system performance in terms of availability and device power consumption, context information is collected and exploited by the network to efficiently set up D2D pairs. As can be seen from Figure C-10, Sensor #2 experiences good channel propagation for its cellular link and its remaining battery power is sufficient for providing relay services, BS selects it to act as sensor relay for Sensor #4 and Sensor #5. Such context aware pairing could reduce the signalling related to mMTC D2D pairing and lead to increased battery lifetime for remote UEs.

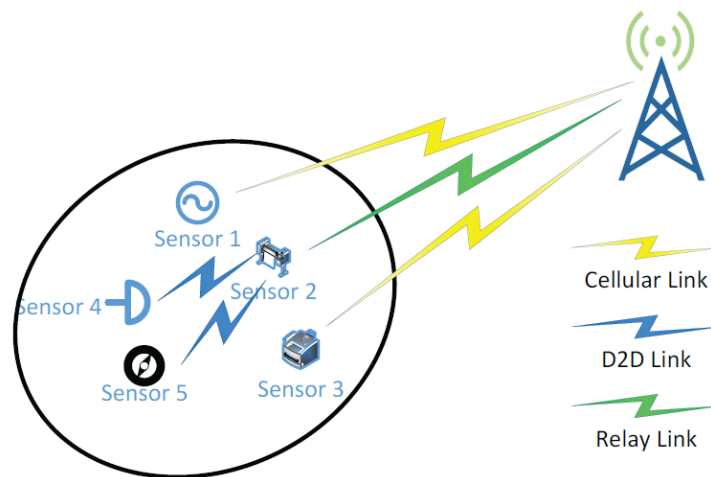


Figure C-10. Exploitation of D2D communication for mMTC.

In this work, three different transmission modes exist for different mMTC UEs, as follows:

- cellular transmission mode, in which the devices upload their reports to the BS with cellular links;
- relay transmission mode, in which the devices are configured by the network to relay the reports from remote UEs and meanwhile transmit their own reports to the BS;
- dedicated D2D transmission mode, in which the remote UEs transmit their reports to relay UEs.

In order to optimize the system performance, the focus of the proposed scheme is the selection of transmission mode for each UE. Thus, a smart transmission mode selection (TMS) algorithm should be implemented in the BS, taking into account the context information. This context information includes all information related for TMS, e.g. channel state information (CSI) between BS and UEs, location and battery level information of UEs. In this work, the proposed context-aware TMS can be divided into two steps:

- 1) clustering sensor devices into different groups;
- 2) selection of transmission mode for each UE.

From an efficiency point of view, D2D communication should be applied in cases where transmitter and receiver are nearby. Thus, a clustering approach is required at the BS to make sure that a relay UE only serves remote UEs in its proximity. The following steps are implemented to perform our proposed scheme:

- 1) Among all sensors with cellular SINR values higher than a predefined value (10 dB used in this work), K sensors are randomly selected as centroids of K clusters.
- 2) Take one another sensor and associate it to the cluster that has the shortest distance from its centroid to this sensor.
- 3) Repeat step 2) until every sensor is associated to a cluster.

Once the result of clustering algorithm is obtained, the selection of transmission mode for each sensor can be performed inside its cluster. For UEs who cannot meet the battery life requirement, D2D communication is exploited. The equation below describes the condition of remote UEs whose battery life requirement cannot be met by cellular links:

$$\frac{BC_{(i,j)}}{EC_{(i,j)}} < BL_{threshold}$$

$BC_{(i,j)}$ denotes the battery capacity of user-j in cluster-i and $EC_{(i,j)}$ is the energy consumption of that user by cellular link for a time unit of Δt . Moreover, users that cannot reach the BS with a cellular link can be assumed to have an infinite value of energy consumption for Δt . Thus, these users also fulfil the inequality and D2D communication is also applied to improve their availability. Last but not least, the requirement of battery life is denoted by $BL_{threshold}$.

If some UEs are classified as remote UEs in a cluster, the BS checks whether some UEs in the same cluster fulfil the following conditions for being relays:

$$\frac{BC_{(i,j)}}{EC_{(i,j)}} > BL_{threshold}$$

$$PL_{(i,j)}^{cellular} \geq PL_{threshold}$$

The first equation represents the condition that user-j in cluster-i can meet the battery life requirement by using cellular transmission. In other words, this user has enough battery capacity to serve as a relay for other remote UEs in cluster-i. In the second equation, $PL_{(i,j)}^{cellular}$ is the pathloss value of the cellular link and $PL_{threshold}$ is a threshold value to check whether the channel condition of cellular link is good enough. In this work, a value of 140 dB is set as the threshold value.

Once the BS obtains the list of feasible relay UEs in one cluster, it picks up one relay UE and sends the D2D setup command to both the relay UE and remote UE(s). Upon receiving the D2D setup command, channel conditions between the relay and remote UEs are estimated to inspect if the D2D communication can contribute to a better energy efficiency. If the D2D setup procedure is successful, the established D2D link is exploited for uplink transmission of packet(s) from remote UE(s). The corresponding signalling schemes are detailed in [MII16-D61], where the collection of the related context information is also illustrated.

In order to evaluate the proposed technologies, a system level simulator is implemented in this work and aligned tightly with real world. A dense urban environment is generated with a Madrid Grid model being applied [MET13-D61]. In order to achieve a cell radius higher than 866 m [3GPP16-38913], multiple replicas of Madrid Grid are generated in the system level simulator, as shown in Figure C-11.

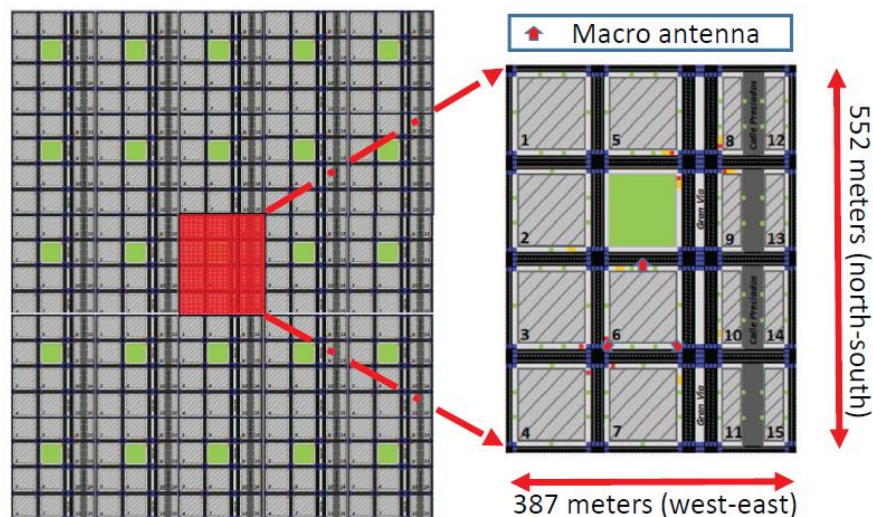


Figure C-11. Environment and deployment model.

Table C-3. Additional simulation parameters.

Frequency	900 MHz
Number of sensors	20 000
Max. transmission power of sensors	23 dBm
Periodicity of uplink packets	5 minutes
Number of reports per day	288 (1 report every 5 minutes as defined in [MET13-D61])
Channel models	cellular links: as proposed by [3GPP15-45820], D2D links: as proposed by [3GPP13-132030]
Total transmission power	45% PA efficiency + 60 mW/s for other circuitry [3GPP15-45820]
Receiver power	100 mW (total consumption to receive packets, including processing made at the device [TLS+13])
C (battery capacity)	5 Wh
Target battery life	10 years

Additional parameters used in simulation are shown in Table C-3. Other parameters are aligned with [ITUR08-M2135] [MII16-D61] and therefore are not mentioned here. Please note that, the time duration for transmission of one uplink report is related with user-specific modulation and coding scheme (MCS) which in turns is a function of the SINR value of that user. An example is given in Figure C-12 to show mapping from SNR value of 8.5 dB to modulation and coding scheme in LTE network. In order to fit the transmission strategy with radio link quality, transmitter selects the modulation and coding scheme #9 which provides the maximal data rate with a BLER less than 10%. The radio link performance of LTE network is used to characterize both cellular and D2D links in this work. Meanwhile, for a relay UE, the time it uses to receive packets from remote UEs is a function of both MCSs of remote UEs and the total number of its connected remote UEs.

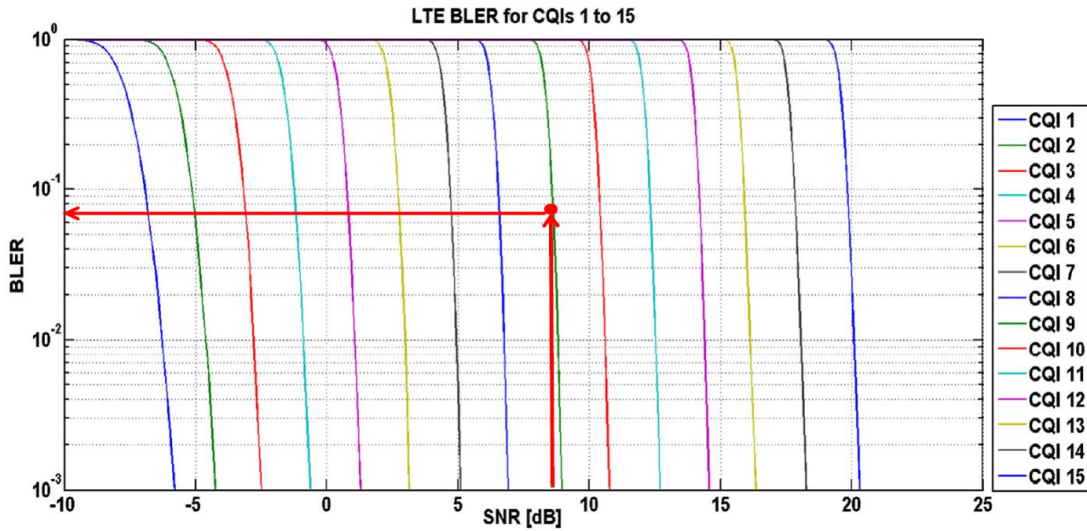


Figure C-12. Mapping from SNR to coding and modulation scheme.

In addition to the results shown in Section 4.2.4 for this TeC, the system performance of two sets of users are inspected separately in Figure C-13, with respect to their radio conditions. As shown in the left figure, regarding UEs who are in outage of LTE, 94% of them can be served by D2D communication and 60% of them can even be served for more than 10 years (3650 days) by their equipped batteries. Although these users are served by D2D links and they consume less power for UL transmission compared with direct cellular links, there are still a big set of users which cannot achieve battery life of 10 years. The reason is that some sensors cannot act as relay nodes any more, due to the high battery drain from forwarding packets from remote UEs to BS in previous days. Besides that, the performance of UEs that are in coverage of cellular network is provided at the right hand of Figure C-13. In that figure, 85% of UEs can meet the battery life requirement of 10 years in LTE system, while this value has been improved to 95% by using our D2D scheme.

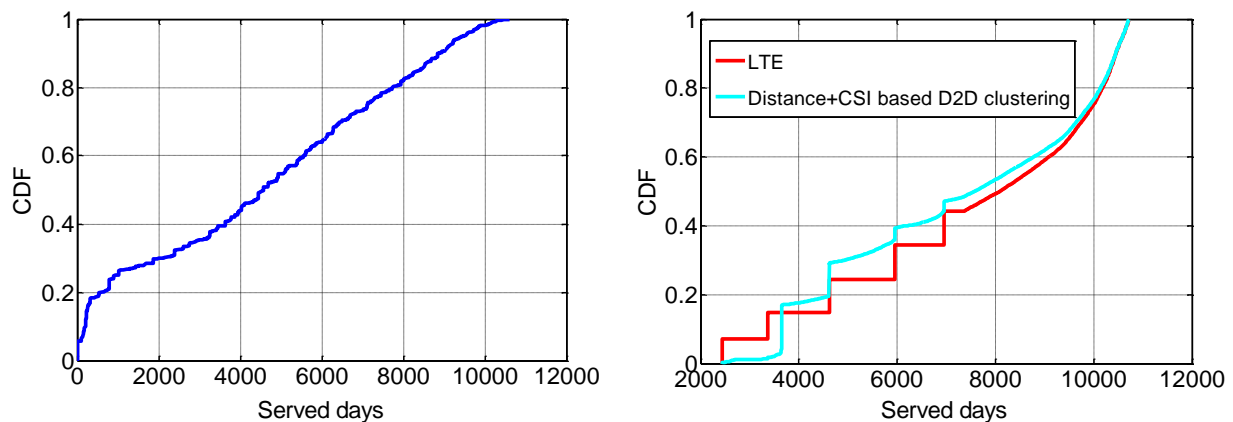


Figure C-13. CDF plot of mMTC devices a) in outage of LTE b) in the coverage of LTE.

C.3 uMTC

C.3.1 AIV harmonization for V2V communication

This TeC focuses on AIV harmonization and, in particular and as an example, on V2V communications for safety and autonomous driving services where we use two harmonized AIVs: one using the cmW band and the other using the mmW band.

In cooperative C-ITS, vehicles periodically broadcast status packets to keep their neighbours informed about their surroundings. In order to support autonomous driving, status updates should be more frequent than to support traffic safety. The current spectrum allocated to V2V is located in the cmW band: 10 MHz for traffic safety at 5.9 GHz. Unfortunately, the free spectrum in the cmW band is scarce and prized and it could be difficult to get more spectrum allocated to V2V in this band to support the higher load required by autonomous driving. In this TeC, exploitation of mmW band is proposed to overcome this problem. Although in mmW bands the communication range is, in general, shorter than in cmW region, in autonomous driving only the vehicles in the close vicinity of the transmitter need to receive the autonomous driving information, i.e. having a long communication range is not critical. Therefore, in the considered approach a portion of packets is sent through cmW band and the rest over mmW band. The packets sent using cmWs cater for traffic safety applications, while those needed specifically for autonomous driving are sent using mmW frequencies.

As prerequisites for the application of this concept, a pool of frequencies devoted to V2V communication available to all vehicles (i.e. not operator dependent) is assumed, as well as the existence of a central entity in charge of the coordination of V2V resources (assuming a multi-operator control) that could be semi-distributed in clusters.

The basis for the evaluation of this concept is UC5 from [MII16-D21] with the Madrid Grid realistic urban environment. As in [MII16-D21], the traffic model considers packets of 1600 bytes, but their periodicity is 10 ms instead of 100 ms due to the assumption that autonomous driving requires more frequent transmissions. Each packet is transmitted in 1 ms sub-frames over a 5 MHz band. Note that transmissions over 10 MHz have been also considered but provided worse results. Physical configuration (power, gains, etc.) follows the specification in [MII16-D21] (see Section 3.3.5 for details). Transmission frequencies of 5.9 GHz for the cmW band and 73 GHz for mmW band are used. For both frequencies the same channel model is used, but different values for vehicle obstruction losses are accounted: 10 dB for cmW and 30 dB for mmW. Those losses assume a knife-edge diffraction model and the location of the radio transmitters and receivers at the car bumper height. Signalling for the coordination is modelled as a constant portion of the resources. RRM entity for D2D communication is centralized and aims at maximizing the distance between vehicles using the same physical resources. To achieve this, the central RRM entity is assumed to know the position of the users. The density of users considered is 1000 vehicles/km² that is the highest value envisioned in [MII16-D11] for urban scenarios.

In this evaluation, the main KPI is the reliability. This KPI is measured through PRR as defined in [MII16-D21]. However, in contrast to [MII16-D21], the E2E delay requirement is set to 10 ms in

this evaluation. Compared to [MII16-D21], an additional deviation of this evaluation is related to the use of mmW and cmW instead of only cmW. Figure C-14 shows the PRR curves for the transmission of 10 ms periodic packets over only cmW or mmW bands considering multiple bandwidths. In order to achieve a reliability higher than 99.999% for the shortest distances, 100 MHz in both cmW and mmW are needed. In cmW, for longer distances such as 50 m, the reliability is much higher than in mmW. Unfortunately, in order to get a reliability in the order of the 90% at 50 m, a bandwidth of 100 MHz is required in cmW. In mmW, it is not clear whether such high level of reliability could be achieved at 50 m even using more bandwidth.

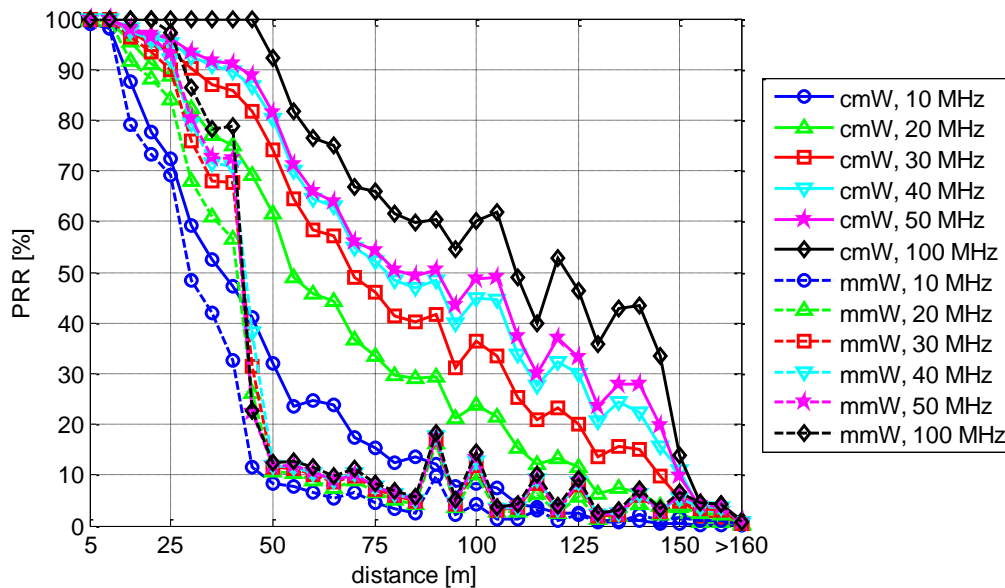


Figure C-14. PRR vs. distance between vehicles for transmissions over pure cmW AIV and a pure mmW AIV.

The proposed technique enables an optimal use of two AIVs. To achieve this, 1 out of 10 transmitted packets is sent over a bandwidth of 10 MHz in cmW, and is used for both traffic safety and autonomous driving. The remaining 9 packets are sent over 100 MHz in mmW and can be used for autonomous driving. Such approach results in better PRR for the traffic safety packets than for the autonomous driving packets, especially at larger communication distances, as depicted in Figure 4-12. Nevertheless, what is required for the autonomous driving packets is to be correctly received in short distances, as explained above, and this is precisely what we achieve for those packets. In fact, for short distances (up to 15 m) we achieve a reliability higher than the 99.999%. Note that, with this configuration, we use in total 110 MHz bandwidth. In a pure mmW transmission, it does not seem feasible to achieve similar results. On the other hand, similar results could be obtained in a pure cmW transmission with 100 MHz bandwidth, but this configuration is not possible today due to lack of free spectrum in cmW band.

C.4 TeCs addressing mixed services

C.4.1 Regular resource grid for new waveform

C.4.2 Flexible multi-service scheduling framework

In this section, additional results to those presented in the main body are included. The study focuses on the impact of the traffic type, protocol used (e.g. Transmission Control Protocol (TCP)), file size, system load and user channel conditions on the selection of the optimal TTI size to schedule a user in a particular instant. The simulation methodology and assumptions are similar to those presented in the main body, and for more details the reader is referred to [PNS+16]. The modelling of TCP follows the Reno model [PFT+00]. When a TCP packet (with the maximum segment size of 1500 B) is generated at the traffic source, it is subject to a core network (CN) latency of 2 ms before arriving at the BS. The corresponding TCP acknowledgment (ACK) from UE in the UL is transmitted with the same TTI size as in the DL. Conveying the TCP ACK from the BS to the traffic source is again subject to the CN latency. The traffic model follows a Poisson arrival process with file sizes of 50 kB and 500 kB, and variations in the total offered load are simulated to assess the end-user throughput.

The evaluation results shown in Figure C-15 indicate that for low offered loads, with both small file size downloads (dominated by the TCP slow-start phase) and with large file downloads, the best performance is achieved with a short TTI that minimizes RTT of TCP ACKs/negative ACKs (NACKs). Higher system load means higher inter-cell interference, which requires extra CCH overhead (i.e. more redundant encoding to guarantee scheduling grants reliability), that especially impacts shorter TTIs and UEs in less favourable radio conditions. In addition, higher loads imply longer queueing delays at the BS, which makes longer TTIs with higher spectral efficiency a more attractive option. For large file sizes, as the load increases, it is more efficient to schedule with a short TTI during the slow-start phase and later, when reaching steady state operation, transmit over longer TTI duration to achieve higher spectral efficiency from reduced CCH overhead (scheduling grants).

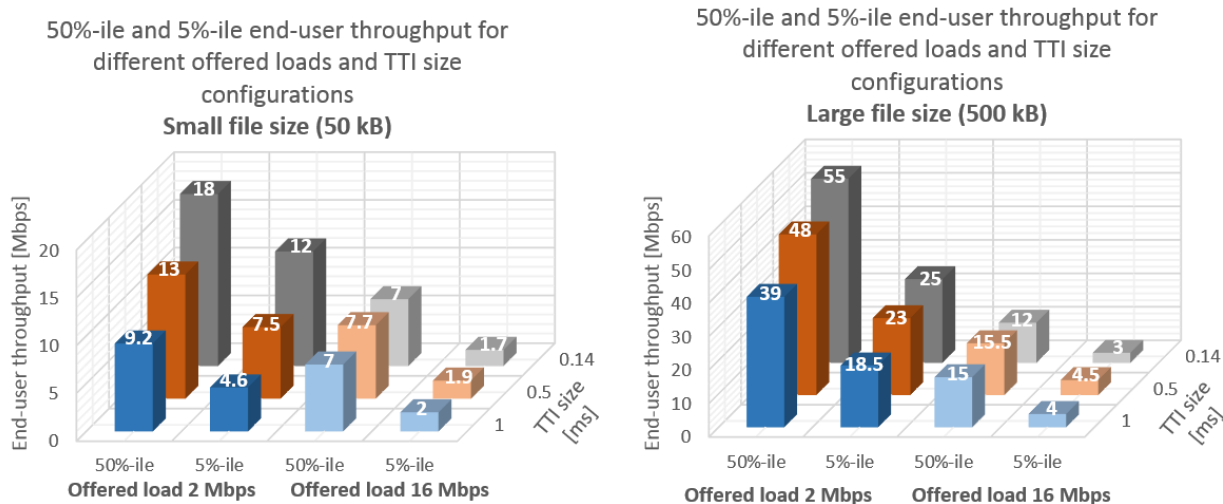


Figure C-15. 5%-ile and 50%-ile end-user throughput for TCP file download with different TTI size, file size and cell offered load.

These results are in line with the observations made in the main body, which indicate that the optimal TTI size to schedule a user depends on several factors, being therefore desirable to have the flexibility to dynamically choose the TTI duration to achieve 5G requirements.

C.4.3 Multi AI traffic steering framework

The basic simulation parameters used for evaluations of dynamic multi-AI traffic steering mechanism depicted in Figure C-16, are similar to the ones used in [MII16-D51] [PME+16], with higher user density of 10000 UEs and 1000 5G-gNBs assumed. The result trends are similar to the case with lower user and base station density, with delay reductions significantly improved with higher amount of density. This is due to the increased number of available links for the AN-O layer to establish a reliable link to deliver user data, due to the higher density of base stations. The normalized mean delay values are shown in Figure C-17. The gains are also higher for higher packet sizes used in normal bursts as compared to short bursts. The reason for this is that for short bursts, using currently available mechanisms, with the ARQ feedback, the network can be informed about the loss of connectivity. For the normal bursts, the dynamic QoS and traffic steering mechanism in AN-O enables fast traffic rerouting using appropriate AIs, depending on the real-time link conditions for the end users.

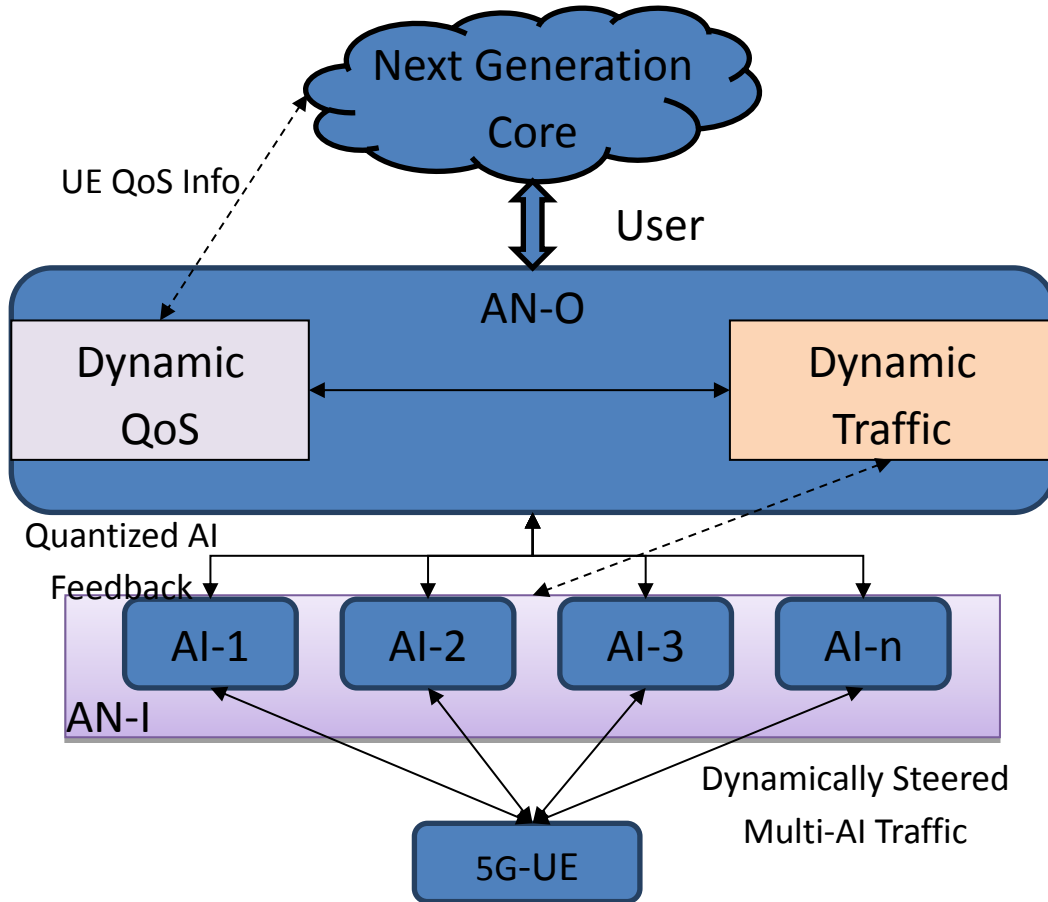


Figure C-16. Overview of the dynamic multi-AI traffic steering mechanism.

Similar to the assumptions in [MII16-D51] [PME+16], we have remained agnostic in terms of the protocol layers in which the functional split between the higher and lower layer RAN functionalities encompassed in the AN-O and AN-I entities. This gives the network operators flexibility to design the network, depending on the services and use cases are being targeted for various deployments. The dynamic traffic steering virtual function implementation could also be designed, depending on the functional split option that is adopted for each deployment.

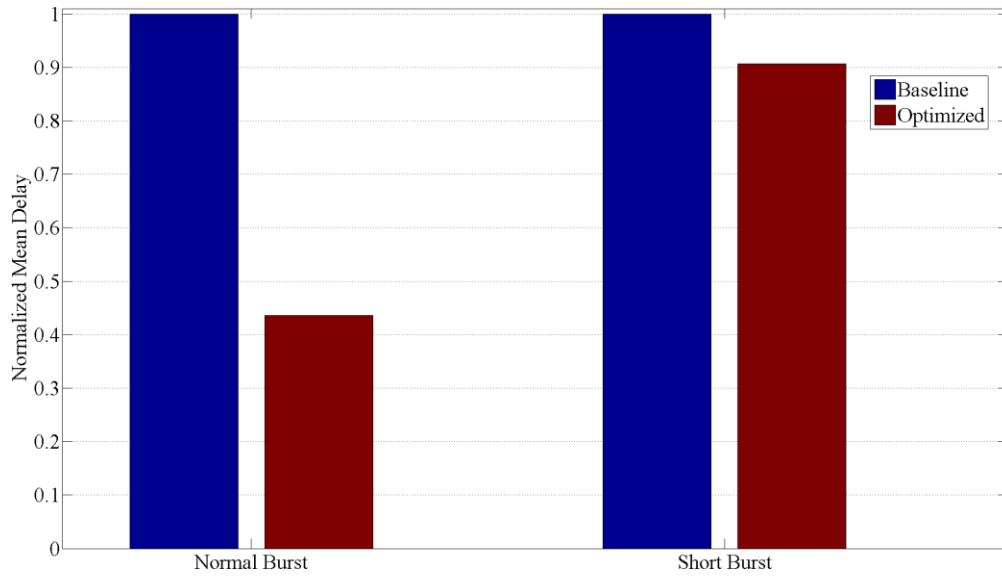


Figure C-17. Normalized mean packet delivery delay.